

AWARD NUMBER: **W81XWH-20-1-0630**

TITLE: **Cathartocytosis: A Novel Cellular Process Essential for Metaplastic Dedifferentiation**

PRINCIPAL INVESTIGATOR: **Jeffrey W. Brown, M.D., Ph.D.**

CONTRACTING ORGANIZATION: **Washington University , St. Louis, MO**

REPORT DATE: **August 2022**

TYPE OF REPORT: **Annual**

PREPARED FOR: U.S. Army Medical Research and Development Command
Fort Detrick, Maryland 21702-5012

DISTRIBUTION STATEMENT: Approved for Public Release;
Distribution Unlimited

The views, opinions and/or findings contained in this report are those of the author(s) and should not be construed as an official Department of the Army position, policy or decision unless so designated by other documentation.

REPORT DOCUMENTATION PAGEForm Approved
OMB No. 0704-0188

Public reporting burden for this collection of information is estimated to average 1 hour per response, including the time for reviewing instructions, searching existing data sources, gathering and maintaining the data needed, and completing and reviewing this collection of information. Send comments regarding this burden estimate or any other aspect of this collection of information, including suggestions for reducing this burden to Department of Defense, Washington Headquarters Services, Directorate for Information Operations and Reports (0704-0188), 1215 Jefferson Davis Highway, Suite 1204, Arlington, VA 22202-4302. Respondents should be aware that notwithstanding any other provision of law, no person shall be subject to any penalty for failing to comply with a collection of information if it does not display a currently valid OMB control number. **PLEASE DO NOT RETURN YOUR FORM TO THE ABOVE ADDRESS.**

1. REPORT DATE August 2022		2. REPORT TYPE Annual		3. DATES COVERED 15Jul2021-14Jul2022	
4. TITLE AND SUBTITLE Cathartocytosis: A Novel Cellular Process Essential for Metaplastic Dedifferentiation				5a. CONTRACT NUMBER W81XWH-20-1-0630	
				5b. GRANT NUMBER CA191105	
				5c. PROGRAM ELEMENT NUMBER	
6. AUTHOR(S) Jeffrey W. Brown, M.D., Ph.D. E-Mail: browniw@wustl.edu				5d. PROJECT NUMBER	
				5e. TASK NUMBER	
				5f. WORK UNIT NUMBER	
7. PERFORMING ORGANIZATION NAME(S) AND ADDRESS(ES) Washington University CB8124 660 South Euclid Ave. St. Louis, MO 63110-1010				8. PERFORMING ORGANIZATION REPORT NUMBER	
9. SPONSORING / MONITORING AGENCY NAME(S) AND ADDRESS(ES) U.S. Army Medical Research and Development Command Fort Detrick, Maryland 21702-5012				10. SPONSOR/MONITOR'S ACRONYM(S)	
				11. SPONSOR/MONITOR'S REPORT NUMBER(S)	
12. DISTRIBUTION / AVAILABILITY STATEMENT Approved for Public Release; Distribution Unlimited					
13. SUPPLEMENTARY NOTES					
4. ABSTRACT I have discovered that the epitope recognized by mAb Das-1 and which is aberrantly expressed in foregut metaplasia and cancer are two closely related epitopes 3'-Sulfo-LeA and 3'-Sulfo-LeC. The manuscript describing these findings has been published in PLoS ONE and is attached in the appendix. Based on this knowledge we have made significant progress in molecularly characterizing the process of cathartocytosis annotated by this antigen. Our studies have also suggested that this epitope may actually play a functional role in cathartocytosis and thus inhibiting its synthesis in high-risk metaplasia and cancer from synthesizing this antigen may have therapeutic potential for esophageal, gastric, and pancreatic cancer. I have also learned that the proteins that bind these epitopes (Galectin-3, Galectin-4, and Galectin-8 affect metaplasia by inhibiting cathartocytosis (Galectin-3 and Galectin-4) or inhibit differentiation (Galectin-8). I have used these preliminary data to obtain additional funding (K08 DK132496). Over the last year, I have published an additional 4 papers, presented a lecture about this research at the premier, international gastroenterology conference Digestive Disease Week as well as presented posters elsewhere.					
15. SUBJECT TERMS None listed.					
16. SECURITY CLASSIFICATION OF:			17. LIMITATION OF ABSTRACT Unclassified	18. NUMBER OF PAGES 69	19a. NAME OF RESPONSIBLE PERSON USAMRDC
a. REPORT Unclassified	b. ABSTRACT Unclassified	c. THIS PAGE Unclassified			19b. TELEPHONE NUMBER (include area code)

TABLE OF CONTENTS

	<u>Page</u>
1. Introduction	4
2. Keywords	4
3. Accomplishments	4
4. Impact	6
5. Changes/Problems	6
6. Products	7
7. Participants & Other Collaborating Organizations	9
8. Special Reporting Requirements	10
9. Appendices	11

1. INTRODUCTION:

The experiments proposed here serve to antigenically and molecularly characterize the cellular changes that occur as a mature cell becomes metaplastic. The first Aim of this grant was to determine the epitope recognized by the mAb Das-1 that is widely expressed specifically in metaplasia and cancer of the gastrointestinal foregut and elsewhere. The second Aim was to molecularly characterize the cellular protein machinery that orchestrates cathartocytosis.

2. KEYWORDS:

Gastric Cancer, Pancreatic Cancer, Esophageal Cancer, Barrett's Esophagus, Cathartocytosis, 3'-Sulfo Lewis A, Metaplasia

3. ACCOMPLISHMENTS:

- What were the major goals of the project?

Specific Aim 1

Major Task 1: Determine the glycosylation epitope recognized by mAb Das-1

Subtask 1: Submit Das-1 IgM and IgG to NCFG to be run on their comprehensive mammalian glycan array.
Target Date: 7/2020

-100% Complete, PMID: 34910746, PMCID: 8673611

Subtask 2: Validate hits with competitive ELISAs, western blots, and IHC/IF. Target Date: 12/2020

-100% Complete, PMID: 34910746, PMCID: 8673611

Subtask 3: Determine the importance of this glycosylation epitope by knocking down the relevant glycosylation enzymes in cell culture Target Date: 12/2021

-90% Complete

Milestone: Identification and confirmation of the glycosylation epitope recognized by mAb Das-1.

Target Date: 12/2021

-100% Complete, PMID: 34910746, PMCID: 8673611

Specific Aim 2

Major Task 2: Identifying the subcellular trajectories membrane takes in the process of cathartocytosis in cell culture

Subtask 1: Clone shRNA vectors to knock down proteins essential to autophagy (canonical and noncanonical), multivesicular body, and autophagolysosome. Target Date 9/2020

-100% Complete

Subtask 2: Validate efficacy of the cloned shRNA vectors. Target Date: 9/2020

-90% Complete

Subtask 3: Tandem protein mass spectroscopy of membrane secreted by LS174T and LS180 cell lines. Target Date: 12/2020

-100% Complete

Subtask 4: Determine the effect of knockdown on membrane secretion *in vitro* using ELISA and western blot. 7/2021

-85% Complete

Milestone Achieved: Identification of membrane shuttling pathways essential to cathartocytosis

-85% Complete

Major Task 3: Validate the importance of the identified proteins in our established murine models of metaplasia using genetic knockouts

Subtask 1: Obtain IACUC and DoD approval for animal use

-Washington University IACUC Approval: March 19, 2020

-DoD ACURO Approval: June 4, 2020

-100% Complete

Subtask 2: Obtain and breed genetic knockouts, heterozygotes, and control littermates based on *in vitro* cell culture results. Target Date: 7/2023

-100% Complete

Subtask 3: Validate that these genetic knockouts block cathartocytosis in our established murine models of induced metaplasia Milestone Achieved: Identification and confirmation of the glycosylation epitope recognized by mAb Das-1. Target Date: 7/2023

-100% Complete

Milestone Achieved: Publish 1-2 manuscripts presenting the molecular details of cathartocytosis that advance the field of cancer biology. Target Date: 7/2023

-50% Complete, Preparing the first manuscript. Hope to submit by 7/2022

- **What was accomplished under these goals?**

Specific Aim 1

I have identified the clinically important epitope aberrantly expressed in cancer and recognized by the monoclonal antibody Das-1 is 3'-Sulfo Lewis A and the afucosylated form 3'-Sulfo Lewis C. This was published.

Specific Aim 2

Using cell culture and colocalization in murine tissue, I have narrowed down the subcellular trajectory significantly. Our data has suggested that the membrane is initially enveloped in a autophagosome, which fuses with the lysosome to form the autophagolysosome.

Subsequently the autophagolysosome is sorted through the multivesicular body which then fuses with the apical membrane to release the membrane permitting rapid dedifferentiation. By way of identifying the antigen (Specific Aim 1), I have determined that galectins play a key role in cathartocytosis. I have obtained three global galectin knockouts (Galectin-3, Galectin-4, and Galectin-8) that preferentially bind 3'-Sulfated Galactose containing glycans and these have very interesting phenotypes that I am currently characterizing.

-Galectin-3 knockout blocks cathartocytosis

-Galectin-8 knockout has a significantly delayed maturation of the gastric chief cells

I am in the process of completely characterizing these knockouts in cell culture as well as in murine models of metaplasia. The interaction of sulfomucins with Galectin knockouts have not been described and as such this is a novel mechanism used by cells to dedifferentiate in the process of metaplasia and oncogenesis. I have also obtained two additional murine alleles. I have generated the Gal3st2fl/fl mouse, to specifically knockout the enzyme that adds the 3'-Sulfate to 3'-Sulfo-LeA. I have also obtained the Papss2fl/fl mouse from Dr. Xie (University of Pittsburgh), which will allow me to conditionally delete the enzyme that creates 3'-Phosphoadenosine-5'-Phosphosulfate (PAPS), an

essential precursor to all sulfation reactions. These two murine alleles will allow me to determine the precise function of the sulfation reaction to metaplasia and cancer.

- **What opportunities for training and professional development has the project provided?**
 - The funds provided by this grant coupled with mentorship provided by Jason Mills and Nick Davidson have allowed me to become proficient and independent with several necessary techniques including shRNA, overexpression in both organoids and cell lines. Further, Jason has taught me how to analyze RNAseq data necessary to determine the phenotype of the Galectin-8 mouse. And I am becoming much more competent at studying vesicular trafficking and expect to be independent by the end of this grant – 7/2023. With respect to the professional development and skills, I have become much stronger grant writer as evidence by the grants I have obtained since obtaining this award. I believe I have also become a much better presenter via the several invitations I have received to present the work funded by this grant.
- **How were the results disseminated to communities of interest?**
 - The results have been disseminated in publications as well as in both oral and poster presentations at national and international conferences.
- **What do you plan to do during the next reporting period to accomplish the goals?**
 - I plan to complete the remaining experiments in Aim 2 and publish results.

4. **IMPACT:**

- **What was the impact on the development of the principal discipline(s) of the project?**

By identifying the glycosylation epitope recognized by the Das-1 epitope, which is expressed in metaplasia and cancer throughout the proximal gastrointestinal tract, we have been able to identify proteins essential to transforming normal, homeostatic cells into metaplasia. Three such proteins are Galectin-3, Galectin-4, and Galectin-8. Over the last year, we have discovered that mice without Galectin-3 (Galectin-3 knockout) are unable to secrete these mucins (failed cathartocytosis) and interestingly because of this, these mice do not turn on transcription factors (e.g. Sox9) characteristic of metaplasia and cancer. Thus it appears that completing cathartocytosis is a necessary “checkpoint” in the progression to metaplasia and cancer. As such, inhibiting Galectin-3 appears to be a novel target to prevent these

- **What was the impact on other disciplines?**

Nothing to report

- **What was the impact on technology transfer?**

Nothing to report

- **What was the impact on society beyond science and technology?**

Nothing to report

5. **CHANGES/PROBLEMS:**

- **Changes in approach and reasons for change**

Nothing to report

- **Actual or anticipated problems or delays and actions or plans to resolve them**

Nothing to report

- **Changes that had a significant impact on expenditures**

Nothing to report

- **Significant changes in use or care of human subjects, vertebrate animals, biohazards, and/or select agents**

Nothing to report

- **Significant changes in use or care of human subjects**

Nothing to report

- **Significant changes in use or care of vertebrate animals.**

Nothing to report

- **Significant changes in use of biohazards and/or select agents**

Nothing to report

6. PRODUCTS:

Publications, conference papers, and presentations

Radyk MD, Peña BL, Spatz LB, **Brown JW**, Burclaff J, Cho CJ, Kefalov Y, Shih C-C, Fitzpatrick JAJ, Mills JC. ATF3 Induces RAB7 to Govern Autodegradation in Paligenosis, a Conserved Cellular Plasticity Program. *EMBO Reports* 2021, 22(9): e51806. PMID: 34309175, PMC8419698.

Brown JW. Gut Check: Can Other Microbes or Communities Phenocopy *H. pylori*'s Early Gastric Pathology? *Gut* 2022, 71(7): 1241-2. PMID: 34556521.

Brown JW,* Cho CJ,* Mills JC. Paligenosis: Cellular Remodeling During Tissue Repair. *Annual Reviews of Physiology* 2022: 84: 461-83. PMID: 34705482 *Co-First Author

Brown JW,[†] Das KK, Kalas V, Das KM, Mills JC.[†] mAb Das-1 Recognizes 3'-Sulfated Lewis A/C which is Aberrantly Expressed during Metaplastic and Oncogenic Transformation of Several Gastrointestinal Epithelia. *PLoS ONE* 2021, 16(12; e0261082): 1-14. PMID: 34910746, PMC8673611. [†]Co-Corresponding Author.

Books or other non-periodical, one-time publications.

Nothing to report

Other publications, conference papers, and presentations.

Selected for oral presentation at DDW 2022, the premier, international GI research conference.

Brown JW, Lin X, Kefalov Y, Das KK, Mills JC. Undescribed roles for Galectins and Glycosylation Epitopes in Modulating Differentiation States at Homeostasis and in Metaplasia. San Diego, CA (May, 2022). *Selected For Oral Presentation at DDW.

Reference: *Gastroenterology* 2022, in press

Poster presentation:

Brown JW, Lin X, Kefalov Y, Das KK, Mills JC. 3'-Sulfo-Le^{A/C} Annotates Cathartocytosis, A Novel Subcellular Process Used by Cells to Efficiently Dedifferentiate during Metaplastic and Oncogenic

Transformation. 2021 Annual Meeting of the Society for Glycobiology, San Diego, CA (November, 2021).

Reference: *Glycobiology* 2021: 31(12): 1684-5.

- **Website(s) or other Internet site(s)**

Nothing to report

- **Technologies or techniques**

Nothing to report

- **Inventions, patent applications, and/or licenses**

Nothing to report

- **Other Products**

Nothing to report

7. PARTICIPANTS & OTHER COLLABORATING ORGANIZATIONS

- **What individuals have worked on the project?**

Name:	Jeffrey W. Brown, M.D., Ph.D.
Project Role:	Principal Investigator
Researcher Identifier (e.g. ORCID ID):	000-0002-3992-9613
Nearest person month worked:	6
Contribution to Project:	Jeffrey W. Brown oversees the completion and participates in all aspects of the project.
Funding Support:	Department of Defense W81XWH-20-1-0630 American Gastroenterological Association: AGA2021-5101 National Institutes of Health: R21 AI156236 National Institutes of Health: K08 DK132496 Doris Duke Charitable Foundation: Doris Duke Fund to Retain Clinical Scientists Washington University Division Funds
Name:	Xiaobo Lin, Ph.D.
Project Role:	Senior Scientist
Researcher Identifier (e.g. ORCID ID):	0000-0003-1422-0568
Nearest person month worked:	6
Contribution to Project:	Xiaobo Lin manages the mouse colony and performs many of the mouse experiments.
Funding Support:	Division Funds
Name:	Yan-Alexander Kefalov
Project Role:	Research Technician
Researcher Identifier (e.g. ORCID ID):	N/A
Nearest person month worked:	12
Contribution to Project:	Yan-Alexander Kefalov clones constructs and performs cell culture experiments.
Funding Support:	W81XWH-20-1-0630

- **Has there been a change in the active other support of the PD/PI(s) or senior/key personnel since the last reporting period?**

Over the last year I have obtained the following (3) additional grants.

K08 DK132496 Principal Investigator 4/1/2022-1/31/2027
 “Neoglycosylation Epitopes in Metaplasia and Cancer”
 National Institutes of Health

Doris Duke Fund to Retain Principal Investigator 7/1/2021-6/30/2022

Clinical Scientists

“Das-1 Reactivity as a Serologic and Biliary Biomarker for Inflammatory Strictures”

Doris Duke Charitable Foundation

DDRCC Supplemental Principal Investigator

12/30/2021-10/1/2022

“Galectin-8 Promotes Cellular Differentiation”

GTAC Services via Digestive Disease Research Core Center under the parent grant P30-DK052574

- **What other organizations were involved as partners?**

Nothing to Report

8. SPECIAL REPORTING REQUIREMENTS

- **COLLABORATIVE AWARDS:**

- **QUAD CHARTS:**

9. APPENDICES:

RESEARCH ARTICLE

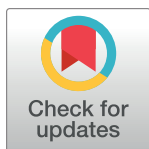
mAb Das-1 recognizes 3'-Sulfated Lewis A/C, which is aberrantly expressed during metaplastic and oncogenic transformation of several gastrointestinal Epithelia

Jeffrey W. Brown^{1*}, Koushik K. Das¹, Vasilios Kalas^{2,3}, Kiron M. Das⁴, Jason C. Mills^{1,5,6}✉

1 Division of Gastroenterology, Department of Medicine, Washington University in St. Louis, School of Medicine, St. Louis, Missouri, United States of America, **2** Washington University in St. Louis, School of Medicine, St. Louis, Missouri, United States of America, **3** Physician Scientist Training Program, Department of Medicine, McGaw Medical Center of Northwestern University, Chicago, Illinois, United States of America, **4** Division of Gastroenterology, Rutgers Robert Wood Johnson Medical School, New Brunswick, New Jersey, United States of America, **5** Department of Pathology and Immunology, Washington University in St. Louis, School of Medicine, St. Louis, Missouri, United States of America, **6** Department of Developmental Biology, Washington University in St. Louis, School of Medicine, St. Louis, Missouri, United States of America

✉ Current address: Department of Medicine, Baylor College of Medicine, Houston, Texas, United States of America

* brownjw@wustl.edu (JWB); jason.mills@bcm.edu (JCM)



OPEN ACCESS

Citation: Brown JW, Das KK, Kalas V, Das KM, Mills JC (2021) mAb Das-1 recognizes 3'-Sulfated Lewis A/C, which is aberrantly expressed during metaplastic and oncogenic transformation of several gastrointestinal Epithelia. PLoS ONE 16(12): e0261082. <https://doi.org/10.1371/journal.pone.0261082>

Editor: Nicholas Clemons, Peter MacCallum Cancer Centre, AUSTRALIA

Received: July 29, 2021

Accepted: November 23, 2021

Published: December 15, 2021

Copyright: © 2021 Brown et al. This is an open access article distributed under the terms of the [Creative Commons Attribution License](https://creativecommons.org/licenses/by/4.0/), which permits unrestricted use, distribution, and reproduction in any medium, provided the original author and source are credited.

Data Availability Statement: All data described here will be publicly available and searchable on the center for functional glycomics website. <http://www.functionalglycomics.org> Based on the most recent glycomic array white paper – the MIRAGE guidelines (Struwe Glycobiology 2016) – this is the preferred method for dissemination of these type of data.

Funding: This study received support from the following sources: JWB is supported by the

Abstract

Introduction

Multiple previous studies have shown the monoclonal antibody Das-1 (formerly called 7E₁₂H₁₂) is specifically reactive towards metaplastic and carcinomatous lesions in multiple organs of the gastrointestinal system (e.g. Barrett's esophagus, intestinal-type metaplasia of the stomach, gastric adenocarcinoma, high-grade pancreatic intraepithelial neoplasm, and pancreatic ductal adenocarcinoma) as well as in other organs (bladder and lung carcinomas). Beyond being a useful biomarker in tissue, mAb Das-1 has recently proven to be more accurate than current paradigms for identifying cysts harboring advanced neoplasia. Though this antibody has been used extensively for clinical, basic science, and translational applications for decades, its epitope has remained elusive.

Methods

In this study, we chemically deglycosylated a standard source of antigen, which resulted in near complete loss of the signal as measured by western blot analysis. The epitope recognized by mAb Das-1 was determined by affinity to a comprehensive glycan array and validated by inhibition of a direct ELISA.

Results

The epitope recognized by mAb Das-1 is 3'-Sulfo-Lewis A/C (3'-Sulfo-Le^{A/C}). 3'-Sulfo-Le^{A/C} is broadly reexpressed across numerous GI epithelia and elsewhere during metaplastic and carcinomatous transformation.

Department of Defense, through the PRCRP program under Award No. W81XWH-20-1-0630, NIH T32 DK007130-42, the Digestive Disease Research Core Centers Pilot and Feasibility Grant as part of P30 DK052574, the American Gastroenterological Association AGA2021-5101, the National Institute of Diabetes and Digestive and Kidney Diseases R21 AI156236, and the Doris Duke Charitable Foundation, Fund to Retain Clinical Scientists. JCM is supported by the National Institute of Diabetes and Digestive and Kidney Diseases (R21 DK111369, R01 DK094989, R01 DK105129, R01 DK110406, P30 DK056338), the Alvin J. Siteman Cancer Center-Barnes Jewish Foundation Cancer Frontier Fund, The National Institutes of Health National Cancer Institute (P30 CA09182, R01 CA239645, R01 CA246208), and the BETRNet (U54 CA163060). The National Center for Functional Glycomics Glycan Array resource and much appreciated assistance with the analysis was supported by R24 GM098791, R24 GM137763, and P41 GM103694. VK was supported by the Medical Scientist Training Program Training grant T32 GM07200. Development of mAb Das-1 was supported in part by National Institute of Diabetes and Digestive and Kidney Diseases research grants R01 DK47673 and R01 DK63618, awarded to KMD.

Competing interests: The authors have read the journal's policies and have the following competing interests to declare: KMD and KKD have been granted a patent for the use of Das-1 in the detection of cancerous pancreatic lesions (patent# US9575073B2; <https://patentimages.storage.googleapis.com/de/90/97/d650045c1ed674/US9575073.pdf>). KKD is providing Das-1 antibody to Interpace Biosciences for commercial use in risk stratifying pancreatic cystic lesions. This does not alter our adherence to PLOS ONE policies on sharing data and materials. JWB, VK, and JCM have no conflicts of interest.

Abbreviations: BSA, Bovine Serum Albumin; DAB, 3,3'-Diaminobenzidine; DTT, Dithiothreitol; ELISA, Enzyme Linked Immunosorbent Assay; Gal, Galactose; GlcNAc, N-Acetylglucosamine; Le^A, Lewis A; Le^C, Lewis C; Le^X, Lewis X; PBS, Phosphate Buffered Saline; TFMS, Trifluoromethanesulfonic Acid.

Discussion

3'-Sulfo-Le^{A/C} is a clinically important antigen that can be detected both intracellularly in tissue using immunohistochemistry and extracellularly in cyst fluid and serum by ELISA. The results open new avenues for tumorigenic risk stratification of various gastrointestinal lesions.

Introduction

The monoclonal antibody Das-1 has been used extensively to study metaplasia and cancer in numerous tissues over the last 30 years (Table 1). Das-1 shows broad reactivity in human fetal tissue; [1] however, in adults at homeostasis, expression is primarily restricted to biliary and colonic epithelium as well as skin [2]. Despite, the absence of reactivity in normal healthy tissues of the GI foregut, the epitope is reexpressed when these tissues undergo metaplasia that increases risk for cancer and when carcinomatous transformation occurs [3–19]. Thus, the epitope recognized by Das-1 fulfills the criteria for being a true oncofetal antigen. In addition to expression in human tissues, we have recently validated the utility of Das-1 in identifying high risk pancreatic cystic lesions in a large multicenter trial, where we demonstrated that a simple ELISA for Das-1 in cyst fluid outperforms all clinical guidelines in identifying pancreatic cysts harboring malignancy [7,8].

In this study, we aim to identify the oncofetal antigen recognized by mAb Das-1 that has been used as a biomarker for high-risk metaplasia and cancer across numerous tissues in both histology as well as body fluids (serum and pancreatic cyst fluid). Here, using chemical deglycosylation, a comprehensive glycan array, and validation by inhibition of a direct ELISA, we demonstrate that the clinically important epitope of Das-1 is 3'-Sulfo-Le^{A/C}.

Results

Immunohistochemistry of foregut metaplasias and cancers demonstrates that mAb Das-1 reactive material is expressed both intracellularly and is secreted (Fig 1). The latter phenomenon explains why it is detectable in extracellular fluid adjacent to high-grade dysplasia and cancer [7,8].

Chemical deglycosylation with trifluoromethanesulfonic acid (TFMS) of a source of concentrated antigen recognized by Das-1 (media conditioned by the LS180 cell line, see Method section) resulted in near complete loss of Das-1 binding in western blot analysis (93% and 85% as measured by IgM and IgG, respectively; Fig 2) indicating the Das-1 epitope depended on glycans. Like most glycoproteins, the mucin used here contains a heterogeneous population of glycans [20]. Thus, we determined glycan specificity of the Das-1 IgM and Das-1 IgG antibodies against a comprehensive array of 584 glycans. Both Das-1 IgM and Das-1 IgG preferentially recognized Le^{A/C} that had been sulfated at the 3' site of galactose (Fig 3). Thus, 3'-Sulfo-Galβ(1–3)GlcNAc (3'-Sulfo-Le^C) appears to be the fundamental epitope recognized by the Das-1 antibody and that the α(1–4) linked fucose in 3'-Sulfo-Le^A likely modestly increases affinity. The antibody also recognizes some disulfated glycans, albeit with lower apparent affinity. The antibodies display little-to-no affinity for the non-sulfated, sialylated, or 6'-mono-sulfated counterparts, which are listed as pertinent negatives below the highest ranked hits (S1 Fig). Recognition of the epitope was also independent of net charge, as Mannose-6-Phosphate, another negatively charged sugar, was not recognized by either antibody (S1 Fig). Relative to the IgG, the IgM isotype had similar epitope specificity but had detectable affinities against

Table 1. Summary of the prior literature describing Das-1 reactivity after metaplastic and/or oncogenic transformation of adult tissues that do not natively express this antigen at homeostasis.

Tissue	Transformation	Reference
Bladder	Cancer	Pantuck <i>et al.</i> , <i>J Urol</i> 1997;158:1722–7. PMID: 9334587
		Pantuck <i>et al.</i> , <i>Br J Urol</i> 1998;82:426–30. PMID: 9772883
Esophagus	Barrett's	Das <i>et al.</i> , <i>Ann Intern Med</i> 1994;120(9):753–6. PMID: 7511878
		DeMeester <i>et al.</i> , <i>Am J Gastroenterol</i> 2002;97(10):2514–23. PMID: 12385432
		Hahn <i>et al.</i> , <i>Am J Surg Pathol</i> 2009;33(7):1006–15. PMID: 19363439
Lung	Cancer	Deshpande <i>et al.</i> , <i>Pathobiology</i> 2002;70(6):343–7. PMID: 12865630
Pancreas	Cancer	Das <i>et al.</i> , <i>Gut</i> 2014;63(10):1626–34. PMID: 24277729
		Das <i>et al.</i> , <i>Gastroenterology</i> 2019;157(3):720–30. PMID: 31175863
		Das <i>et al.</i> , <i>Hum Pathol</i> . 2021;111:36–44. PMID: 33524436
		Heidarian <i>et al.</i> , <i>J Am Soc Cytopathol</i> . 2021;10:249–54. PMID: 33541830
Small Bowel	Adenoma	Onuma <i>et al.</i> , <i>Am J Gastroenterol</i> 2001;96(8):2480–5. PMID: 11513194
Stomach	Intestinal-Type Metaplasia	Glickman <i>et al.</i> , <i>Am J Surg Pathol</i> 2001;25(1):87–94. PMID: 11145256
		DeMeester <i>et al.</i> , <i>Am J Gastroenterol</i> 2002;97(10):2514–23. PMID: 12385432
		Mirza <i>et al.</i> , <i>Gut</i> 2003;52(6):807–12. PMID: 12740335
		Piazuelo <i>et al.</i> , <i>Mod Pathol</i> 2004;17(1):62–74. PMID: 14631367
		Watari <i>et al.</i> , <i>Int J Cancer</i> 2012;130(10):2349–58. PMID: 21732341
Stomach	Cancer	Mirza <i>et al.</i> , <i>Gut</i> 2003;52(6):807–12. PMID: 12740335
		O'Connell <i>et al.</i> , <i>Arch Pathol Lab Med</i> 2005;129(3):338–47. PMID: 15737028
		Feng <i>et al.</i> , <i>Exp Ther Med</i> 2013;5(6):1555–8. PMID: 23837030
		Kawanaka <i>et al.</i> , <i>Br J Cancer</i> 2016;114(1):21–9. PMID: 26671747
		Watari <i>et al.</i> , <i>Int J Cancer</i> 2012;130(10):2349–58. PMID: 21732341

<https://doi.org/10.1371/journal.pone.0261082.t001>

broader range of glycans (Fig 3), as might be expected due to the greater avidity of its pentameric quaternary structure.

To confirm the epitope specificity, we performed a direct ELISA using Das-1 against the heterogeneously glycosylated high molecular weight mucin carrying the antigen and found that both Das-1 IgG and IgM were inhibited by 3'-Sulfo-Le^A, in a dose-dependent manner (Fig 4), and neither the sialylated (3'-Sialyl-Le^A; i.e. CA19-9) nor unsulfated adducts were able to inhibit the reaction. Due to the high avidity of pentameric IgM (10 antigen binding sites) against mucins containing numerous glycosylation epitopes, we were only able to achieve 46% inhibition at 200 μM of the freely diffusing glycans compared to the 88% inhibition we achieved with the Das-1 IgG at the same concentration. The IC₅₀ for IgG in this experiment was 48.9 μM. Despite only differing by the Galactose-GlcNAc-fucose arrangement (Fig 4 Key), Le^X (type II) adducts were not able to competitively inhibit Das-1 binding in the ELISA. Further, the assay was not inhibited by sulfated galactose in the absence of the adjacent GlcNAc in Le^{A/C} (Fig 4). Thus, both the affinity and inhibitory studies presented here are consistent with 3'-Sulfo-Le^{A/C} being the epitope recognized by both Das-1 IgG and IgM.

Discussion

Aberrant glycosylation patterns (especially acidic modification including sialylation and sulfation) have been identified in numerous types of cancer, and probing for neo-glycosylation epitopes is a common clinical practice used to (1) detect cancer, (2) monitor therapeutic response, and/or (3) evaluate for recurrence. However, typically the utility of these glycosylation epitopes is restricted to a small set of cancers (e.g. CA19-9 for pancreatic cancer). In

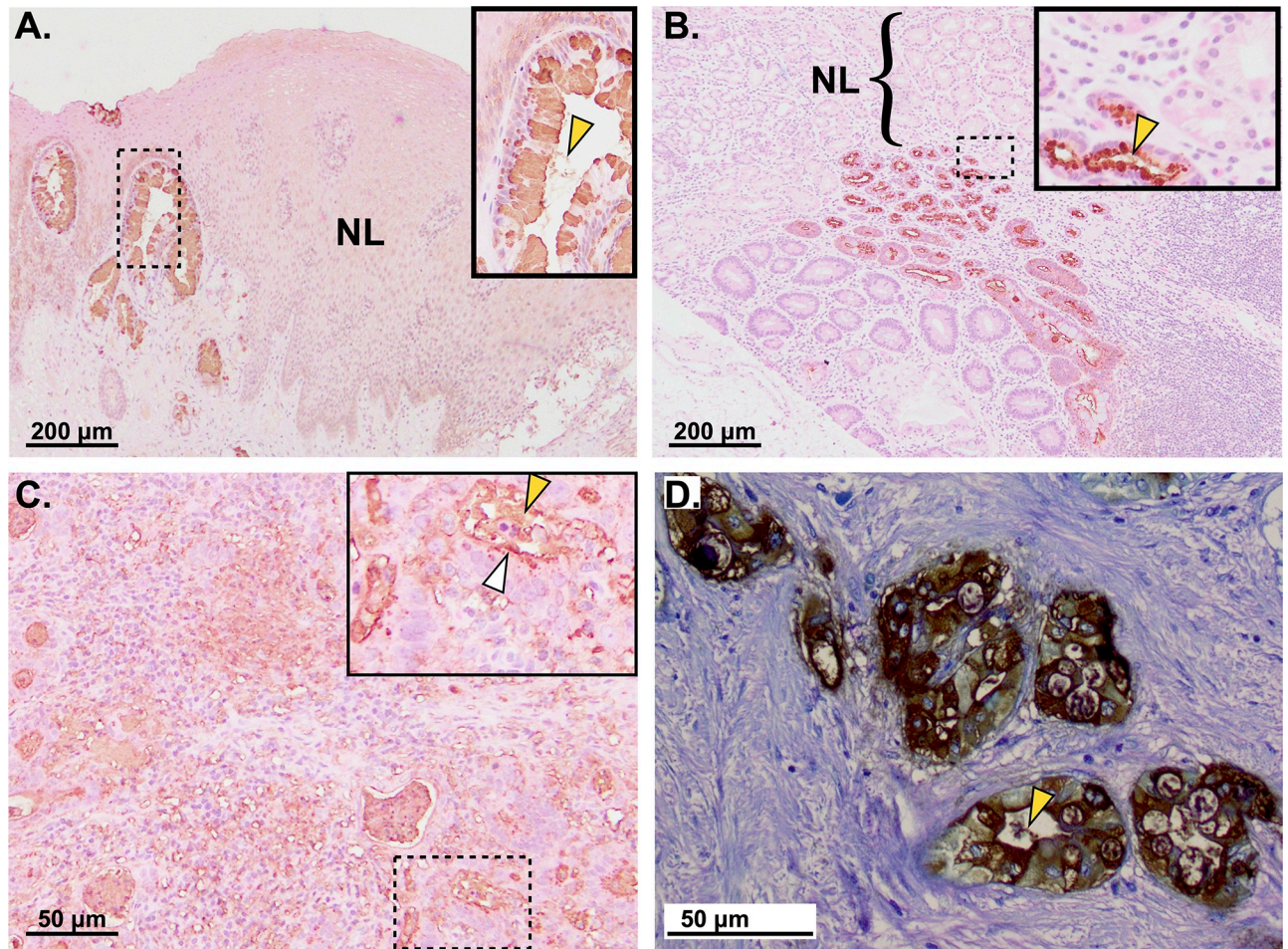


Fig 1. Unlike normal tissue, metaplastically and oncogenically transformed foregut tissues become reactive to mAb Das-1. Immunohistochemistry of A. Barrett's Esophagus, B. Intestinal Metaplasia of the Stomach (from tissue adjacent to gastric cancer), C. Gastric Cancer, D. Pancreatic Ductal Adenocarcinoma. Scale bars presented in bottom left corner of each panel. Bracket labeled "NL" to highlight the absence of staining in either the esophageal squamous tissue or normal stomach; contrast with incomplete intestinal-type metaplasia, which expresses 3'-Sulfo-Le^A. Insets show higher-magnification of boxed areas. White arrowhead: Das-1 staining at a cell apex; yellow arrowhead: 3'-Sulfo-Le^A that has been secreted into the extracellular space.

<https://doi.org/10.1371/journal.pone.0261082.g001>

contrast, 3'-Sulfo-Le^{A/C} appears to be aberrantly expressed among numerous pre-neoplastic lesions and cancers (Fig 1, Table 1).

Sulfation, much like phosphorylation, is a posttranslational modification that adds a negatively charged moiety and can be used to regulate cellular processes. Sulfate groups can be detected using high-iron diamine staining; however, this technique has been removed from most commercial laboratories due to toxicity concerns [21]. Furthermore, this technique is specific only to the reactive sulfate group and not the glycan carrying this moiety. Since there are no commercially available lectins or antibodies currently available that are specifically reactive to glycans carrying a terminal sulfate, this posttranslational modification is poorly understood [22,23]. In an attempt to study sulfation, Rick Cummings' group recently developed a novel sea lamprey variable lymphocyte receptor reactive to 3'-Sulfo-Le^X and characterized expression in a survey of normal adult tissue [23]. Other groups have used recombinantly expressed proteins like selectins; however, these lectins recognize terminally sialylated glycans in addition to those with terminal sulfates [22]. Thus, in addition to the diagnostic utility of

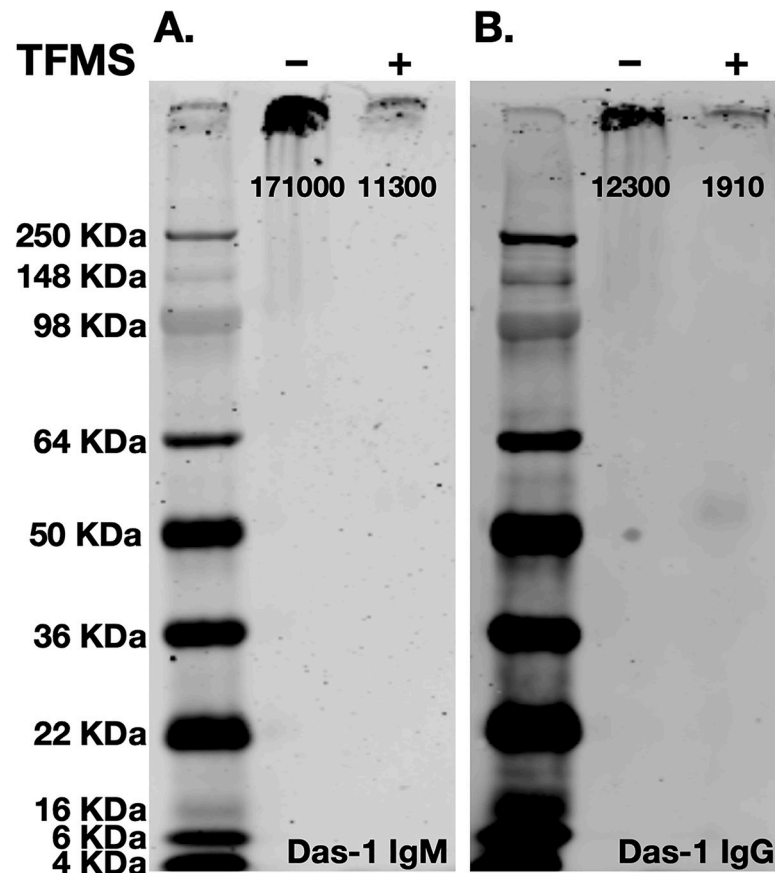


Fig 2. Das-1 IgG and IgM recognize a glycosylation epitope. Chemical deglycosylation of the antigen results in near complete loss of signal as measured by western blot analysis using (A) Das-1 IgM and (B) Das-1 IgG. Quantification of band intensity is presented below each band.

<https://doi.org/10.1371/journal.pone.0261082.g002>

this antibody, the specific reactivity towards 3'-Sulfo-Le^{A/C} that we reported here for mAb Das-1 provides a unique opportunity to study the cellular consequences of expressing this poorly understood post-translational modification.

This study is not without limitations. First, the high molecular weight mucins carrying 3'-Sulfo-Le^{A/C} are extremely difficult to electrophoretically resolve due to their extremely large size and heterogeneity in glycosylation as well as potentially protein carriers (e.g. compare Fig 1 to Issa *et al.*, 2011 [24] whom used a different, historic antibody against 3'-Sulfo-Le^A). Second, it is possible that despite being very comprehensive that the glycan array was lacking an epitope for which the Das-1 antibody has even greater affinity than 3'-Sulfo-Le^{A/C}. Third, because 3'-Sulfo-Le^C is not commercially available, we were not able to directly test whether the Das-1 antibodies could be inhibited by this sugar in solution. We have provided indirect evidence for interaction for interaction with 3'-Sulfo-Le^C with murine models of oncologic progression. In mice, *Fut3* (the only enzyme that can add an $\alpha(1-4)$ linked fucose) is a pseudogene [25] and, as a consequence, mice are only able to synthesize 3'-Sulfo-Le^C and not 3'-Sulfo-Le^A. Das-1 reactivity towards murine models of gastric intestinal metaplasia (data reviewed, but not shown) and pancreatic cancer (S2 Fig) demonstrate that reactivity phenocopies human disease [15,26,27].

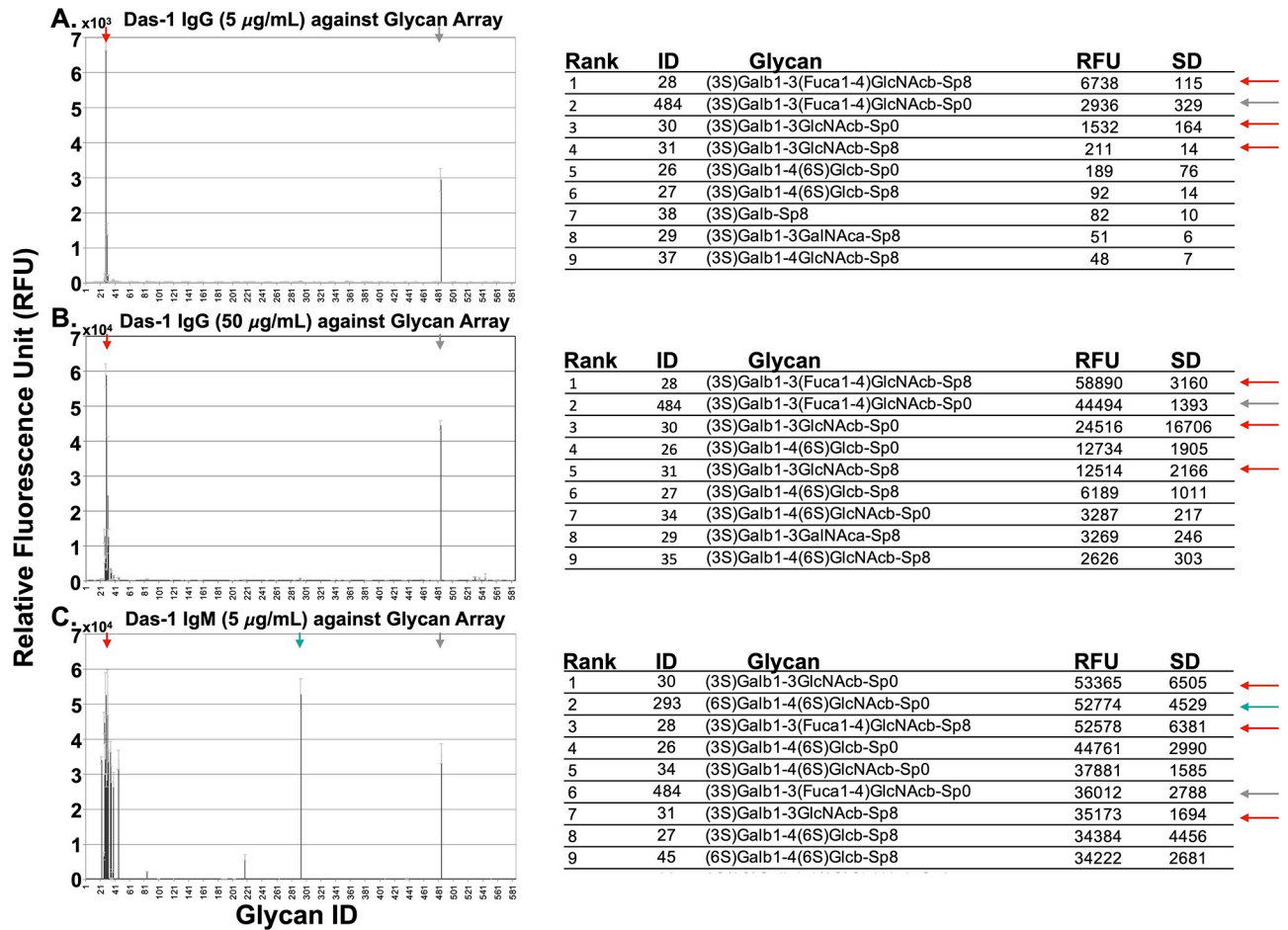


Fig 3. The results of the glycan arrays. Das-1 IgG (at 5 & 50 µg/mL) and Das-1 IgM (at 5 µg/mL) are plotted in A, B, and C respectively as the average relative fluorescence units (of 6 technical replicates) plus/minus standard deviation. The top 9 glycans for each arrays are listed to the right of each figure. Colored arrows emphasize that Das-1 IgG and Das-1 IgM recognize the same set of glycans. The complete data sets are provided in [S1 Dataset](#) (5 µg/mL IgG), [S2 Dataset](#) (50 µg/mL IgG), and [S3 Dataset](#) (5 µg/mL IgM) and are available for download on the Consortium for Functional Glycomics website (www.functionalglycomics.org).

<https://doi.org/10.1371/journal.pone.0261082.g003>

3'-Sulfo-Le^A has been implicated in diverse cellular processes. For example, swallowed salivary 3'-Sulfo-Le^A on Muc5B has been shown to be a potent ligand for the gastric pathogen *H. pylori* [28]. The bacterial receptor for 3'-Sulfo-Le^A is believed to be neutrophil-activating protein (NapA) [29,30], which is invariably expressed across human strains of *H. pylori* [31]. The importance of NapA as a major virulence factor has been demonstrated in murine models: vaccination of mice with recombinantly expressed NapA provides protection against *H. pylori* challenge, which is consistent with anti-NapA antibodies being present in the majority of people infected with *H. pylori* [32]. Thus, swallowed salivary 3'-Sulfo-Le^A may serve as a decoy to saturate this virulence factor and limit *H. pylori* entry into the gastric glands. 3'-Sulfo-Le^A has been demonstrated to be a potent ligand for selectins (e.g. E-Selectin [33,34], L-Selectin [35–37], and P-Selectin [36]). Further, it has also been shown to bind proteins on macrophages (cysteine-rich domain of the macrophage mannose receptor [38]) as well as dendritic cells (dendritic cell immunoreceptor [39]). It remains to be determined why tumors of the foregut invariably express and secrete this 3'-Sulfo-Le^{A/C}: whether it serves an intracellular function, is to avoid immune surveillance, or to modulate the microbiome.

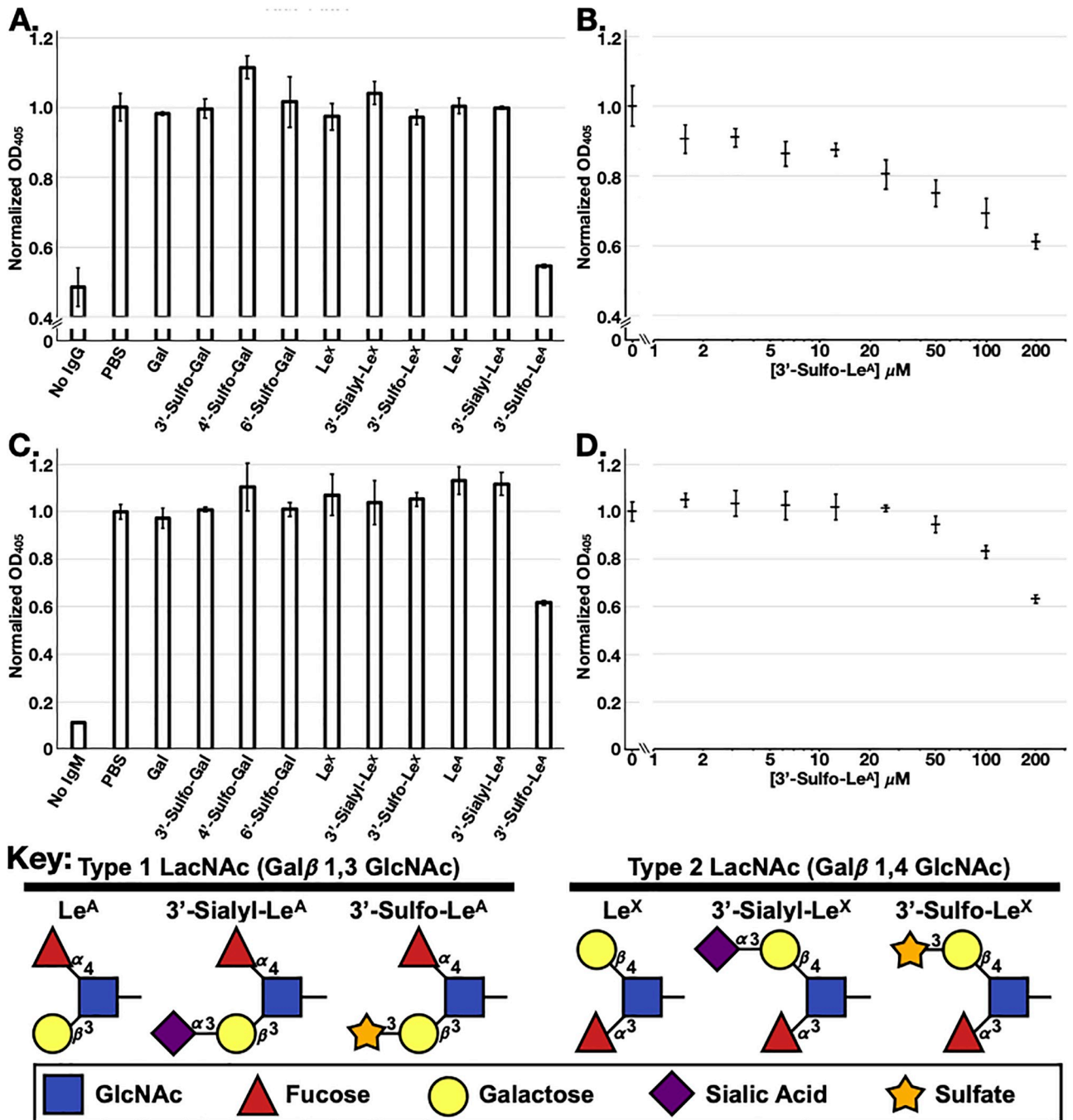


Fig 4. Das-1 IgG and IgM specifically recognize 3'-Sulfo-Le^A. Direct ELISA using Das-1 IgG (A) or Das-1 IgM (C) in the absence or presence of several free glycans in solution at 200 μM. Direct ELISA using Das-1 IgG (B) or Das-1 IgM (D) against a titration series of 3'-Sulfo-Le^A. Data reported as average ± standard deviation of three technical replicates normalized to the reaction without glycans (PBS). Key: Schematic diagram of the relevant Lewis antigens is provided for reference.

<https://doi.org/10.1371/journal.pone.0261082.g004>

The progression from normal tissue to metaplasia to cancer has arguably been best described in the stomach by seminal work of Pelayo Correa and others [40–43]. The pre-cancerous state of chronic atrophic gastritis is characterized by appearance of metaplastic cells deep in the gastric glands [44]. Such Spasmolytic Polypeptide Expressing Metaplasia (SPEM)

or pseudopyloric metaplasia cells express Sialyl-Le^X antigens that promote binding of the pro-inflammatory, carcinogenic bacteria *H. pylori* [45,46]. Expression of these sialomucins within the columnar epithelial cells is also a defining feature of Type II, incomplete, intestinal-type metaplasia in the stomach [21]. Transition from sialylation to sulfation is the sole feature distinguishing Type II from Type III gastric intestinal metaplasia with the latter being associated with increased risk for progression to cancer [21,47–49]. Consistent with our data, another group has historically generated an antibody (91.9H) that recognizes 3'-Sulfo-Le^A and is reactive with Barrett's esophagus [50] and GIM [51]; and phenocopies high iron diamine staining for sulfation in Barrett's and GIM [51]. This antibody recognizes this antigen only in the context of a tetra- or penta-saccharide [52], while here we exclusively used trisaccharides and thus demonstrate that Das-1 recognizes the terminal 3'-Sulfo-Le^A trisaccharide and does not require other adjacent sugars.

Uncovering the diagnostically important 3'-Sulfo-Le^A modification has important implications. For one, new technologies for specifically detecting this glycan (e.g. mass spectroscopy [53]) may lead to even greater sensitivity in diagnosis of metaplasia and cancer at earlier stages and in a wider variety of fluids and tissues. Moreover, reproducibility of the Das-1 sandwich ELISA [7,8] for clinical laboratory applications may be improved by using pure 3'-Sulfo-Le^A as a standard as opposed to the current practice for Das-1: using antigen concentrated from a colon cancer cell line [7,8].

It remains to be determined (1) *why* metaplastic and cancerous tissue of the GI foregut ubiquitously express this antigen, (2) the *necessity* of this epitope for metaplastic and oncogenic transformation, (3) what proteins or lipids carry this epitope, and (4) the molecular mechanism by which this epitope is released in pancreatic cyst fluid [7,8] as well as in the serum of individuals with cancer [53,54]. If the cellular processes annotated by these 3'-Sulfo-Le^A antigens confer a proliferative or survival advantage to cancer then specifically inhibiting the sulfation reaction may provide a novel therapeutic strategy for these lethal cellular transformations.

Methods

For western blots, lyophilized antigen derived from media conditioned by the LS180 colon cancer cell line (ATCC CL-187) [7] was deglycosylated using anhydrous trifluoromethanesulfonic acid (TFMS) per manufacturer (Sigma-Aldrich, USA) protocol. Briefly, 140 μ L of TFMS and 15 μ L of anisole were added to lyophilized mucin for 3 hours at 2–8°C. 4 μ L of Bromophenol Blue was added to follow the neutralization reaction, which was accomplished by adding 60% pyridine solution in a dropwise fashion in a methanol-dry ice bath. Following the deglycosylation reaction, both control and TFMS treated antigen were diluted to the same final volume with Laemmli buffer with 50 mM DTT prior to being applied to the gel. The control reaction was treated in an identical fashion (lyophilization, anisole, and pyrimidine) to the experimental condition; the only difference was that TFMS was omitted. Western blot was performed using nitrocellulose blocked with 5% BSA in PBS. Das-1 IgM or IgG were used at 1 μ g/mL and Goat anti-Mouse IgM (LiCOR 926–32280) or Donkey Anti-Mouse IgG (LiCOR 926–32212) were used at 1:5000 and imaged on a Odyssey CLX.

Both the original Das-1 IgM as well as Das-1 IgG (developed from a hybridoma that had undergone spontaneous isotype switch and thus with identical *in vivo* reactivity) were assayed against a comprehensive array of 584 glycans provided by the National Center for Functional Glycomics. Briefly, the array was generated from a library of natural and synthetic mammalian glycans with amino linkers printed onto N-hydroxysuccinimide (NHS)-activated glass microscope slides forming covalent amide linkages [55]. The glycan spotting concentration was

100 μ M. 6 technical replicates were performed for each antibody. Detailed methods section is available at <https://ncfg.hms.harvard.edu/protocols/glycan-binding-assay-unlabeled-monoclonal-antibody>. Here, Das-1 IgM was tested at 5 μ g/ml and Das-1 IgG at 5 μ g/ml and 50 μ g/ml with 1% BSA (Boval LY-0081) in 20 mM Tris pH 7.4, 150 mM NaCl, 2 mM CaCl₂, 2 mM MgCl₂, 0.05% Tween-20 against the array for 1 hour at room temperature. Secondary anti-mouse IgM (488) or anti-Mouse IgG (488) were used at 5 μ g/ml in the same buffer and conditions. The Das-1 IgM and IgG antibodies were provided to CFG and as a fee-for-service and the analysis against the glycan array was completed blinded.

Epitope specificity was confirmed by ELISA of wells coated with antigen (0.5 μ g/well), incubated in PBS overnight at 4°C, blocked with 1% BSA (Sigma A7906) in PBS, and then incubated with 2.5 μ g of either Das-1 IgG or Das-1 IgM \pm 200 μ M of the respective carbohydrate in PBS. The reactions were developed after incubation with alkaline phosphate-conjugated anti-mouse IgG (Sigma A1418) or IgM (Sigma A9688) at 1:20000 in PBS with 1% BSA and absorption at 405 nm measured after adding phosphatase substrate (Sigma S0942) in 0.001M MgCl₂, 0.05M Na₂CO₃ pH 9.6. Separate assays measured effects of competitive inhibition with 0 to 200 μ M 3'-Sulfo-Le^A. After coating the wells with antigen, all incubations were one hour in duration and performed at room temperature and the wells were washed three times with PBS containing 0.1% Tween-20 between each step.

The IC₅₀ for IgG titration curve was calculated using Eq 1, where Abs is ELISA absorption at 405nm, [3'-SulfoLe^A] is the concentration of small molecule inhibitor, Max was set to 1 and Min to 0.485 (no IgG control, Fig 4A). The IC₅₀ and cooperativity were simultaneously refined via minimizing least squares using Excel's Solver add-in. IC₅₀ for IgG was 48.9 μ M and cooperativity was 0.585. Identical analysis of the IgM inhibition study (with Min set to 0.112) suggests that the IC₅₀ is \sim 239 μ M and the transition more cooperative at \sim 1.78; however, these values should be viewed as estimates because the freely diffusible 3'-Sulfo-Le^A only partially inhibited the high-order avidity between pentameric IgM and multivalent glycosylated mucins (46% inhibition at 200 μ M).

$$Abs = 1 - \frac{Max - Min}{1 + \left(\frac{IC_{50}}{[3'SulfoLe^A]}\right)^{Cooperativity}}$$

Immunohistochemistry of paraffin embedded tissue was performed in a standard fashion. Briefly dewaxing was accomplished with HistoClear and the slides were hydrated using an ethanol series. Antigen retrieval was with a pressure cooker (5 minutes) in 10 mM citrate, pH 6.0. Blocking using 2% BSA (Sigma A7906). Tissue was probed with 1 μ g/mL Das-1 IgM in PBS with 2% BSA and 0.2% Triton X-100 overnight at 4C. Biotinylated goat anti-Mouse IgM (Vector Lab BA-2020) was used as a secondary (1:200 dilution in PBS with 2% BSA and 0.2% Triton X-100 for 1 hour at room temperature). Vectastain ABC Elite kit (Peroxidase; Vector PK-6100) diluted in in PBS with 2% BSA and 0.2% Triton X-100 for 1 hour at room temperature followed by 3.3'-Diaminobenzidine (DAB) for 1 minute at room temperature.

JWB & JCM are the guarantor of this work and, as such, had full access to all of the data in the study and takes responsibility for the integrity of the data and the accuracy of the data analysis.

Supporting information

S1 Fig. In depth presentation of pertinent positive and negative glycan results. Das-1 IgG (at 5 & 50 μ g/mL) and Das-1 IgM (at 5 μ g/mL) are plotted logarithmically in A, B, and C respectively as the average relative fluorescence units (of 6 technical replicates) plus/minus

standard deviation. The top 20 glycans for each arrays are listed below each array along with pertinent negative results. The complete data sets are provided in [S1 Dataset](#) (5 µg/mL IgG), [S2 Dataset](#) (50 µg/mL IgG), and [S3 Dataset](#) (5 µg/mL IgM) and are available for download on the Consortium for Functional Glycomics website (www.functionalglycomics.org). (PDF)

S2 Fig. Das-1 reactivity in a murine model of pancreatic cancer progression phenocopies human pathology. Das-1 is not reactive to (A) normal pancreata or (B) acinar-to-ductal metaplasia; however, demonstrates a (C) variegated reactivity towards high-grade Pan-IN, which becomes confluent in (D) pancreatic ductal carcinoma (PDAC) and (E) invasive PDAC. This pattern phenocopies what we have observed our survey of human pancreatic cancer progression (Das *et al.* (2021) Human Pathology 111: 36–44). (TIFF)

S1 Dataset. Complete glycan array dataset of Das-1 IgG (5 ug/uL) against the CFG glycan array. This dataset will also be released for public download at www.functionalglycomics.org. (XLSX)

S2 Dataset. Complete glycan array dataset of Das-1 IgG (50 ug/uL) against the CFG glycan array. This dataset will also be released for public download at www.functionalglycomics.org. (XLSX)

S3 Dataset. Complete glycan array dataset of Das-1 IgM (5 ug/uL) against the CFG glycan array. This dataset will also be released for public download at www.functionalglycomics.org. (XLSX)

S1 Raw images.
(TIFF)

Acknowledgments

We thank Jamie Heimburg-Molinario and Richard D. Cummings for both performing and analyzing the glycan array data. We thank Kian-Huat Lim for providing us with slides of KPC mouse.

Author Contributions

Conceptualization: Jeffrey W. Brown, Koushik K. Das, Vasilios Kalas, Kiron M. Das, Jason C. Mills.

Data curation: Jeffrey W. Brown, Koushik K. Das, Vasilios Kalas, Jason C. Mills.

Formal analysis: Jeffrey W. Brown, Koushik K. Das, Jason C. Mills.

Funding acquisition: Jeffrey W. Brown, Jason C. Mills.

Investigation: Jeffrey W. Brown.

Methodology: Jeffrey W. Brown, Vasilios Kalas, Jason C. Mills.

Resources: Kiron M. Das.

Writing – original draft: Jeffrey W. Brown, Koushik K. Das, Kiron M. Das, Jason C. Mills.

Writing – review & editing: Jeffrey W. Brown, Koushik K. Das, Jason C. Mills.

References


1. Badve S, Logdberg L, Sokhi R, Sigal SH, Botros N, Chae S, et al. An antigen reacting with das-1 monoclonal antibody is ontogenically regulated in diverse organs including liver and indicates sharing of developmental mechanisms among cell lineages. *Pathobiology*. 2000; 68(2):76–86. Epub 2000/07/06. <https://doi.org/10.1159/000028117> PMID: 10878504.
2. Das KM, Vecchi M, Sakamaki S. A shared and unique epitope(s) on human colon, skin, and biliary epithelium detected by a monoclonal antibody. *Gastroenterology*. 1990; 98(2):464–9. Epub 1990/02/01. [https://doi.org/10.1016/0016-5085\(90\)90839-s](https://doi.org/10.1016/0016-5085(90)90839-s) PMID: 1688539.
3. Pantuck AJ, Bancila E, Das KM, Amenta PS, Cummings KB, Marks M, et al. Adenocarcinoma of the urachus and bladder expresses a unique colonic epithelial epitope: an immunohistochemical study. *J Urol*. 1997; 158(5):1722–7. Epub 1997/10/23. [https://doi.org/10.1016/s0022-5347\(01\)64109-0](https://doi.org/10.1016/s0022-5347(01)64109-0) PMID: 9334587.
4. Das KM, Prasad I, Garla S, Amenta PS. Detection of a shared colon epithelial epitope on Barrett epithelium by a novel monoclonal antibody. *Ann Intern Med*. 1994; 120(9):753–6. Epub 1994/05/01. <https://doi.org/10.7326/0003-4819-120-9-199405010-00006> PMID: 7511878.
5. DeMeester SR, Wickramasinghe KS, Lord RV, Friedman A, Balaji NS, Chandrasoma PT, et al. Cytokeratin and DAS-1 immunostaining reveal similarities among cardiac mucosa, CIM, and Barrett's esophagus. *Am J Gastroenterol*. 2002; 97(10):2514–23. Epub 2002/10/19. <https://doi.org/10.1111/j.1572-0241.2002.06033.x> PMID: 12385432.
6. Deshpande CG, Shah RN, Yeldandi A, Papreddy K, Badve S. Expression of Das-1 in primary lung adenocarcinomas represents reactivation of an oncofetal pulmonary antigen. *Pathobiology*. 2002; 70(6):343–7. Epub 2003/07/17. <https://doi.org/10.1159/000071274> PMID: 12865630.
7. Das KK, Xiao H, Geng X, Fernandez-Del-Castillo C, Morales-Oyarvide V, Daglilar E, et al. mAb Das-1 is specific for high-risk and malignant intraductal papillary mucinous neoplasm (IPMN). *Gut*. 2014; 63(10):1626–34. Epub 2013/11/28. <https://doi.org/10.1136/gutjnl-2013-306219> PMID: 24277729.
8. Das KK, Geng X, Brown JW, Morales-Oyarvide V, Huynh T, Pergolini I, et al. Cross Validation of the Monoclonal Antibody Das-1 in Identification of High-Risk Mucinous Pancreatic Cystic Lesions. *Gastroenterology*. 2019; 157(3):720–30 e2. Epub 2019/06/09. <https://doi.org/10.1053/j.gastro.2019.05.014> PMID: 31175863.
9. Mirza ZK, Das KK, Slate J, Mapitigama RN, Amenta PS, Griffel LH, et al. Gastric intestinal metaplasia as detected by a monoclonal antibody is highly associated with gastric adenocarcinoma. *Gut*. 2003; 52(6):807–12. Epub 2003/05/13. <https://doi.org/10.1136/gut.52.6.807> PMID: 12740335.
10. Piazuolo MB, Haque S, Delgado A, Du JX, Rodriguez F, Correa P. Phenotypic differences between esophageal and gastric intestinal metaplasia. *Mod Pathol*. 2004; 17(1):62–74. Epub 2003/11/25. <https://doi.org/10.1038/sj.modpathol.3800016> PMID: 14631367.
11. Watari J, Moriichi K, Tanabe H, Kashima S, Nomura Y, Fujiya M, et al. Biomarkers predicting development of metachronous gastric cancer after endoscopic resection: an analysis of molecular pathology of *Helicobacter pylori* eradication. *Int J Cancer*. 2012; 130(10):2349–58. Epub 2011/07/07. <https://doi.org/10.1002/ijc.26275> PMID: 21732341.
12. O'Connell FP, Wang HH, Odze RD. Utility of immunohistochemistry in distinguishing primary adenocarcinomas from metastatic breast carcinomas in the gastrointestinal tract. *Arch Pathol Lab Med*. 2005; 129(3):338–47. Epub 2005/03/02. <https://doi.org/10.5858/2005-129-338-UOIIDP> PMID: 15737028.
13. Feng XS, Wang YF, Hao SG, Ru Y, Gao SG, Wang LD. Expression of Das-1, Ki67 and sulfuric proteins in gastric cardia adenocarcinoma and intestinal metaplasia lesions. *Exp Ther Med*. 2013; 5(6):1555–8. Epub 2013/07/10. <https://doi.org/10.3892/etm.2013.1038> PMID: 23837030.
14. Kawanaka M, Watari J, Kamiya N, Yamasaki T, Kondo T, Toyoshima F, et al. Effects of *Helicobacter pylori* eradication on the development of metachronous gastric cancer after endoscopic treatment: analysis of molecular alterations by a randomised controlled trial. *Br J Cancer*. 2016; 114(1):21–9. Epub 2015/12/17. <https://doi.org/10.1038/bjc.2015.418> PMID: 26671747.
15. Das KK, Brown JW, Fernandez Del-Castillo C, Huynh T, Mills JC, Matsuda Y, et al. mAb Das-1 Identifies Pancreatic Ductal Adenocarcinoma and High-grade Pancreatic Intraepithelial Neoplasia with High Accuracy. *Hum Pathol*. 2021. Epub 2021/02/02. <https://doi.org/10.1016/j.humpath.2021.01.003> PMID: 33524436.
16. Pantuck AJ, Murphy DP, Amenta PS, Das KM, Cummings KB, Weiss RE. The monoclonal antibody 7E12H12 can differentiate primary adenocarcinoma of the bladder and prostate. *Br J Urol*. 1998; 82(3):426–30. Epub 1998/10/17. <https://doi.org/10.1046/j.1464-410x.1998.00755.x> PMID: 9772883.
17. Onuma EK, Amenta PS, Jukkola AF, Mohan V, Borra S, Das KM. A phenotypic change of small intestinal epithelium to colonocytes in small intestinal adenomas and adenocarcinomas. *Am J Gastroenterol*. 2001; 96(8):2480–5. Epub 2001/08/22. <https://doi.org/10.1111/j.1572-0241.2001.04056.x> PMID: 11513194.

18. Hahn HP, Blount PL, Ayub K, Das KM, Souza R, Spechler S, et al. Intestinal differentiation in metaplastic, nongoblet columnar epithelium in the esophagus. *Am J Surg Pathol*. 2009; 33(7):1006–15. Epub 2009/04/14. <https://doi.org/10.1097/PAS.0b013e31819f57e9> PMID: 19363439.
19. Heidarian A, Das KK, Mino-Kenudson M, Fernandez-Del Castillo C, Pitman MB. Cytology adds value to monoclonal antibody Das-1 testing for detection of high-risk pancreatic cysts. *J Am Soc Cytopathol*. 2021. Epub 2021/02/06. <https://doi.org/10.1016/j.jasc.2021.01.002> PMID: 33541830.
20. Capon C, Wieruszkeski JM, Lemoine J, Byrd JC, Leffler H, Kim YS. Sulfated lewis X determinants as a major structural motif in glycans from LS174T-HM7 human colon carcinoma mucin. *J Biol Chem*. 1997; 272(51):31957–68. Epub 1998/01/24. <https://doi.org/10.1074/jbc.272.51.31957> PMID: 9405387.
21. Shah SC, Gawron AJ, Mustafa RA, Piazuolo MB. Histologic Subtyping of Gastric Intestinal Metaplasia: Overview and Considerations for Clinical Practice. *Gastroenterology*. 2020; 158(3):745–50. Epub 2019/12/31. <https://doi.org/10.1053/j.gastro.2019.12.004> PMID: 31887261.
22. Tang H, Partyka K, Hsueh P, Sinha JY, Kletter D, Zeh H, et al. Glycans related to the CA19-9 antigen are elevated in distinct subsets of pancreatic cancers and improve diagnostic accuracy over CA19-9. *Cell Mol Gastroenterol Hepatol*. 2016; 2(2):201–21 e15. Epub 2016/03/22. <https://doi.org/10.1016/j.jcmgh.2015.12.003> PMID: 26998508.
23. McKittrick TR, Bernard SM, Noll AJ, Collins BC, Goth CK, McQuillan AM, et al. Novel lamprey antibody recognizes terminal sulfated galactose epitopes on mammalian glycoproteins. *Commun Biol*. 2021; 4(1):674. Epub 2021/06/05. <https://doi.org/10.1038/s42003-021-02199-7> PMID: 34083726.
24. Issa SM, Schulz BL, Packer NH, Karlsson NG. Analysis of mucosal mucins separated by SDS-urea agarose polyacrylamide composite gel electrophoresis. *Electrophoresis*. 2011; 32(24):3554–63. Epub 2011/11/29. <https://doi.org/10.1002/elps.201100374> PMID: 22120911.
25. Gersten KM, Natsuka S, Trinchera M, Petryniak B, Kelly RJ, Hiraiwa N, et al. Molecular cloning, expression, chromosomal assignment, and tissue-specific expression of a murine alpha-(1,3)-fucosyltransferase locus corresponding to the human ELAM-1 ligand fucosyl transferase. *J Biol Chem*. 1995; 270(42):25047–56. Epub 1995/10/20. <https://doi.org/10.1074/jbc.270.42.25047> PMID: 7559635.
26. Brown JW, Das KK, Willet SG, Radyk MD, Burclaff J, Mills JC. Cathartocytosis, A Novel Cellular Process Essential for Metaplastic Dedifferentiation. *Gastroenterology*. 2019; 156(6):S82.
27. Brown JW, Das KK, Kalas V, Das KM, Mills JC. 3'-Sulfated Lewis A is a Biomarker for Metaplastic and Carcinomatous Transformation of Several Gastrointestinal Epithelia. *Gastroenterology*. 2021; 160(6):S71.
28. Veerman EC, Bank CM, Namavar F, Appelmeik BJ, Bolscher JG, Nieuw Amerongen AV. Sulfated glycans on oral mucin as receptors for *Helicobacter pylori*. *Glycobiology*. 1997; 7(6):737–43. Epub 1997/10/06. <https://doi.org/10.1093/glycob/7.6.737> PMID: 9376676.
29. Namavar F, Sparrius M, Veerman EC, Appelmeik BJ, Vandenbroucke-Grauls CM. Neutrophil-activating protein mediates adhesion of *Helicobacter pylori* to sulfated carbohydrates on high-molecular-weight salivary mucin. *Infect Immun*. 1998; 66(2):444–7. Epub 1998/02/07. <https://doi.org/10.1128/IAI.66.2.444-447.1998> PMID: 9453593.
30. Teneberg S, Miller-Podraza H, Lampert HC, Evans DJ Jr., Evans DG, Danielsson D, et al. Carbohydrate binding specificity of the neutrophil-activating protein of *Helicobacter pylori*. *J Biol Chem*. 1997; 272(30):19067–71. Epub 1997/07/25. <https://doi.org/10.1074/jbc.272.30.19067> PMID: 9228091.
31. Evans DJ Jr., Evans DG, Takemura T, Nakano H, Lampert HC, Graham DY, et al. Characterization of a *Helicobacter pylori* neutrophil-activating protein. *Infect Immun*. 1995; 63(6):2213–20. Epub 1995/06/01. <https://doi.org/10.1128/iai.63.6.2213-2220.1995> PMID: 7768601.
32. Satin B, Del Giudice G, Della Bianca V, Dusi S, Laudanna C, Tonello F, et al. The neutrophil-activating protein (HP-NAP) of *Helicobacter pylori* is a protective antigen and a major virulence factor. *J Exp Med*. 2000; 191(9):1467–76. Epub 2000/05/03. <https://doi.org/10.1084/jem.191.9.1467> PMID: 10790422.
33. Yuen CT, Lawson AM, Chai W, Larkin M, Stoll MS, Stuart AC, et al. Novel sulfated ligands for the cell adhesion molecule E-selectin revealed by the neoglycolipid technology among O-linked oligosaccharides on an ovarian cystadenoma glycoprotein. *Biochemistry*. 1992; 31(38):9126–31. Epub 1992/09/29. <https://doi.org/10.1021/bi00153a003> PMID: 1382586.
34. Yuen CT, Bezouska K, O'Brien J, Stoll M, Lemoine R, Lubineau A, et al. Sulfated blood group Lewis(a). A superior oligosaccharide ligand for human E-selectin. *J Biol Chem*. 1994; 269(3):1595–8. Epub 1994/01/21. PMID: 7507478.
35. Galustian C, Lubineau A, le Narvor C, Kiso M, Brown G, Feizi T. L-selectin interactions with novel mono- and multisulfated Lewisx sequences in comparison with the potent ligand 3'-sulfated Lewis a. *J Biol Chem*. 1999; 274(26):18213–7. Epub 1999/06/22. <https://doi.org/10.1074/jbc.274.26.18213> PMID: 10373422.

36. Galustian C, Childs RA, Stoll M, Ishida H, Kiso M, Feizi T. Synergistic interactions of the two classes of ligand, sialyl-Lewis(a/x) fuco-oligosaccharides and short sulpho-motifs, with the P- and L-selectins: implications for therapeutic inhibitor designs. *Immunology*. 2002; 105(3):350–9. Epub 2002/03/29. <https://doi.org/10.1046/j.1365-2567.2002.01369.x> PMID: 11918697.
37. Galustian C, Childs RA, Yuen CT, Hasegawa A, Kiso M, Lubineau A, et al. Valency dependent patterns of binding of human L-selectin toward sialyl and sulfated oligosaccharides of Le(a) and Le(x) types: relevance to anti-adhesion therapeutics. *Biochemistry*. 1997; 36(17):5260–6. Epub 1997/04/29. <https://doi.org/10.1021/bi962887a> PMID: 9136888.
38. Leteux C, Chai W, Loveless RW, Yuen CT, Uhlir-Hansen L, Combarous Y, et al. The cysteine-rich domain of the macrophage mannose receptor is a multispecific lectin that recognizes chondroitin sulfates A and B and sulfated oligosaccharides of blood group Lewis(a) and Lewis(x) types in addition to the sulfated N-glycans of lutropin. *J Exp Med*. 2000; 191(7):1117–26. Epub 2000/04/05. <https://doi.org/10.1084/jem.191.7.1117> PMID: 10748230.
39. Bloem K, Vuist IM, van den Berk M, Klaver EJ, van Die I, Knippels LM, et al. DCIR interacts with ligands from both endogenous and pathogenic origin. *Immunol Lett*. 2014; 158(1–2):33–41. Epub 2013/11/19. <https://doi.org/10.1016/j.imlet.2013.11.007> PMID: 24239607.
40. Saenz JB, Mills JC. Acid and the basis for cellular plasticity and reprogramming in gastric repair and cancer. *Nat Rev Gastroenterol Hepatol*. 2018; 15(5):257–73. Epub 2018/02/22. <https://doi.org/10.1038/nrgastro.2018.5> PMID: 29463907.
41. Correa P. Human gastric carcinogenesis: a multistep and multifactorial process—First American Cancer Society Award Lecture on Cancer Epidemiology and Prevention. *Cancer Res*. 1992; 52(24):6735–40. Epub 1992/12/15. PMID: 1458460.
42. de Vries AC, van Grieken NC, Looman CW, Casparie MK, de Vries E, Meijer GA, et al. Gastric cancer risk in patients with premalignant gastric lesions: a nationwide cohort study in the Netherlands. *Gastroenterology*. 2008; 134(4):945–52. Epub 2008/04/09. <https://doi.org/10.1053/j.gastro.2008.01.071> PMID: 18395075.
43. Ota H, Katsuyama T, Nakajima S, El-Zimaity H, Kim JG, Graham DY, et al. Intestinal metaplasia with adherent *Helicobacter pylori*: a hybrid epithelium with both gastric and intestinal features. *Hum Pathol*. 1998; 29(8):846–50. Epub 1998/08/26. [https://doi.org/10.1016/s0046-8177\(98\)90455-5](https://doi.org/10.1016/s0046-8177(98)90455-5) PMID: 9712427.
44. Goldenring JR. Pyloric metaplasia, pseudopyloric metaplasia, ulcer-associated cell lineage and spasmolytic polypeptide-expressing metaplasia: reparative lineages in the gastrointestinal mucosa. *J Pathol*. 2018; 245(2):132–7. Epub 2018/03/07. <https://doi.org/10.1002/path.5066> PMID: 29508389.
45. Saenz JB, Vargas N, Mills JC. Tropism for Spasmolytic Polypeptide-Expressing Metaplasia Allows *Helicobacter pylori* to Expand Its Intragastric Niche. *Gastroenterology*. 2019; 156(1):160–74 e7. Epub 2018/10/06. <https://doi.org/10.1053/j.gastro.2018.09.050> PMID: 30287170.
46. Teal E, Dua-Awereh M, Hirshorn ST, Zavros Y. Role of metaplasia during gastric regeneration. *Am J Physiol Cell Physiol*. 2020; 319(6):C947–C54. Epub 2020/08/07. <https://doi.org/10.1152/ajpcell.00415.2019> PMID: 32755448.
47. Filipe MI, Potet F, Bogomoletz WV, Dawson PA, Fabiani B, Chauveinc P, et al. Incomplete sulphomucin-secreting intestinal metaplasia for gastric cancer. Preliminary data from a prospective study from three centres. *Gut*. 1985; 26(12):1319–26. Epub 1985/12/01. <https://doi.org/10.1136/gut.26.12.1319> PMID: 4085908.
48. Hakkinen I, Viikari S. Occurrence of fetal sulphoglycoprotein antigen in the gastric juice of patients with gastric diseases. *Ann Surg*. 1969; 169(2):277–81. Epub 1969/02/01. <https://doi.org/10.1097/00000658-196902000-00016> PMID: 4974368.
49. Jass JR, Filipe MI. A variant of intestinal metaplasia associated with gastric carcinoma: a histochemical study. *Histopathology*. 1979; 3(3):191–9. Epub 1979/05/01. <https://doi.org/10.1111/j.1365-2559.1979.tb02996.x> PMID: 468122.
50. Azuma N, Endo T, Arimura Y, Motoya S, Itoh F, Hinoda Y, et al. Prevalence of Barrett's esophagus and expression of mucin antigens detected by a panel of monoclonal antibodies in Barrett's esophagus and esophageal adenocarcinoma in Japan. *J Gastroenterol*. 2000; 35(8):583–92. Epub 2000/08/24. <https://doi.org/10.1007/s005350070057> PMID: 10955596.
51. Bodger K, Campbell F, Rhodes JM. Detection of sulfated glycoproteins in intestinal metaplasia: a comparison of traditional mucin staining with immunohistochemistry for the sulfo-Lewis(a) carbohydrate epitope. *J Clin Pathol*. 2003; 56(9):703–8. Epub 2003/08/29. <https://doi.org/10.1136/jcp.56.9.703> PMID: 12944557.
52. Loveless RW, Yuen CT, Tsuiji H, Irimura T, Feizi T. Monoclonal antibody 91.9H raised against sulfated mucins is specific for the 3'-sulfated Lewis(a) tetrasaccharide sequence. *Glycobiology*. 1998; 8(12):1237–42. Epub 1998/12/22. <https://doi.org/10.1093/glycob/8.12.1237> PMID: 9858646.

53. Tanaka-Okamoto M, Mukai M, Takahashi H, Fujiwara Y, Ohue M, Miyamoto Y. Various sulfated carbohydrate tumor marker candidates identified by focused glycomic analyses. *Glycobiology*. 2017; 27(5):400–15. Epub 2016/12/28. <https://doi.org/10.1093/glycob/cww133> PMID: 28025252.
54. Zheng J, Bao WQ, Sheng WQ, Guo L, Zhang HL, Wu LH, et al. Serum 3'-sulfo-Lea indication of gastric cancer metastasis. *Clin Chim Acta*. 2009; 405(1–2):119–26. Epub 2009/04/28. <https://doi.org/10.1016/j.cca.2009.04.017> PMID: 19394320.
55. Blixt O, Head S, Mondala T, Scanlan C, Huflejt ME, Alvarez R, et al. Printed covalent glycan array for ligand profiling of diverse glycan binding proteins. *Proc Natl Acad Sci U S A*. 2004; 101(49):17033–8. Epub 2004/11/26. <https://doi.org/10.1073/pnas.0407902101> PMID: 15563589.

ATF3 induces RAB7 to govern autodegradation in paligenosis, a conserved cell plasticity program

Megan D Radyk¹, Lillian B Spatz¹, Bianca L Peña¹, Jeffrey W Brown¹, Joseph Burclaff¹, Charles J Cho¹, Yan Kefalov¹, Chien-Cheng Shih², James AJ Fitzpatrick^{2,3,4} & Jason C Mills^{1,5,6,*} 

Abstract

Differentiated cells across multiple species and organs can re-enter the cell cycle to aid in injury-induced tissue regeneration by a cellular program called paligenosis. Here, we show that activating transcription factor 3 (ATF3) is induced early during paligenosis in multiple cellular contexts, transcriptionally activating the lysosomal trafficking gene *Rab7b*. ATF3 and RAB7B are upregulated in gastric and pancreatic digestive-enzyme-secreting cells at the onset of paligenosis Stage 1, when cells massively induce autophagic and lysosomal machinery to dismantle differentiated cell morphological features. Their expression later ebbs before cells enter mitosis during Stage 3. *Atf3*^{-/-} mice fail to induce RAB7-positive autophagic and lysosomal vesicles, eventually causing increased death of cells *en route* to Stage 3. Finally, we observe that ATF3 is expressed in human gastric metaplasia and during paligenotic injury across multiple other organs and species. Thus, our findings indicate ATF3 is an evolutionarily conserved gene orchestrating the early paligenotic autodegradative events that must occur before cells are poised to proliferate and contribute to tissue repair.

Keywords acinar-ductal metaplasia; BHLHA15; plasticity; RAB5; spasmodic polypeptide-expressing metaplasia

Subject Categories Autophagy & Cell Death; Stem Cells & Regenerative Medicine

DOI 10.15252/embr.202051806 | Received 28 September 2020 | Revised 4 June 2021 | Accepted 18 June 2021

EMBO Reports (2021) e51806

Introduction

Injury in adult organisms can trigger differentiated cells to reprogram to an embryonic-like, progenitor state. The change from a differentiated cell to a proliferating progenitor-like cell has been shown in nearly every organ, for example, kidney (Kusaba *et al.*, 2014),

lung (Hong *et al.*, 2001; Tata *et al.*, 2013), stomach (Nam *et al.*, 2010; Leushacke *et al.*, 2017; Radyk *et al.*, 2018; Willet *et al.*, 2018; Meyer *et al.*, 2019), pancreas (Mills & Sansom, 2015; Willet *et al.*, 2018), intestine (van Es *et al.*, 2012; Jones *et al.*, 2019), and liver (Raven *et al.*, 2017; Chen *et al.*, 2020). As early as 1900, it was proposed that such cellular retooling was a fundamental feature shared by cells, suggesting an evolutionarily conserved program that mature cells could invoke to reroute their energy from performing differentiated cell functions (like secretion of digestive enzymes) to instead undergo mitosis (Adami, 1900).

In the last few years, we have begun to delineate the shared features of injury-induced conversion of mature cells to regenerating proliferative cells (a process termed paligenosis) (Willet *et al.*, 2018). Paligenosis progresses via three distinct, sequential stages: (i) autodegradation of mature cell structures via lysosomal and autophagy pathways, (ii) shift to expression of a progenitor or embryonic gene network, and (iii) re-entry into the cell cycle. Much evidence indicates metaplasias largely arise via cell plasticity (often paligenosis), in particular spasmodic polypeptide-expressing metaplasia (SPEM) in the stomach and acinar-to-ductal metaplasia (ADM) in the pancreas (Storz, 2017; Burclaff & Mills, 2018; Meyer & Goldenring, 2018). Metaplasia is a lesion characterized by expression of progenitor/embryonic genes, often with increased proliferation, ultimately leading to increased risk for tumorigenesis. Recently, it has become clear that metaplasia in healthy organisms is an evolutionarily conserved injury response that is usually simply a transient, regenerative state that allows tissue to recruit mature cells to help repair injury after large-scale damage (Goldenring, 2018; Saenz & Mills, 2018; Saenz *et al.*, 2018; Burclaff *et al.*, 2020). It is likely that increased cancer risk occurs when metaplasia is chronic and/or with repeated injury (Amieva & Peek, 2016; Giroux & Rustgi, 2017; Storz, 2017; Jin & Mills, 2019; Wroblewski *et al.*, 2019). Accordingly, loss of a key paligenosis gene, *Ddit4*, increases tumorigenesis by allowing cells to proliferate even with DNA damage present (Miao *et al.*, 2021). This further demonstrates the need to better understand paligenosis as a process that guards against cancer initiation.

1 Division of Gastroenterology, Department of Medicine, Washington University School of Medicine, St. Louis, MO, USA

2 Washington University Center for Cellular Imaging, Washington University School of Medicine, St. Louis, MO, USA

3 Departments of Neuroscience and Cell Biology & Physiology, Washington University School of Medicine, St. Louis, MO, USA

4 Department of Biomedical Engineering, Washington University in St. Louis, St. Louis, MO, USA

5 Department of Developmental Biology, Washington University School of Medicine, St. Louis, MO, USA

6 Department of Pathology and Immunology, Washington University School of Medicine, St. Louis, MO, USA

*Corresponding author: Tel: +1 713 798 4607; Fax: +1 713 798 0951; E-mail: jason.mills@bcm.edu

†Present address: Section of Gastroenterology and Hepatology, Departments of Medicine and Pathology, Baylor College of Medicine, Houston, TX, USA

Given the evolutionarily conserved role of paligenosis as a mechanism underlying both regeneration and tumorigenesis, we attempted to identify the core set of genes that might be largely dedicated to executing paligenosis. Such paligenosis genes are expected to be evolutionarily conserved, shared across all tissue types, and required only for injury-induced proliferation of differentiated cells but not in dedicated stem cells or during embryonic development. We recently showed that two genes meeting those criteria are *Ddit4* (mentioned above) and *Ifrd1*. DDIT4 is invoked early in paligenosis to quench mTORC1, which must be shut off for the massive autophagy and lysosomal activity of Stage 1, while IFRD1 is essential to restore mTORC1 activity for entry into S phase (Miao *et al*, 2020b).

Here, we dissect the conserved genetic program that drives the activation of the autodegradation activity in Stage 1. We focus on mechanisms conserved across two exocrine cell populations in two different organs: gastric zymogenic chief cells (ZCs) and pancreatic acinar cells (ACs). These, almost entirely postmitotic, cells live months to years in the absence of injury. ZCs and ACs have large, polarized morphologies with abundant rough endoplasmic reticulum (rER) and numerous, large secretory granules. Their secretory architecture is maintained almost entirely by a two-step transcriptional regulation program with X-box-binding protein 1 (Huh *et al*, 2010; Hess *et al*, 2011) transcriptionally activating the secretory granule trafficking transcription factor MIST1 (encoded by *Bhlha15*) (Pin *et al*, 2001; Ramsey *et al*, 2007; Lo *et al*, 2017; Dekaney *et al*, 2019). MIST1 induces and maintains expression of numerous transcriptional targets whose gene products in turn coordinate cellular organization, vesicular trafficking, and stress responses (Kowalik *et al*, 2007). For example, MIST1 binds to and directly upregulates the pro-exocrine secretory apparatus Rab proteins RAB26 and RAB3D by direct transcriptional upregulation of their genes (Tian *et al*, 2010; Mills & Taghert, 2012; Jin & Mills, 2014). MIST1 is an unique transcription factor; in that, it acts as a scaling factor for cell architecture and maturity by regulating abundance of cell trafficking proteins (Mills & Taghert, 2012).

Rab proteins, like RAB26, RAB3D, and RAB27, are important in gastric zymogenic chief cells and pancreatic acinar cells because they help maintain secretory cell function and cell state (Ohnishi *et al*, 1996; Tian *et al*, 2010; Jin & Mills, 2014; Hou *et al*, 2015; Lo *et al*, 2017). Other Rab GTPases, like RAB5, RAB7, and RAB9, organize the endolysosomal system. RAB5 traffics the early endosome, RAB7 traffics the late endosome, lysosome, and autophagosome, and RAB9 traffics late endosomes as they transition to the trans-Golgi network (Wandinger-Ness & Zerial, 2014; Langemeyer *et al*, 2018). There are over 70 human Rab GTPases, which exhibit some overlap in function but can also exhibit distinct functions based on intrinsic characteristics or through protein cofactors. For example, RAB7A and RAB7B are both known to control late endosome maturation and lysosome biogenesis (Guerra & Bucci, 2016); however, they cannot be defined as isoforms because they do not share conserved motifs (Pereira-Leal & Seabra, 2000). The function of RAB7A is generally restricted to late endosomes and facilitates the transition to lysosomes (Bucci *et al*, 2000), while RAB7B can control endosomal transport to the trans-Golgi network (Guerra & Bucci, 2016) and can interact with cystine protease ATG4B to modulate autophagy (Kjos *et al*, 2017).

We will show that activating transcription factor 3 (ATF3) is induced during paligenotic injury in diverse organs, working to

reverse the MIST1 cell maturation program early in Stage 1. ATF3 is a highly conserved transcription factor with clear orthologues even in primitive multicellular organisms like sea anemones (*Nematostella vectensis*; <https://omabrowser.org/oma/home/>) (Altenhoff *et al*, 2018). ATF3 is rapidly induced following injury, and *Atf3* loss in multiple organisms and tissues generally exhibits phenotypes after injury (Hartman *et al*, 2004; Li *et al*, 2010; Wang *et al*, 2012; Brooks *et al*, 2015; Gey *et al*, 2016; Fazio *et al*, 2017; Zhao *et al*, 2017; Zhu *et al*, 2018). ATF3 has also been shown to transcriptionally repress MIST1 (Fazio *et al*, 2017).

Here, we show that ATF3 has a surprising role in vesicle trafficking: it binds to and transcriptionally activates *Rab7b* (also previously identified as *Rab42*; Itoh *et al*, 2006; Marubashi & Fukuda, 2020), which helps govern the maturation of late endosomes to lysosomes (Yang *et al*, 2004; Progida *et al*, 2010; Stroupe, 2018). We show RAB7 expression increases dramatically in early paligenotic exocrine cells, forming large accumulations of vesicles and co-labeling, as expected, with autophagic and lysosomal vesicles. Using *ATF3* overexpression and knockdown constructs in human epithelial cells and *Atf3*^{-/-} mice, we show that autodegradative machinery depends on ATF3, partly through transcriptional regulation of *Rab7b*. Owing to failed degradation in Stage 1, *Atf3*^{-/-} mice also have markedly aberrant later stages of paligenosis with increased cell death and decreased proliferation and repair in paligenosis Stage 3. We also find ATF3 expression focally in human SPEM, suggesting ATF3 is a staple in early transitions to metaplasia. These data indicate that ATF3 is a key evolutionarily conserved paligenosis gene that acts as one of the first proteins activated in paligenotic injury. It works principally to induce autodegradation, in part, by increasing the lysosome and autophagy coordinator *Rab7b*.

Results

Degradation of specialized cell features follows exocrine cell injury

To better characterize the early, autodegradation phase of paligenosis at ultrastructural resolution, we identified the organelles and trafficking features that characterize the earliest morphological changes after injury. To induce stomach injury, we used high-dose tamoxifen (HDT), which has been described by our laboratory and others to quickly and synchronously elicit a stomach injury and induce SPEM independent of estrogen receptor activity or sex of mice (Huh *et al*, 2012; Saenz *et al*, 2016; Leushacke *et al*, 2017; Keeley *et al*, 2019). To induce pancreas injury, we repeatedly treated with the secretagogue cerulein, which has long been described to cause damage to the exocrine pancreas (Adler *et al*, 1985; Niederau *et al*, 1985; Saluja *et al*, 1985; Willet *et al*, 2018). Injury timelines and how the time points correspond to paligenosis stages are indicated in Fig EV1A and B.

We analyzed the initial downscaling stage of paligenosis via focused ion beam-scanning electron microscopy (FIB-SEM) three-dimensional (3D) nanotomography (Fig 1A and Movies EV1–EV4). FIB-SEM of vehicle-treated ZCs compared to 24-h HDT-treated ZCs revealed a dense accumulation of lysosomes and autolysosomes in the basal region of the cell, where the cell's rER network and many mitochondria are concentrated. In addition to loss of rER, we saw exocrine granule degradation as well as swelling and fragmenting of

mitochondria. The ultrastructural changes were corroborated by immunofluorescence at 6 and 24-h HDT showing gradual loss of GIF⁺ exocrine granules coincident with increased LAMP1⁺ lysosomes (Fig 1B). Transmission electron microscopy (tEM) showed that ZCs following 24-h HDT injury harbored increased lysosomes and double-membrane bound vesicles (consistent with autophagosomes) filled with cell components, such as granules, ER, and cytosol (Fig 1C). Granular census was also reduced (Fig 1D), consistent with downscaling of mature cell architecture and an increase in single- and double-membraned vesicles, which we summarize and quantify as autodegradation events (Fig 1E). Similarly, we saw decreased granule number and increased autodegradation events in pancreatic ACs following repeated cerulein (CER) injury for one day (Fig 1F–H). These results support our initial description (Willet *et al*, 2018) that Stage 1 of paligenosis consists of an increase in both lysosomal and autophagic degradation pathways and further clarifies which organelles are targeted for degradation.

We wanted to determine whether lysosomes and autophagosomes are required for paligenosis progression in the stomach, so we treated mice with hydroxychloroquine (HCQ; 60 mg/kg/day). Intraperitoneal injection of HCQ dampens autophagic activity by blocking autophagosome–lysosome fusion (Rosenfeldt *et al*, 2013; Cao *et al*, 2017). A 3-day course of HCQ significantly decreased the fraction of stomach units that exhibit SPEM (Fig EV1C–F). We also saw many ZCs that appeared to never downscale their granules (meaning they did not undergo the autodegradative processes Stage 1), as marked by sustained GIF expression and residually large apical cytoplasm (Fig EV1D–F). Thus, lysosomes and autophagosomes are necessary for Stage 1 of paligenosis and, consequently, for subsequent progression of cells to Stage 2, which is characterized by induction of SPEM markers.

The massive degradation events occurring early in paligenosis indicated that cellular membrane trafficking was dramatically altered and pointed to alterations in the Rab family of small GTPases. RABs facilitate vesicle and organelle movement and are especially important for cells with secretory functions, like exocrine cells in the stomach and pancreas (Johnson *et al*, 2004; Faust *et al*, 2008; Fukuda, 2008; Tian *et al*, 2010; Jin & Mills, 2014; Takahashi *et al*, 2017). RAB function can be regulated at the transcriptional level in exocrine cells (Johnson *et al*, 2004; Tian *et al*, 2010). Accordingly, we found a significant increase in *Rab7b* (though not *Rab5*, *Rab7a*, *Rab9*) mRNA at 12-h HDT treatment: the time when the majority of ZCs are in Stage 1 of paligenosis (Fig 1I). Our analysis of a previously published dataset (Kowalik *et al*, 2007) also suggests that *Rab7b* is expressed in pancreatic acinar cells following cerulein-induced pancreatitis. Together the findings suggest that, like *Rab26* and *Rab3d*, *Rab7b* is transcriptionally controlled in exocrine cells.

ATF3 binds to and directly induces the *Rab7b* gene during paligenotic downscaling

While there was little RAB7 expression in vehicle-treated stomach and pancreas, we observed large balloons and crescents of RAB7+ vesicles during stage 1 of paligenosis in stomach and pancreas (Fig 2A and D). Note that we have not found an antibody that can distinguish RAB7B from RAB7A in tissue sections, so we used total RAB7 antibody for these immunostaining studies. However, we favor the interpretation that the majority of the RAB7+ vesicles are likely

RAB7B vesicles, given qRT–PCR and Western blot showed only *Rab7b* mRNA and RAB7B protein are induced consistently after paligenotic injury in pancreas and stomach (Fig EV2A and B). In contrast, there was no consistent pattern of increased expression in any of the following paligenotic injury scenarios in pancreas and stomach: total RAB7 protein by Western blot of whole tissue (Fig EV2A and B), *Rab7a* mRNA by qRT–PCR from whole tissue (Fig 1I), and RAB7A protein by Western blot of whole tissue (Fig EV2A and B).

We reasoned that the transcriptional upregulation of *Rab7b* specifically within early paligenosis might give us a route to identify, for the first time, early transcriptional regulators of the paligenosis process. Our previous work showed that MIST1 activates *Rab* transcription (e.g., *Rab3d* and *Rab26*) by binding within well-conserved *cis*-regulatory regions within the first intron. Thus, we used the MEME Suite web server (Bailey *et al*, 2009) and FIMO (Find Individual Motif Occurrences) software (Grant *et al*, 2011) to identify transcription factor binding sites within the first intron of *Rab7b*. A putative ATF3-binding motif was identified within this region. More detailed analysis using Contra v3 (Kreft *et al*, 2017) (<http://bioit2.irc.ugent.be/contra/v3>) (Fig EV3A–C) further corroborated that a potential ATF3 site was highly evolutionarily conserved across mammals. ATF3 was previously characterized in the early stages of cerulein-induced pancreatitis in mice (Fazio *et al*, 2017; Data ref: Fazio *et al*, 2017) and our *in silico*-predicted ATF3-binding site matched a site from chromatin immunoprecipitation sequencing (ChIP–Seq) analysis of genomic ATF3 binding early after cerulein injury from the published dataset (Fig EV3A–C). ATF3 was also an appealing target because it was previously described as one of the most highly upregulated genes in a mouse model of SPEM (Nozaki *et al*, 2008; Miao *et al*, 2020b). Thus, the data pointed to ATF3 as a key transcription factor early in paligenosis, potentially activating *Rab7* to facilitate the massive autophagic changes in Stage 1.

Accordingly, ATF3 was rapidly induced specifically within ZCs and ACs following injury (Fig 2A and D), and *Atf3* transcript and ATF3 protein were also both increased in whole tissue analysis of the stomach and pancreas (Fig 2B and C). ATF3 was dramatically increased early in paligenosis Stage 1, but its expression returned to almost homeostatic levels in paligenosis Stage 3. Moreover, ATF3 binding to the *Rab7b* gene in stomach tissue was confirmed using ChIP (Fig 2E) with primers designed to amplify genomic DNA including the consensus ATF3 intronic binding site described above (Fazio *et al*, 2017). We used an equivalent intronic region in the *Rab9a* gene (which has similar function and gene structure; Mackiewicz & Wyroba, 2009) as a negative control and a previously identified ATF3-binding site within the *Atf3* gene as a positive control (as ATF3 can transcriptionally regulate itself (Inoue *et al*, 2004)). As predicted, ATF3 specifically bound both to *Atf3* and *Rab7b* (vs. non-specific IgG and *Rab9* negative controls) with binding greatly increased early (6 h) after injury. Thus, induction of ATF3 activity and the consequent activation of *Rab7* occurs very early following injury; indeed, it is the earliest conserved molecular event we have so far identified in paligenosis.

ATF3 can act as a transcriptional activator or repressor depending on the gene and the context (Hai *et al*, 1999). To confirm that ATF3 activated *Rab7b* and to test if their molecular interaction was conserved across species, we used AGS cells (a human gastric epithelial line) to generate stable cell clones that overexpressed ATF3 or stably repressed *ATF3* using shRNAs. AGS cells did not express

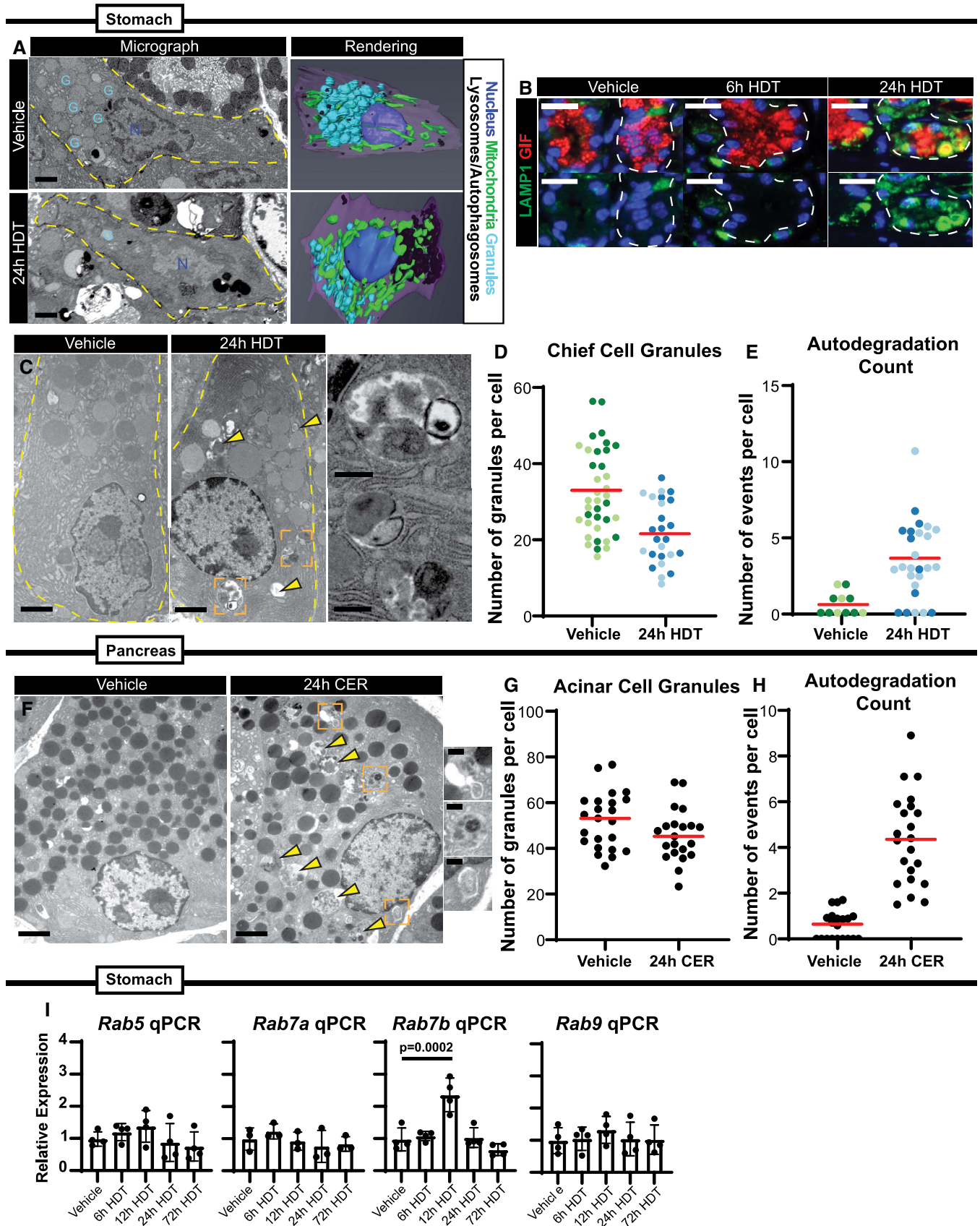


Figure 1.

Figure 1. Secretory cell structure is dismantled rapidly and in a choreographed pattern in paligenosis.

- A *Left*—Single-level electron micrograph images of zymogenic chief cells (ZCs) after 24-h vehicle or high-dose tamoxifen (HDT) treatment from FIB-SEM 3D tomography. G = representative secretory granules; N = nuclei. Scale bar, 2 μ m. *Right*—Stacked EM images rendered into 3D projections using Amira software. Cells outlined by dashed yellow line.
- B Representative immunofluorescence images of stomach unit bases at homeostasis, 6-hour, and 24-h HDT stained with GIF (red, granules) and LAMP1 (green, lysosomes) Scale bar, 25 μ m. Stomach unit base outlined by dashed white line.
- C Representative TEM images of normal and injured ZCs (scale bar, 2 μ m). *Right* (insets)—higher magnification images of boxed regions from left show emergence of double-membraned autophagic vesicles engulfing mature granules, mitochondria, and rough ER 24-h after HDT injury. Scale bar, 500 nm. Arrowheads mark vesicular degradation events in the cell lacking double membranes. Cells outlined by dashed yellow line.
- D Graph of the number of zymogenic chief cell granules per cell in vehicle vs. 24-h HDT treatment. Each data point = total granules in a cell in a single TEM section with cells from 2 separate mice plotted together (each cell is a data point; cells from the same mouse are grouped by color shade). Red line indicates mean across all the mice.
- E Graph of the number of degradation events scored as in D. A degradation event was counted if electron dense-cargo or organelles were surrounded by a single membrane (lysosome) or double membrane (autophagosome). Red line indicates mean across all the mice.
- F Representative TEM images of normal and injured acinar cells. Scale bar, 2 μ m. *Right* (insets)—higher magnification images of boxed regions from left show emergence of double-membraned autophagic vesicles engulfing mature granules, mitochondria, and rough ER 24-h after cerulein (CER) injury. Scale bar, 500 nm. Arrowheads mark degradation events without double membranes.
- G Graph of the number of acinar cell granules per cell in vehicle vs. 24-h CER treatment. Each data point = total granules in a cell in a single cell counted from one mouse. Red line indicates mean.
- H Graph of the number of degradation events scored in vehicle vs. 24-h CER treatment. Each data point = total events in a cell in a single cell counted from one mouse. Red line indicates mean.
- I mRNA expression by qRT-PCR of *Rab5*, *Rab7a*, *Rab7b*, and *Rab9*. Significance determined by one-way ANOVA, Tukey post-hoc. Each data point represents the mean of triplicate technical replicates from a single mouse, $n = 3-4$ mice in independent experiments. Error bars denote standard deviation.

substantial endogenous ATF3, though cells expressing anti-ATF3 shRNA (ATF3-KD) still expressed less (Fig 3A). ATF3-KD caused statistically significant decrease in RAB7B mRNA and fewer cells with detectable RAB7 protein, and conversely, when ATF3 protein was overexpressed (ATF3-OE), we saw an induction of RAB7 protein and mRNA (Fig 3A and B). Of note, many of the ATF3-OE cells showed large RAB7⁺ globular and crescentic vesicular formations phenocopying those seen *in vivo* in paligenotic murine cells (Fig 3C). Our *in vivo* data suggested that ATF3 could induce autophagy in part via directly increasing RAB7 abundance. Supporting our hypothesis, we noted increased cathepsin D (CTSD)-positive lysosomes in cells with higher expression of ATF3 correlating consequently with increased RAB7B (Fig 3C). To determine whether RAB7B was sufficient, even in the absence of ATF3, to induce these large vesicles observed *in vivo* and *in vitro*, we forced expression of FLAG-tagged, WT RAB7B in ATF3-KD cells. Figure 3D shows the large vesicular phenotype is even more dramatic with RAB7B overexpression. On the other hand, transfection with RAB7B^{T22N}, a GTPase-dead RAB7B mutant (GTPase cycling is critical for RABs to traffic and maintain vesicular compartments), abrogated the phenotype (Fig 3D). These results are consistent with previous reports that RAB7B^{T22N} impairs endolysosomal trafficking necessary for maturation of cathepsin D, which is activated in its pro-form in the lysosome (Progida *et al*, 2010). Taken together, ATF3 is sufficient to transcriptionally activate RAB7B, and RAB7B itself (whether ATF3-induced or transfected) is sufficient to activate the endolysosomal pathway to facilitate cell autodegradation. While ATF3, a transcription factor, may also induce other genes that activate autodegradation pathways, our results indicate RAB7B appears to be a principal target in paligenosis.

ATF3 is required for massive lysosome and autophagy induction in Stage 1 of paligenosis

To determine whether loss of *Atf3* results in decreased *Rab7* *in vivo*, we studied paligenosis in stomach and pancreas of *Atf3*^{-/-} mice (Hartman *et al*, 2004). It is important to note that these mice have a

global loss of *Atf3*, meaning *Atf3* is neither in differentiated nor in progenitor cells. However, since we only see ATF3 induction in differentiated cells after injury, *Atf3*'s main role is primarily in differentiated cells. In addition, we observed ATF3 induction in ACs in the pancreas, where there is no adult stem cell population, again suggesting that ATF3 mainly functions in differentiated cells after injury. In WT mice, we observed scant RAB7 in vehicle tissue of the stomach or pancreas, but following injury in WT animals, we saw the previously observed RAB7⁺ vesicles and large circular aggregates. Many of the large RAB7-vesicles were lysosomes or autolysosomes as indicated by enclosed CTSD (Fig 4A and B). Although low-abundance RAB7 could still be detected in ZCs and ACs of *Atf3*^{-/-} mice, the large RAB7-positive vesicles were predominantly lacking. Injury induced RAB7⁺ vesicles in WT mice, but in *Atf3*^{-/-} mice, we did not observe upregulation of large RAB7⁺ vesicles (Fig 4A and B).

Cathepsin D is a marker of both lysosomes and autolysosomes, so we next examined whether loss of ATF3 and RAB7 affected autophagic trafficking. We observed that the autophagic vesicle marker MAP1LC3B (LC3) was induced in Stage 1 of paligenosis in the stomach, consistent with previous work and our EM analysis indicating increased autophagic trafficking (Willet *et al*, 2018; Meyer *et al*, 2019; Fig 4C). Such LC3⁺ autophagic puncta were not induced in the absence of ATF3. We confirmed ATF3-dependent induction of lysosomes and autophagosomes using TEM (Fig 4D and E).

The results indicate ATF3 is induced rapidly in paligenosis and is required for RAB7-associated autophagy/lysosomal trafficking. Thus, ATF3 is both necessary and sufficient to induce the endolysosome-traffic protein RAB7 and is critical for the massive induction of autodegradative machinery that cells use in Stage 1 of paligenosis to downscale much of their mature cell architecture.

ATF3 loss results in less repair and more cell death after secretory cell injury

Paligenosis is a stepwise process, that can be inhibited between each stage. We have previously shown that blocking autodegradative

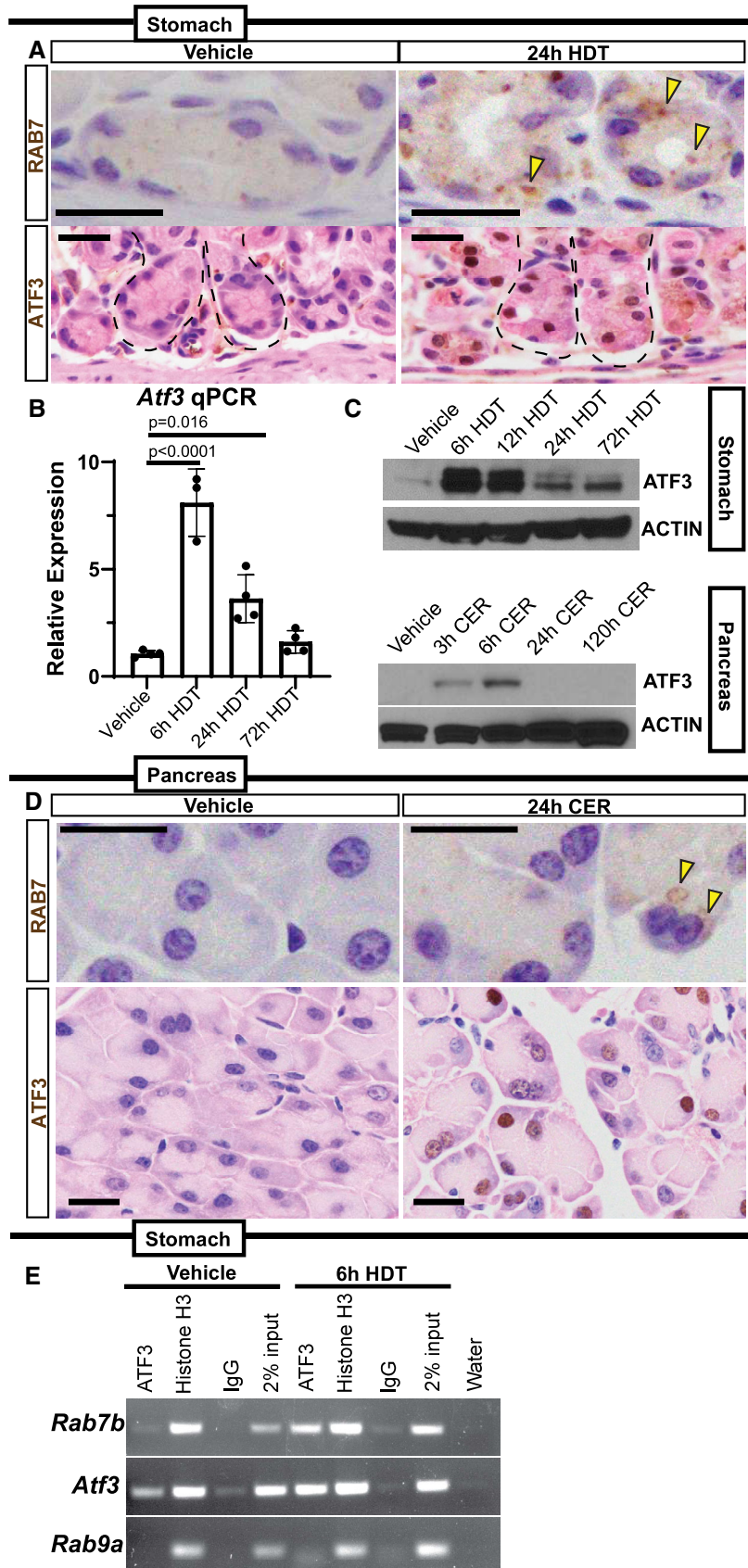


Figure 2.

Figure 2. ATF3 transcriptionally upregulates *Rab7b* early in paligenosis, and RAB7 protein is associated with large lysosomal aggregates.

- A *Top*—Representative RAB7 expression in base of stomach units (ZCs) in vehicle or 24-h HDT by immunohistochemistry. Arrowheads point to RAB7 vesicle aggregates. Scale bar 20 μ m. *Bottom*—Representative ATF3 expression in base of stomach units (ZCs) by immunohistochemistry. ATF3 appears in nuclei following 24-h high-dose tamoxifen (HDT). Scale bar 20 μ m. Stomach unit base outlined by dashed black line.
- B *Atf3* mRNA expression by qRT-PCR in vehicle, 6, 24, and 72-h HDT treatment. Each data point represents the mean of triplicate technical replicates from a single mouse, $n = 3-4$ mice in independent experiments. Significance determined by one-way ANOVA, Tukey. Error bars denote standard deviation.
- C Western blot of ATF3 expression over HDT and CER time courses with β -Actin loading control.
- D *Top*—Representative RAB7 staining in pancreatic acinar cells. Arrowheads indicate RAB7 vesicles. Scale bar 20 μ m. *Bottom*—Representative ATF3 expression in pancreatic acinar cells. Nuclei express ATF3 after 24-h cerulein (CER) injury. Scale bar 20 μ m.
- E ChIP-PCR on mouse stomach tissue at vehicle and 6-hour HDT. Chromatin probed with ATF3, Histone H3 antibodies, or a Rabbit IgG control. Also included is the 2% chromatin input and water to control for DNA contamination. *Rab7b* amplicon is from a conserved, putative ATF3-binding site in the first intron. Amplicon from *Atf3* is a positive control from a previously characterized ATF3-binding site; negative control is from a site in *Rab9a* lacking putative ATF3-binding motifs.

function during paligenosis impairs regeneration (Willet *et al*, 2018). We reasoned the aberrant induction of autodegradation in the absence of ATF3 would affect the fraction of cells able to progress to Stage 2 (expressing metaplastic/progenitor genes) and Stage 3 (entering the cell cycle). Stage 2 is easily measured by induction of the epitope for the lectin GSII in ZCs, with the resultant cells (known as SPEM cells) co-labeling with GSII and ZC markers (like PGC or GIF). *Atf3*^{-/-} mice showed profound loss of progression to Stage 2, with only rare SPEM cells (Figs 5A and EV4A–C). Stage 2 failure was corroborated by a second SPEM marker CD44v (Fig EV4A; Khurana *et al*, 2013; Engevik *et al*, 2016; Meyer *et al*, 2019). Moreover, the failure to produce Stage 2 SPEM cells correlated with reduced proliferation (Figs 5B and C, and EV4D). Note that progenitors higher up in the gastric unit (in the isthmus and neck) are induced to proliferate via a non-paligenotic mechanism (Willet *et al*, 2018; Choi *et al*, 2019; Miao *et al*, 2020a; Miao *et al*, 2020b). As expected, those non-paligenotic cells were still induced to proliferate after injury, so overall proliferation in the injured stomach was less affected by loss of ATF3 than paligenotic proliferation specifically (Fig EV4D; cf: Fig 5B vs. Fig 5C showing basal, paligenotic proliferation).

We noticed that the lack of paligenotic progression to stages 2 and 3 did not indicate mature cells were delayed in the paligenotic process, as many of the bases of gastric units, where ZCs or paligenotic cells should be, were simply missing. This pattern was consistent with dropout of whole gastric unit bases, a phenomenon we have previously described when there is a failure to progress through paligenosis (Willet *et al*, 2018; Miao *et al*, 2020b). Inability to complete paligenosis resulted in marked base dropout with approximately 1/3 of gastric unit bases missing (Fig 5D). As might be expected, the increased base dropout in *Atf3*^{-/-} correlated with significantly increased cleaved-CASP3 positivity, indicating cell death by apoptosis (Fig EV4E and F). In the pancreas, ATF3 was also required for paligenosis progression, as *Atf3*^{-/-} ACs had significantly higher cleaved-CASP3 expression (Fig 5E and F) as well as decreased Stage 3 proliferation induction (Fig 5G and H).

Overall, the results indicate that the failure to upregulate autodegradation in Stage 1, in the absence of *Atf3*, led to the failure to progress through Stage 2 of paligenosis and finally resulted in increased cell death in Stage 3, in both stomach and pancreas.

ATF3 is critical for injury responses across organs

Our studies thus far showed that ATF3 could regulate autodegradative activity in a conserved way across tissue and species by

regulating RAB7. In addition, loss of ATF3 caused the same Stage 1 failure with associated overall paligenosis failure in two different organs, suggesting that early ATF3 induction might be a conserved feature of paligenosis. HDT injury-producing SPEM in mice is a model of the SPEM that occurs in chronic atrophic gastritis in humans (Petersen *et al*, 2017). Using human stomach samples of tissue adjacent to gastric tumor tissue, we have previously extensively characterized (Lennerz *et al*, 2010; Radyk *et al*, 2018; Willet *et al*, 2018), we observed expression of ATF3 in SPEM. However, as might be expected, given ATF3 expression was early and transient following injury in mice, and most SPEM is chronic and mitotically quiescent in humans (Willet *et al*, 2018; Burclaff *et al*, 2020) scattered, potentially transitional SPEM cells were ATF3-positive (Fig 6). Morphologically normal human gastric epithelial cells lacked ATF3 expression (Fig 6).

As ATF3 is highly conserved, we took advantage of a previously published Axolotl single-cell RNA-sequencing analysis of limb regeneration (Gerber *et al*, 2018; Data ref: Gerber *et al*, 2018) that shows high correlation with gene expression in mouse paligenosis (Miao *et al*, 2020b). We found that, like the previously identified paligenosis gene IFRD1, ATF3 is induced during limb regeneration. RAB7B is induced at the next time point after ATF3 (Fig EV5A), as represented by the fraction of cells that express these genes throughout the course of repair after limb amputation. We previously showed that regenerative proliferation in kidney and liver occurs by paligenosis (Willet *et al*, 2018), and activation of muscle satellite cells following injury (Yue *et al*, 2020) also appears to involve a paligenosis-like process involving emergence from quiescence. We assayed genes whose expression was increased after paligenotic injury in all 5 organs: stomach, pancreas, liver, kidney, and muscle to determine potential core paligenosis genes (Fig EV5B). We found only 7 genes were upregulated in all 5 datasets: *Atf3*, *Cebpb*, *Hmox1*, *Ier3*, *Ifrd1* (Fahling *et al*, 2013; Data ref: Fahling *et al*, 2013; Kowalik *et al*, 2007; Data ref: Kowalik *et al*, 2007; Moore *et al*, 2015; Data ref: Moore *et al*, 2015; Otu *et al*, 2007; Data ref: Otu *et al*, 2007; Yue *et al*, 2020; Data ref: Yue *et al*, 2020), *Junb*, and *Zfp36*. Thus, the results indicate *Atf3* may play a conserved role in mediating paligenosis across multiple tissues and species.

Discussion

Our work here shows that ATF3, induced early in Stage 1 of paligenosis, is required for initiation of the autodegradative machinery. Though there are likely additional targets critical for ATF3

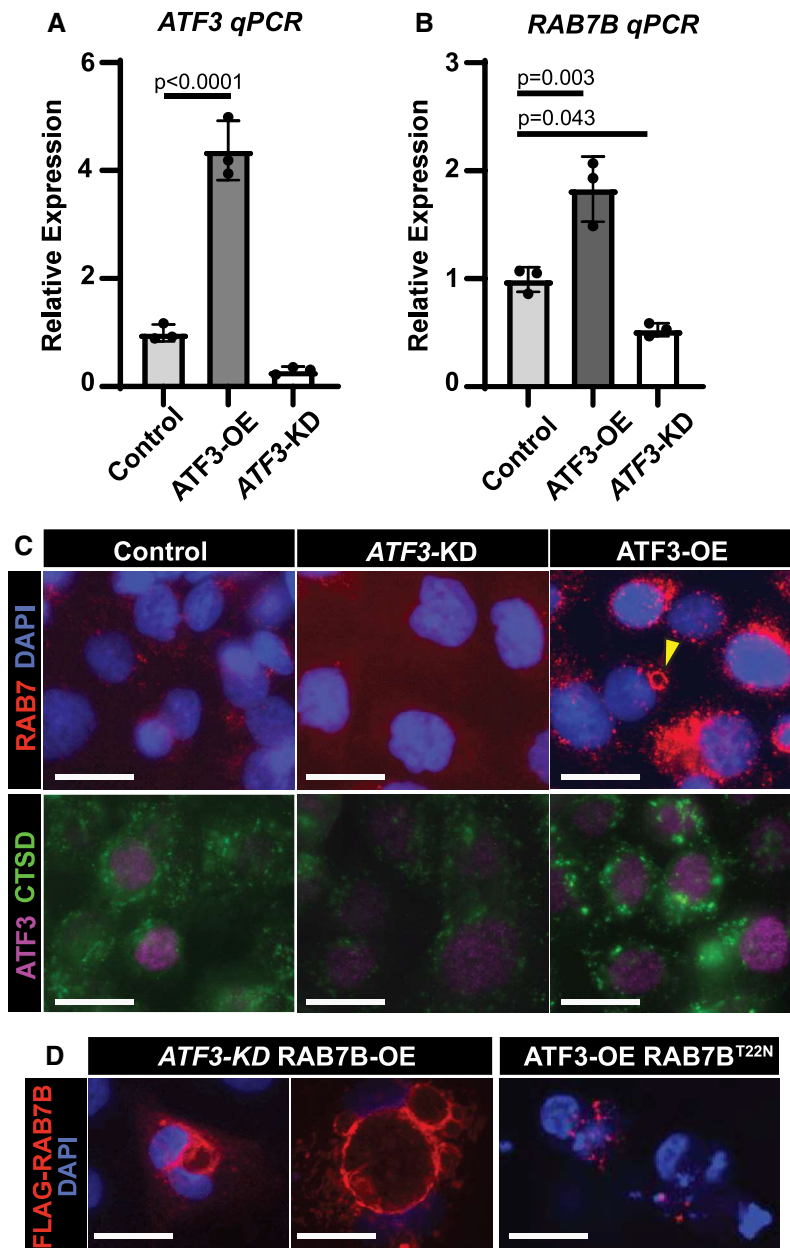


Figure 3. ATF3 transcriptionally upregulates RAB7B in vitro to govern formation of autodegradative vesicles.

- A mRNA expression of *ATF3* by qRT-PCR in control, *ATF3* knockdown (KD), and *ATF3* overexpression (OE) AGS cell lines generated using a PiggybacTM transposon system. Significance by one-way ANOVA, Dunnett post-hoc. Data point = mean of technical triplicates in a single mouse. $n = 3$ mice. Error bars denote standard deviation.
- B mRNA expression of *RAB7B* by qRT-PCR in AGS cell lines from 3A. Statistics and plotting as for panel A.
- C *Top*—Immunofluorescence for RAB7 (red) and DAPI (blue, nuclei) in control, *ATF3* knockdown (KD), and *ATF3* overexpression (OE) AGS cells. Arrowhead indicates aggregated RAB7 vesicular formation similar to those observed in tissue. *Bottom*—Immunofluorescence for *ATF3* (purple) and cathepsin D (CTSD, green, lysosomes) in AGS cells. Scale bar, 20 μ m.
- D *Left*—Immunofluorescence for anti-FLAG (RAB7B) (red) and DAPI (blue, nuclei) in *ATF3* knockdown; RAB7B overexpression (*ATF3*-KD RAB7B-OE) AGS cells show large vesicular structures. *Right*—Immunofluorescence for anti-FLAG (RAB7B) (red) and DAPI (blue, nuclei) in *ATF3* overexpression; RAB7B GTPase mutant (*ATF3*-OE RAB7B^{T22N}) AGS cells fail to make vesicles. Scale bar, 20 μ m.

actions in paligenosis, we show both in mouse paligenosis models and in human epithelial cells that *ATF3* binds and activates *Rab7b*, which encodes a protein critical in turn for trafficking autophagic vesicles and lysosomes. *ATF3* is necessary for RAB7 induction and for induction of a large complement of autophagolysosomes. *ATF3*

induction after paligenotic injury is conserved across tissues and species with *ATF3* increased even in human metaplasia.

The concept of an evolutionarily conserved program, paligenosis, which mechanizes cell plasticity for mature cells, like pancreatic or gastric exocrine cells, is recent. Paligenosis, as originally defined, is

Figure 4. *Atf3* coordinates cellular autodegradation after injury in paligenosis stage I.

- A Representative immunofluorescence images of pancreatic acinar cells after vehicle or 24-h cerulein (CER) treatment stained for RAB7 (red) and cathepsin D (CTSD, green, lysosomes). Top row is wild-type, bottom row is *Atf3*^{-/-}. Yellow arrowhead highlights RAB7 and CTSD co-expression. White arrowhead points to an area of RAB7 expression only. Scale bar, 20 μ m.
- B Representative immunofluorescence images of gastric chief cells after vehicle or 24-h high-dose tamoxifen (HDT) treatment stained for RAB7 (red) and cathepsin D (CTSD, green, lysosomes). Top row is wild-type, bottom row is *Atf3*^{-/-}. Yellow arrowhead highlights RAB7 and CTSD co-expression. White arrowhead points to an area of RAB7 expression only. Scale bars 20 μ m. Stomach unit base outlined by dashed white line.
- C Representative immunofluorescence images of gastric chief cells after vehicle or 24-h HDT treatment stained for pepsinogen C (PGC, red, granules) and MAP1LC3B (green, autophagy marker). Top row is wild-type, bottom row is *Atf3*^{-/-}. Stomach unit base outlined by dashed white line.
- D Transmission electron micrograph images of zymogenic chief cells (ZCs) after 24-h vehicle or HDT treatment in WT (top) and *Atf3*^{-/-} mice (bottom). Scale bar, 1 μ m. Arrowheads indicate cell components being degraded.
- E Quantification of degradation events per cell counted from EM images of ZCs after 24-h HDT treatment in WT and *Atf3*^{-/-} mice as shown in panel 3D. Each data point = total granules in a cell in a single TEM section with cells from 2 separate mice plotted together (data point colors indicate cells from a single mouse). Red line indicates mean across all the mice.

a stepwise program that retools cell architecture to convert a mature cell to a regenerative, progenitor-like phenotype. The three paligenosis stages (1. autodegradation, 2. increased progenitor/metaplastic expression, and 3. cell cycle re-entry) can be genetically and morphologically defined, and progression from stage to stage can be blocked by inhibitors or deletion of key genes (Fig 7). The stepwise, conserved nature of the program allows us to determine whether there are dedicated, paligenosis genes and genetic machinery, independent of tissue and conserved across evolutionary phyla, as is the case with other cellular programs like apoptosis. We recently identified *Ifrd1* and *Ddit4* as paligenosis-governing genes and proposed that paligenosis genes in general would be: (i) largely dispensable for normal development or proliferative activity; (ii) activated primarily during regeneration-inducing injury; and (iii) highly evolutionarily conserved. We argue here that ATF3 is a similar such gene required for paligenosis. It is upregulated early in paligenosis in multiple tissues, is known to be induced by injury, and is conserved from sea anemones to humans, and, in general, organisms null for ATF3 have phenotypes only after injury. Furthermore, we show evidence here that ATF3 is expressed during transition to metaplasia in humans, which is representative of a much larger cohort (> 500) that we are currently analyzing for expression of paligenosis genes. We observe 11% of human metaplastic lesions have focal ATF3 in non-proliferative foci, consistent with ATF3 being upstream of the decision for cells to proliferation.

We describe a model (Fig 7) in which ATF3 is induced early after injury to help transcriptionally upregulate *Rab7b* and other genes important for autophagy and lysosomal accumulation during paligenosis Stage 1. During this time ATF3 also likely transcriptionally represses genes involved in cell differentiation/maturation like *MIST1*, a relationship that has been shown before in pancreas (Fazio et al, 2017). Shortly after Stage 1, ATF3 decreases, and the cell progresses through the remainder of paligenosis. Without *Atf3*, the defects in Stage 1 (autodegradation) obstruct the cell's ability to become regenerative, metaplastic cells. A greater proportion of cells die and tissue repair is compromised. In addition, we describe a new signaling axis for injury-induced cell plasticity by ATF3 transcriptional regulation of *Rab7b* during paligenosis.

Atf3 joins aforementioned *Ddit4* and *Ifrd1* as paligenosis-governing genes (Miao et al, 2020b). At the tissue level, loss of *Atf3* appears most similar to loss of *Ifrd1* as lack of either gene leads to increased cell death in paligenosis Stage 3. While IFRD1 functions to suppress p53-mediated repression of mTORC1, allowing proliferation in Stage 3, ATF3 instead activates autodegradation pathways for proper clearance of differentiated/specialized cell features. Though both ATF3 and IFRD1 have different mechanisms to govern paligenosis, it is clear that failure to clear paligenosis checkpoints, either by inability to upregulate autodegradation (*Atf3*^{-/-}) or by inability to re-activate mTORC1 (*Ifrd1*^{-/-}), leads to decreased tissue recovery after injury. ATF3 and DDIT4 both function in Stage 1 to

Figure 5. *Atf3* loss increases cell death and reduces proliferation after paligenotic injury.

- A Representative immunofluorescence images of gastric units after vehicle or 72-h high-dose tamoxifen (HDT) treatment stained for GIF (red, granules), GSII (green, neck cells and SPEM marker), BRDU (white, proliferation), and DAPI (blue, nuclei). Top row is wild-type, bottom row is *Atf3*^{-/-}. Yellow arrowheads point to areas of base dropout where ZCs have been lost. Scale bar, 50 μ m. Stomach units outlined by dashed white line.
- B Proliferation as quantified by number of BrdU⁺ cells per unit in WT and *Atf3*^{-/-} vehicle \pm HDT. Each data point = mean of counts from 40 to 50 gastric glands from an individual mouse, *n* = 3–4 mice per treatment group. Significance by unpaired two-tailed *t*-test. Error bars denote standard deviation.
- C Plot and statistical analysis as for Panel B but quantifying BrdU⁺ cells only in the bottom 1/3 of the unit, which are derived mostly from paligenosis and not from isthmal and neck stem and progenitor cells.
- D Death of ZCs after injury plotted by quantifying the base dropout rate, which is the fraction of glands that do not reach the muscularis mucosa from the lumen. Each data point is the mean of 80–100 glands from an individual mouse, *n* = 4 mice per treatment group. Significance by unpaired two-tailed *t*-test. Error bars denote standard deviation.
- E Representative immunohistochemistry of cleaved-caspase 3 in pancreatic acinar cells marking apoptosis in vehicle or 24-h cerulein (CER) treatment. Top row is WT, and bottom row is *Atf3*^{-/-}. Scale bar, 50 μ m.
- F Apoptosis quantified following 24-h CER injury by the number of cleaved-caspase 3⁺ cells from a 40 \times field. Each data point is mean of positive cells in 4–5 40 \times fields in an individual mouse, *n* = 3 mice per treatment group. Significance by unpaired two-tailed *t*-test. Error bars denote standard deviation.
- G Representative immunohistochemistry of BrdU in pancreatic acinar cells marking proliferation in vehicle or 7 days of repeated cerulein injury. Top row is WT, and bottom row is *Atf3*^{-/-}. Scale bar, 50 μ m.
- H Quantification of proliferation at peak ADM as counted by the number of BrdU⁺ cells from a 20 \times field following 7 days of cerulein treatment. Plotting and statistical analysis as per panel F.

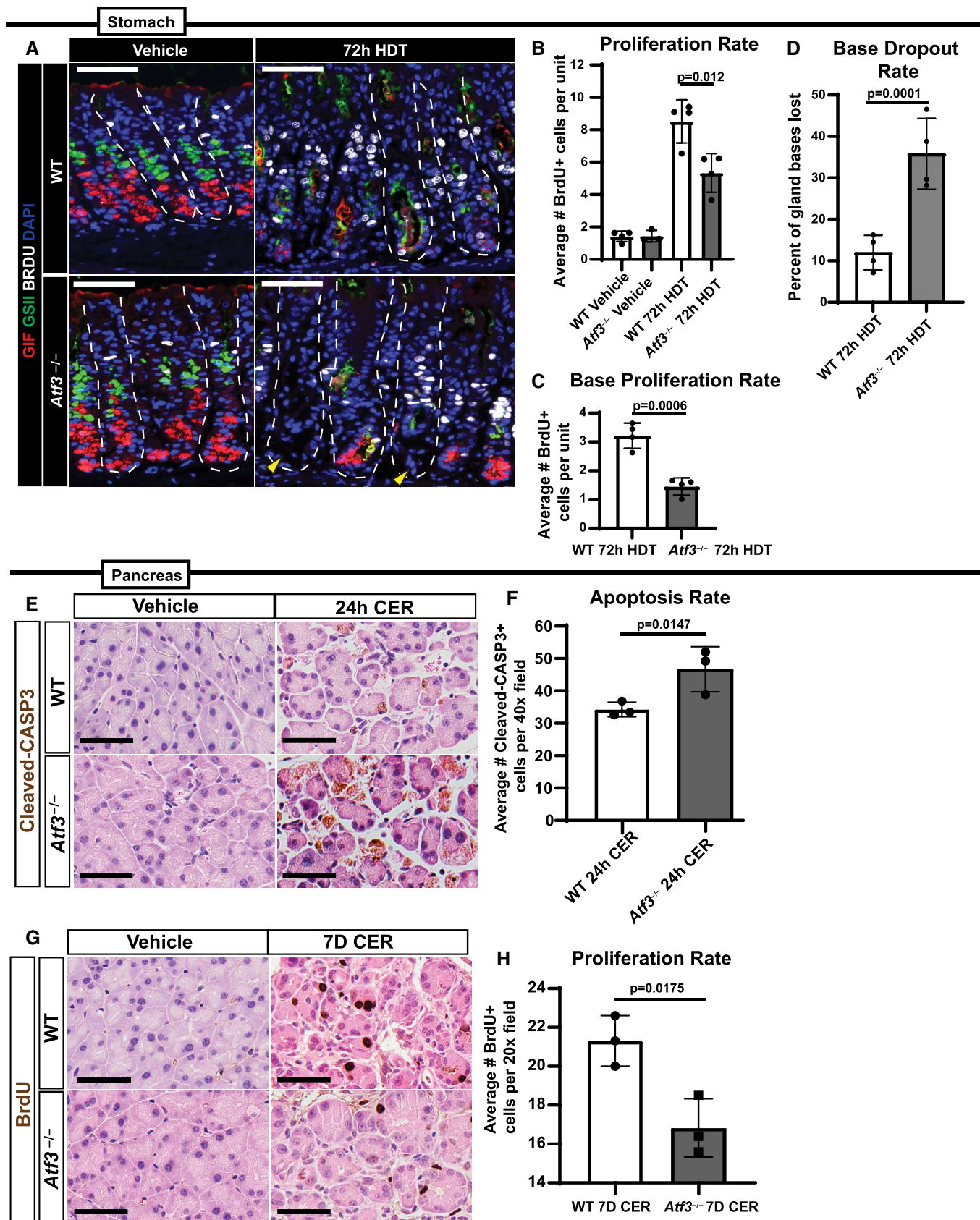


Figure 5.

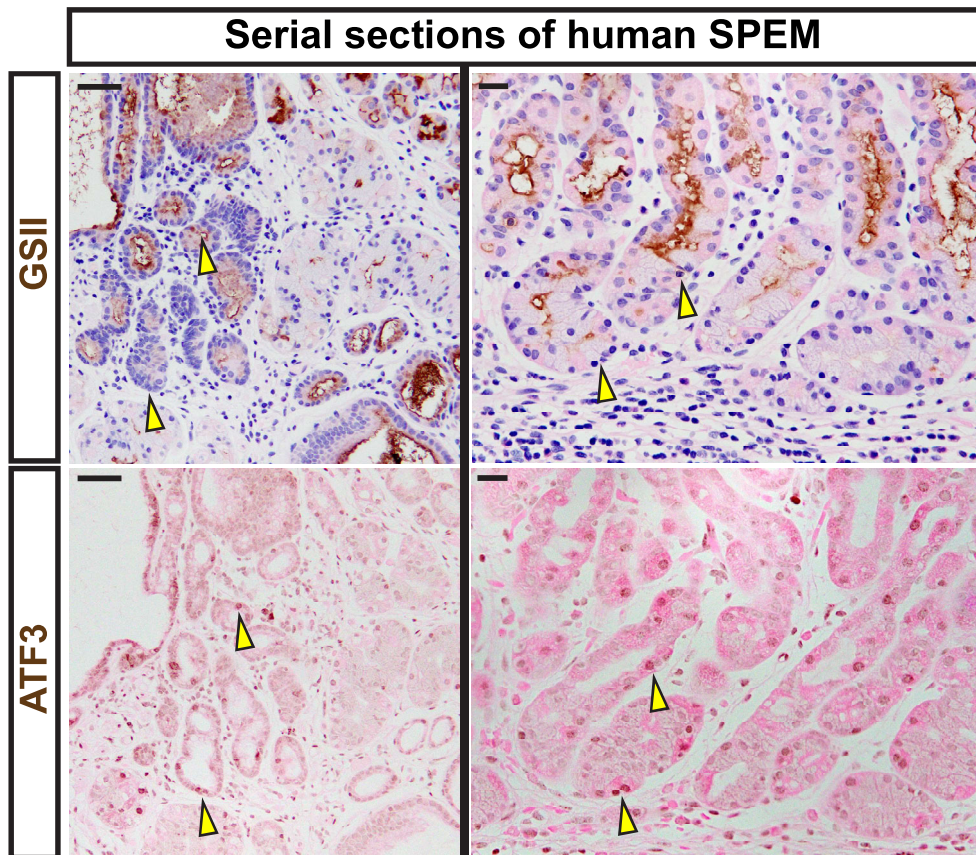


Figure 6. ATF3 is expressed in human SPEM.

Serial sections of human tissue. Representative immunohistochemistry of GSII (top; spasmolytic polypeptide-expressing metaplasia [SPEM] marker and neck cells) counterstained with hematoxylin (blue) and eosin (pink). Representative staining of ATF3 (bottom) counterstained with eosin (pink). Tissue was taken from regions adjacent to gastric adenocarcinoma. Scale bars *left*—50 μm and *right*—20 μm . Arrowheads indicate strongly expressing ATF3 cells and the corresponding region in the same gland labeled with GSII in a serial tissue section. GSII at the base of gastric glands in the body of the stomach indicate transition to SPEM.

control autodegradation. Unlike *Atf3*, however, *Ddit4*^{-/-} mice have increased proliferation. DDIT4 functions during initial stages to deactivate mTORC1; hence, *Ddit4*^{-/-} mice express constitutively high mTORC1 throughout paligenosis, which overrides a checkpoint (Miao *et al*, 2020b). Additionally, loss of *Ddit4* and induction of metaplasia increases tumorigenesis in an N-methyl-N-nitrosourea spontaneous gastric cancer model (Miao *et al*, 2021).

Activating transcription factor 3 is a member of the ATF/CREB family of transcription factors and shares similar binding sites with AP-1 (also from the ATF/CREB and c-Fos/c-Jun families), which regulates immediate early genes following stress/injury. *Atf3* has been implicated in injury settings in many organs including cerebral ischemia (Wang *et al*, 2012), axon regeneration (Hunt *et al*, 2012; Gey *et al*, 2016), acute lung injury (Zhao *et al*, 2017), heart failure (Brooks *et al*, 2015), alcohol liver damage (Tsai *et al*, 2015), liver ischemia-reperfusion injury (Zhu *et al*, 2018), stress-induced β -cell apoptosis (Hartman *et al*, 2004), ADM (Fazio *et al*, 2017; Azizi *et al*, 2021), and acute kidney injury (Li *et al*, 2010). ATF3 is also important for injury responses in *Drosophila* (Zhou *et al*, 2017) and *Axolotl* (Gerber *et al*, 2018). In all those cases, *Atf3* loss exacerbates the injury phenotype but is dispensable for homeostasis and embryonic development, just as we observed here in stomach and

pancreas injury. A recent publication similarly showed that *Atf3* loss leads to decreased ADM and that absence of *Atf3* in a spontaneous cancer mouse model actually prevented KRAS^{G12D}-driven pancreatic cancer (Azizi *et al*, 2021). That may be consistent with our results here, as mutant KRAS-driven cancer depends on ADM, which depends on ATF3 and paligenosis. Cells lacking ATF3 may die rather than transform. Thus, the role of ATF3 in cancer is complex and under active study.

It has not been previously reported that injury-responsive ATF3 accumulation induces autophagy and lysosomal activity, but ATF3 has been reported to interact with individual autophagy pathway members. For example, ATF3 regulates *Beclin-1* (Lin *et al*, 2014) and *Atg5* (Sood *et al*, 2017). There may also exist an autophagy-ATF3 feedback loop because defective autophagy (*Atg4b* loss) impairs ATF3 activity in a mouse lung injury model (Aguirre *et al*, 2014).

To our knowledge, there are no previous reports of ATF transcription factors transcriptionally regulating any Rabs, though potential ATF binding sites have been described to be present in the 5'-flanking region of *Rab7* (Bhattacharya *et al*, 2006). In fact, in general, transcriptional regulation of RABs or regulation of RAB function via titrating protein abundance is usually not studied, with some few exceptions such as MIST1 scaling RABs, and a report of c-

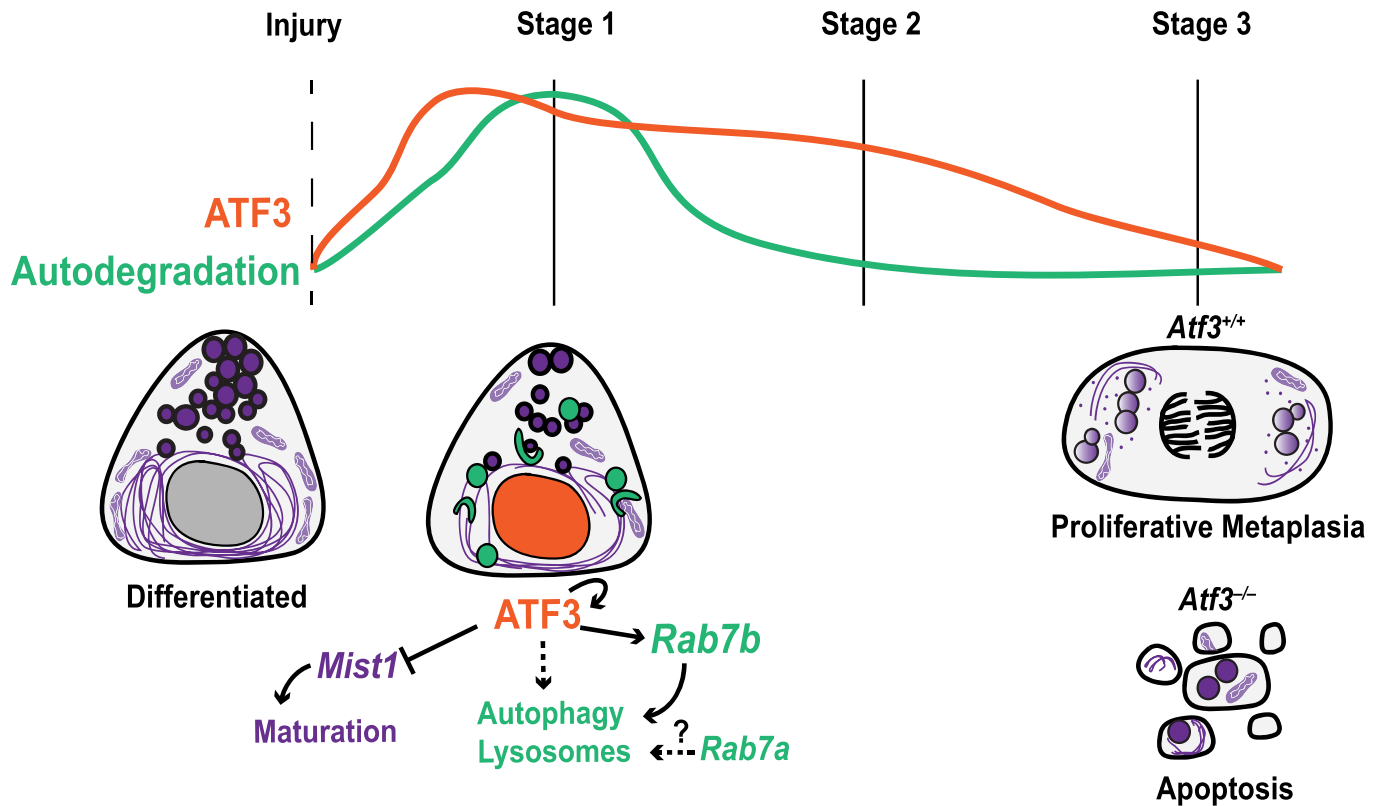


Figure 7. Model of ATF3 function in paligenesis.

ATF3 peaks early after injury and helps to coordinate the induction of autodegradation by transcriptionally activating *Rab7b* and other targets to increase the number of lysosomes and induce autophagy. ATF3 also functions at this same time (Stage 1) to repress scaling and maturation factor *Mist1*.

Myc helping drive melanoma by activating *Rab7* (Alonso-Curbelo *et al*, 2014). However, an ATF-related protein, AP-1, regulates *Rab11a* in B cells in mice (Lizundia *et al*, 2007), suggesting that ATF/CREB transcription factors may have an underappreciated and understudied role in transcriptionally regulating RABs.

RAB7A and RAB7B are regulators of endosomal trafficking and maturation. RAB7 proteins are largely localized to late endosomes and lysosomes to aid in the autophagosome–lysosome fusion and mitochondrion–lysosome contacts (Stroupe, 2018), events undoubtedly important during Stage 1 of paligenesis. As such, complete *Rab7* loss in pancreatic acinar cells impairs autophagic and endocytic pathways in mouse models of pancreatitis (Takahashi *et al*, 2017). Here, we show that *Atf3* loss impairs autophagic and lysosomal pathways, further supporting the notion of ATF3 function through *Rab7b* during paligenesis and injury. There are few studies specifically focused on RAB7B, identified because of its size and sequence similarity to RAB7A. RAB7B has similar functions as RAB7A and was, accordingly, first observed to be associated with lysosomes in monocytes (Yang *et al*, 2004). More recently, RAB7B has been shown to interact with ATG4B on vesicles and negatively regulate autophagy (Kjos *et al*, 2017), indicating it also, like RAB7A, regulates autophagic trafficking. There may not be complete concordance between the two RAB7 proteins, however, as RAB7B may have an added function in some circumstances of aiding retrograde transport from late endosomes or lysosomes to the Golgi (Progida *et al*, 2010).

Using AGS cells, we demonstrated that expression of RAB7B was sufficient to form the large vesicular compartments observed following injury in murine tissue. This effect was independent of ATF3 expression, as vesicles were readily observed with ATF3 knockdown and RAB7B overexpression. In addition, vesicle formation was dependent on RAB7B's GTPase activity, as no vesicles were observed with the RAB7B^{T22N} mutant, even with overexpression of ATF3.

Recent studies have shown the importance of degradation and autophagy in regulating cell plasticity in several organs (Saera-Vila *et al*, 2016; Call & Nichenko, 2020; Li *et al*, 2020; Romermann *et al*, 2020). We speculate that Stage 1 of paligenesis is not only required to change the cell structure to one that is more physiologically progenitor-like but also to generate enough energy for DNA replication and cell division. Ribosomes are an enormous pool for nucleotides, which may be one reason we see so much degradation machinery accumulate in the rER portion of the cell, where there may be release of nucleotides from ribosomes. As mentioned above, functional degradation machinery may also act as a checkpoint indicating a cell is healthy enough to commit to cell cycle re-entry. This was the case when we administered hydroxychloroquine to inhibit lysosome–autophagosome fusion (Fig EV1C–F) and when we blocked lysosome activity during paligenesis (Willet *et al*, 2018) which, like *Atf3* and *Irf1* loss, also ultimately led to increased cell death.

Activating transcription factor 3 may transcriptionally regulate other targets during Stage 1 that do not control degradation. ATF3

can repress *Mist1*, the secretory cell scaling factor expressed only in mature ZCs and ACs; *Mist1* downregulation is a key early step in ZC and AC paligenesis (Kowalik *et al*, 2007; Nozaki *et al*, 2008; Lennerz *et al*, 2010; Karki *et al*, 2015; Meyer *et al*, 2019). It also represses *Sox9* (Fazio *et al*, 2017), a metaplastic gene whose induction defines transition from Stage 1 to Stage 2, supporting the hypothesis that ATF3 plays several roles in Stage 1 of paligenesis. It is not clear how ATF3 is upregulated for paligenesis and metaplasia initiation, but once accumulated, ATF3 acts in a positive feedback loop to regulate itself. Reactive oxygen species are also induced *en route* to SPEM and may contribute to autodegradation and antioxidant pathway activation, as shown by the induction of antioxidant gene xCT, a cysteine/glutamate transporter in SPEM (Meyer *et al*, 2019). Likewise, reactive oxygen species are important for ADM induction and progression to pancreatic adenocarcinoma (Liou *et al*, 2016; Cheung *et al*, 2020).

The current study stimulates several important questions. First, how does metabolism affect the cell fate transitions in paligenesis? We saw dramatic structural changes in mitochondria during paligenesis, which likely reflect changes in metabolism. The metabolic profile of cells as they transition from their normal state to a metaplastic state is not well characterized, though a recent study

demonstrated disrupted acinar cell cholesterol metabolism underlies pancreatitis in mouse models (Mareninova *et al*, 2021). We showed a dependency on dynamic mTORC1 activity during metaplasia (Willet *et al*, 2018) and recent studies show acetyl-CoA metabolism contributes to cell plasticity in the pancreas and potentially tumorigenesis via epigenetic regulation (Carrer *et al*, 2019). Epigenetics also plays a role in SPEM initiation, most recently shown by miR148a repression of DNA-methylating gene DNMT1, a pro-metaplasia gene (Shimizu *et al*, 2020). Second, which cells are poised to undergo paligenesis and become metaplastic? Not all mature cells in a tissue may have the ability to re-enter the cell cycle after injury, but organs experiencing chronic damage (like GI organs) harbor cells that act as facultative progenitors if the injury is severe enough, though the age of cells in the GI system is a factor for their ability to contribute to plasticity (Engevik *et al*, 2016; Weis *et al*, 2017) and some cell types like acid-secreting parietal cells seem unable to return to the cell cycle. Further study of general, conserved genes that govern paligenesis in diverse contexts should help us have a better understanding of regeneration, tumorigenesis, and also potentially how plasticity arose as a way for multicellular organisms to use cells for both specialized, differentiated function and as progenitors after damage.

Materials and Methods

Reagents and Tools table

Reagent/Resource	Reference or Source	Identifier or Catalog number
Experimental Models		
C57BL/6j (<i>M. musculus</i>)	Jackson Lab	Stock No: 000664
<i>Atf3</i> ^{-/-} (<i>M. musculus</i>)	Hartman <i>et al</i> (2004)	
AGS cells (<i>H. sapiens</i>)	ATCC	CLR-1739
XL-10 Gold Ultracompetent Cells	Agilent	Cat #200317
Human patient samples	Lennerz <i>et al</i> (2010), Capoccia <i>et al</i> (2013), Khurana <i>et al</i> , (2013), Radyk <i>et al</i> (2018)	
Recombinant DNA		
<i>ATF3</i> (human)	Sequence cloned out of Addgene #26115 and inserted into a homemade PiggyBac Transposon vector for overexpression (vector also used in ref. Miao <i>et al</i> (2020)	Cat #26115
<i>RAB7B</i> (human)	Origene This sequence template was also used to generate the RAB7B ^{T22N} mutant by amplifying a truncated C-terminal domain and a three-part ligation using oligos encoding the mutant N-terminal domain.	Cat #RC202283

Methods and Protocols

Animal studies and reagents

All experiments involving animals were performed according to protocols approved by the Washington University School of Medicine Animal Studies Committee. Mice were maintained in a specified pathogen-free barrier facility under a 12-h light cycle. All mice used in experiments were 6–8 weeks old. Male and female mice were used for each experiment, and we did not note any differences due to sex. Statistical justification for animal

numbers is based on our previous experience, consultation with biostatisticians, and using the sampling power analysis approach. Animals were randomized when allocating into each treatment groups. Experimental cohorts were randomly designated at birth for specific animals to minimize bias. Wild-type C57BL/6 mice were purchased from Jackson Laboratories (Bar Harbor, ME). *Atf3*^{-/-} mice were bred onto a C57BL/6 background and received from Dr. Tsonwin Hai at the Ohio State University Medical Center. *Atf3*^{-/-} mice were first described in Ref. Hartman *et al* (2004).

Tamoxifen (250 mg/kg body weight; Toronto Research Chemicals, Inc, Toronto, Canada) was administered by intraperitoneal (IP) injection to induce SPEM in the stomach (see Fig EV1 for timeline; Saenz *et al*, 2016). Tamoxifen was prepared in a 10% ethanol and 90% sunflower oil solution by sonication (Sigma, St Louis, MO).

Pancreatitis was induced by 6 hourly IP injections of 50 µg/kg (in 0.9% saline) cerulein (Sigma-Aldrich) given every other day for up to 7 days (see Fig EV1 for timeline). Mice were sacrificed 24-h after the final cerulein injection.

Hydroxychloroquine sulfate (Acros Organics) was dissolved in PBS and administered by intraperitoneal injection at a dose of 60 mg/kg/day (Rosenfeldt *et al*, 2013). See Fig EV1C for injection timeline.

All mice were given an intraperitoneal injection containing BrdU (120 mg/kg) and 5-fluoro-2'-deoxyuridine (12 mg/kg) 90 min before sacrifice to capture cells in S phase at the experimental endpoint.

Immunofluorescence and immunohistochemistry

Mouse tissues were excised, flushed with phosphate-buffered saline (PBS), and then inflated with freshly prepared 4% paraformaldehyde. The stomach was clamped and suspended in fixative in a 50-ml conical overnight, followed by rinses in PBS and 70% ethanol, arrangement in 3% agar in a tissue cassette, and paraffin processing. Sections (5 µm) were cut, deparaffinized, and rehydrated with graded Histo-Clear (National Diagnostics), ethanol, and water, then antigen-retrieved in sodium citrate buffer (2.94 g sodium citrate, 500 µl Tween 20, pH 6.0) using a pressure cooker. Slides were blocked in 5% normal serum, 0.2% Triton X-100, in PBS. Slides were incubated overnight at 4°C in primary antibodies (see Reagent Table), then rinsed in PBS, incubated 1 h at room temperature in secondary antibodies, and/or fluorescently labeled lectin rinsed in PBS, mounted in ProLong Gold Antifade Mountant with 4'-diamidino-2-phenylindole (DAPI) (Molecular Probes).

For immunohistochemistry, steps were identical except the following. An extra quenching step was performed for 15 min in a methanol solution containing 1.5% H₂O₂ before antigen retrieval. Substrate reaction and detection was performed using ImmPACT VIP Peroxidase (horseradish peroxidase) Substrate Kit (Vector Laboratories, Burlingame, CA) as detailed per the manufacturer's protocol, and sections were developed with DAB for desired time and counterstained with hematoxylin and/or eosin. Slides were mounted in Permount Mounting Medium.

Western blot

Approximately 75 mg mouse corpus stomach or pancreas tissue were sonicated in RIPA buffer with 1× protease inhibitor cocktail (Thermo). Protein was separated using NuPAGE 10% Bis-Tris gels and transferred to an Invitrogen nitrocellulose membrane. Membranes were then blocked with 3% bovine serum albumin (BSA) and incubated overnight at 4°C with primary antibodies (see Reagent Table for antibodies). The membranes were rinsed in Tris-buffered saline (TBS) pH 8.0, incubated 1 hour at room temperature in secondary antibody in 5% low-fat milk. Actin antibody was used as a control to ensure equal loading of protein in each gel lane. Secondary antibody signals were imaged and detected by SuperSignal West Pico PLUS Chemiluminescent Substrate Kit.

Imaging and quantifications

Fluorescence microscopy was performed using a Zeiss Axiovert 200 microscope with an Axiocam MRM camera and Apotome II instrument for grid-based optical sectioning. Post-imaging adjustments, including contrast, fluorescent channel overlay, and pseudocoloring, were performed with AxioVision and Adobe Photoshop CS6. Histology of stomach and immunohistochemistry were imaged using an Olympus BX51 light microscope and Olympus SZX12 dissecting microscope w/12 MPixel Olympus DP70 camera. Images were analyzed, and post-imaging adjustments were performed with Adobe Photoshop CS6.

Quantification of BrdU proliferation rates was done by counting 5 or more 20× fields from a whole-slide scanned images from the Hamamatsu NanoZoomer 2.0-HT system.

FIB-SEM 3D Nanotomography

FIB-SEM 3D nanotomography was performed as described in ref. Lo *et al* (2017). Mouse gastric tissues were bisected into fixative containing 2.5% glutaraldehyde and 2% paraformaldehyde in 0.15 M cacodylate buffer containing 2 mM CaCl₂ (pH 7.4), fixed for 15 min at 37°C and then overnight at 4°C, sliced into ~1.5-mm-thick pieces, rinsed in cacodylate buffer for 10 min at room temperature, and subjected to secondary fixation in 1% osmium tetroxide/0.3% potassium ferrocyanide in cacodylate buffer for 1 h on ice. The samples were then washed in ultrapure water and stained *en bloc* in 2% aqueous uranyl acetate for 1 h. After staining, samples were briefly washed in ultrapure water, dehydrated in a graded acetone series, and infiltrated with microwave assistance (Pelco BioWave Pro) into LX112 resin, which was cured in an oven for 48 h at 60°C. Cured blocks were trimmed and mounted onto SEM pins with silver epoxy and faced with a diamond knife. Toluidine blue-stained sections (300 nm thick) were used to locate a region of interest. Blocks were sputter-coated with 10 nm of iridium (Leica, ACE 600) with rotation on a planetary stage to ensure saturation. Regions of interest on a FIB-SEM (Zeiss, Crossbeam 540) were located by secondary electron imaging at 10 KeV. Once a region was found, the sample was prepared using the ATLAS (Fibics) 3D nanotomography engine. In short, a platinum pad was deposited on a 40-µm × 40-µm region of interest with the FIB set to 30 KeV and 1.5 nA. Three vertical lines for focus and stigmation and two angled lines for z-tracking were milled into the platinum pad at 50 pA, and a protective pad of carbon was deposited on top of the milled platinum at 1.5 nA. Following this, a rough trench 50 µm wide and 55 µm deep was milled at 30 nA and polished at 7 nA. Once polishing of the block face was complete, face detection, focusing, and z-tracking were all performed on the fiducial marks that were milled into the platinum pad. Imaging was performed at 2 KeV and 1.1 nA using the EsB (energy selective backscatter) detector with a grid voltage of 1100 V. The block was milled at a current of 700 pA with 20 nm slices, and 2,000 × 1,750 pixel images were acquired at a resolution of 20 nm/pixel with a dwell of 8 or 10 µs and a line average of 3 for a total z-depth of 35 µm.

3D reconstruction

3D reconstruction was performed as described in ref. Lo *et al* (2017). All EM serial images were imported into the Amira 6 3D software package for 3D reconstruction. Areas of interest were manually segmented into data objects with intervening unsegmented slices

("X") based on object volume. For organelles with suboptimal contrast, the thresholding function was used for manual segmentation. The interpolation function was used to highlight areas of interest between manually segmented slices. 3D models were generated from labeled objects. The "Smooth" and "Simplify" functions were used for model generation, and pseudocoloring was used to enhance visualization for each organelle. Animations were created with the Animation Director in the software.

Electron microscopy

For TEM, stomachs were fixed, sectioned, stained, and imaged as previously described (Willet *et al*, 2018). Briefly, tissue was collected as described above, fixed overnight at 4°C in modified Karnovsky's fixative, and sectioned. Tissue was processed by the Washington University in St. Louis Department of Pathology and Immunology Electron Microscopy Facility.

Human cancer cell culture

AGS cells (ATCC) were grown under standard conditions (Advanced DMEM/F12, 10% FBS, Nonessential amino acids, and Pen/Strep at 37°C and 5% CO₂) and were cotransfected with a transposon expressing shRNA against *ATF3* (TRCN0000329691) under a U6 promoter as well as a homemade plasmid expressing hyperactive PiggyBac transposase to generate stable incorporation of the vector into the genome. After selection with puromycin, passaged cells were obtained for experiments within the first 10 passages. To generate *ATF3* overexpression lines, the human *ATF3* sequence was cloned from Addgene #26115 and inserted into a homemade PiggyBac transposon vector for overexpression.

Following selection of stable *ATF3* overexpression or *ATF3* knockdown constructs, the cells were transfected with transposons containing either *wild-type* or T22N point mutant of RAB7B containing an N-terminal 3x-FlagTag. RAB7B template was purchased from OriGene (Catalog #RC202283), and the mutant was generated by amplifying a truncated C-terminal domain and a three-part ligation using oligos encoding the mutant N-terminal domain. All sequences were confirmed by Sanger sequencing services provided by Genewiz. Two days after transfection with RAB7B constructs, the cells were fixed and stained with an anti-FLAG antibody, which permitted specific identification of those doubly transfected cells and to determine the cellular localization of mutated RAB7B^{T22N}.

For immunofluorescence experiments, cells were grown on coverslips and blocking and staining was completed in 12-well culture plates. For imaging, the coverslips were mounted onto slides with ProLong Gold Antifade Mountant with 4'6-diamidino-2-phenylindole (DAPI) (Molecular Probes).

qRT-PCR

RNA was isolated using RNeasy (Qiagen) per the manufacturer's protocol. The integrity of the mRNA was verified with a BioTek Take3 spectrophotometer and electrophoresis on a 2% agarose gel. RNA was treated with DNase I (Invitrogen), and 1 µg of RNA was reverse-transcribed with SuperScript III (Invitrogen) following the manufacturer's protocol. Measurements of cDNA abundance were performed by qRT-PCR using Applied Biosystems QuantStudio 3 Real-time PCR system. Power SYBR Green master mix (Thermo Scientific) fluorescence was used to quantify the relative amplicon amounts of each gene. Primer sequences are located in Table EV1.

ChIP-PCR

Approximately 25 mg of stomach corpus tissue was flash-frozen in liquid nitrogen until IP was performed. The SimpleChIP Plus Enzymatic Chromatic IP Kit (Cell Signaling Technology) was used for tissue prep and IP per the manufacturer's protocol (see Reagent table for antibody concentrations). Tissue was fixed with PFA for 20 min and disaggregated with a Medimachine (BD Biosciences). Standard PCR was used to determine *ATF3* binding at the *Rab7b* first intron (see Table EV2 for primer sequences).

Human patient samples

Human gastric pathological tissue specimens were obtained with approval by the Institutional Review Board of Washington University School of Medicine. Samples used are deidentified tissues archived from standard-of-care procedures. Informed consent was received from all patients for the use of their tissue and experiments conformed to the principles set out in the WMA Declaration of Helsinki and the Department of Health and Human Services Belmont Report. Our research team does not have contact with patients and patient information is deidentified. All specimens are stored behind double-locked doors, and only approved members of the research team have access. Gastric clinical samples have been previously described in Ref. Lennerz *et al* (2010), Capoccia *et al* (2013), Radyk *et al* (2018), Willet *et al* (2018).

Graphing and statistical analysis

Graphs and statistics were done with GraphPad Prism (La Jolla, CA). In cases involving more than two samples to compare, significance was determined using ANOVA with post-hoc correction: Tukey was used to assess statistical significance if multiple conditions were compared; Dunnett post-hoc when comparing multiple samples to a single control. Otherwise, unpaired, two-tailed Student's *t*-test was used to determine significance. Data that would violate normalcy by study design were analyzed by nonparametric Mann-Whitney U-test. Most data (e.g., cell counts) were first analyzed as mean values of measurements from multiple fields across multiple sections of an organ for each animal, and then, the mean of those means was plotted. A *P*-value of ≤ 0.05 was considered significant. Samples were randomized, and measurements were blinded to prevent the introduction of experimental bias. Formal tests for normalcy were not performed. At least the minimum numbers of animals are used to achieve statistical significance in any determinations.

Data availability

This study includes no data deposited in external repositories.

Expanded View for this article is available online.

Acknowledgements

We thank Dr. Tsonwin Hai at the Ohio State University for the *Atf3*^{-/-} mice. We thank Karen Green, Lisa Snipes, and Kevin Boyer of the Department of Pathology Electron Microscopy Center. We acknowledge the AITAC of the Washington University Digestive Disease Center (DDRCC: P30 DK052574) and the NIH Shared Instrumentation Grant S10RR0227552 (for NanoZoomer slide scanning). FIB-SEM nanotomography was performed in the Washington University Center

for Cellular Imaging (WUCCI), which is funded, in part, by the Children's Discovery Institute of Washington University and St. Louis Children's Hospital (CDI-CORE-2015-505 and CDI-CORE-2019-813), the Foundation for Barnes-Jewish Hospital (3770), and Siteman Cancer Center (P30CA091842). MDR was funded by F31CA236506-01 (NIH NCI), the Philip and Sima Needleman Student Fellowship in Regenerative Medicine, and 5T32GM007067-43 (NIH); LBS was supported by Siteman Cancer Center Cancer Pathway Program (P30 CA091842 and T32CA113275). BLP by Washington University Biology Summer Undergraduate Research Fellowship Program (BioSURF) and the Children's Discovery Institute of Washington University and St. Louis Children's Hospital; JWB was supported by the Department of Defense, through the PRCRP program under Award No. W81XWH2010630 (USAMRAA), T32-DK007130 (NIH NIDDK), the Digestive Disease Research Core Centers Pilot and Feasibility Grant as part of P30 DK05257, NIH R21 AI156236, and the American Gastroenterological Association AGA2021-5101; J.B. was supported by National Institutes of Health (NIH) training grant (GM007067) and the Philip and Sima Needleman Student Fellowship in Regenerative Medicine; CJC by T32-CA009547 (NIH NCI); JCM by the National Institute of Diabetes and Digestive and Kidney Diseases (R21 DK111369, R01DK094989, R01DK105129, R01DK110406 R01120680), The National Institutes of Health National Cancer Institute (P30 CA09182, R01 CA239645, R01 CA246208), and the BETRNet (U54 CA163060).

Author contributions

MDR designed and performed experiments, analyzed and interpreted data, performed statistical analyses, and drafted and revised the manuscript; LBS and BLP designed and performed experiments, analyzed and interpreted data, performed statistical analyses, and drafted the manuscript; JWB, JB, CJC, and YK designed and performed experiments. C-CS and JAJF designed the experiments. JCM designed the experiments, provided funding for the study, generated data, performed bioinformatics analyses, and drafted and revised the manuscript.

Conflict of interest

The authors declare that they have no conflict of interest.

References

- Adami JG (1900) On Growth and Overgrowth. In: "Festschrift" in Honor of Abraham Jacobi, MD, LL.D.: To Commemorate the Seventieth Anniversary of His Birth, May Sixth, 1900, Huber F, Sondern FE (eds), pp 422–432. New Rochelle, NY: Knickerbocker Press
- Adler G, Hahn C, Kern HF, Rao KN (1985) Cerulein-induced pancreatitis in rats: increased lysosomal enzyme activity and autophagocytosis. *Digestion* 32: 10–18
- Aguirre A, López-Alonso I, González-López A, Amado-Rodríguez L, Batalla-Solís E, Astudillo A, Blázquez-Prieto J, Fernández AF, Galván JA, dos Santos CC et al (2014) Defective autophagy impairs ATF3 activity and worsens lung injury during endotoxemia. *J Mol Med (Berl)* 92: 665–676
- Alonso-Curbelo D, Riveiro-Falkenbach E, Pérez-Guijarro E, Cifdaloz M, Karras P, Osterloh L, Megías D, Cañón E, Calvo T, Olmeda D et al (2014) RAB7 controls melanoma progression by exploiting a lineage-specific wiring of the endolysosomal pathway. *Cancer Cell* 26: 61–76
- Attenhoff AM, Glover NM, Train C-M, Kaleb K, Warwick Vesztröcy A, Dylus D, de Fariás TM, Zile K, Stevenson C, Long J et al (2018) The OMA orthology database in 2018: retrieving evolutionary relationships among all domains of life through richer web and programmatic interfaces. *Nucleic Acids Res* 46: D477–D485
- Amieva M, Peek Jr RM (2016) Pathobiology of Helicobacter pylori-Induced Gastric Cancer. *Gastroenterology* 150: 64–78
- Azizi N, Toma J, Martin M, Khalid MF, Mousavi F, Win PW, Borrello MT, Steele N, Shi J, Pasca di Magliano M et al (2021) Loss of activating transcription factor 3 prevents KRAS-mediated pancreatic cancer. *Oncogene* 40: 3118–3135
- Bailey TL, Boden M, Buske FA, Frith M, Grant CE, Clementi L, Ren J, Li WW, Noble WS (2009) MEME SUITE: tools for motif discovery and searching. *Nucleic Acids Res* 37: W202–208
- Bhattacharya M, Ojha N, Solanki S, Mukhopadhyay CK, Madan R, Patel N, Krishnamurthy G, Kumar S, Basu SK, Mukhopadhyay A (2006) IL-6 and IL-12 specifically regulate the expression of Rab5 and Rab7 via distinct signaling pathways. *EMBO J* 25: 2878–2888
- Brooks AC, DeMartino AM, Brainard RE, Brittain KR, Bhatnagar A, Jones SP (2015) Induction of activating transcription factor 3 limits survival following infarct-induced heart failure in mice. *Am J Physiol Heart Circ Physiol* 309: H1326–1335
- Bucci C, Thomsen P, Nicoziani P, McCarthy J, van Deurs B (2000) Rab7: a key to lysosome biogenesis. *Mol Biol Cell* 11: 467–480
- Burclaff J, Mills JC (2018) Plasticity of differentiated cells in wound repair and tumorigenesis, part II: skin and intestine. *Dis Model Mech* 11: dmm035071
- Burclaff J, Willet SG, Saenz JB, Mills JC (2020) Proliferation and Differentiation of Gastric Mucous Neck and Chief Cells During Homeostasis and Injury-induced Metaplasia. *Gastroenterology* 158: 598–609
- Call JA, Nichenko AS (2020) Autophagy: an essential but limited cellular process for timely skeletal muscle recovery from injury. *Autophagy* 16: 1344–1347
- Cao B, Parnell LA, Diamond MS, Mysorekar IU (2017) Inhibition of autophagy limits vertical transmission of Zika virus in pregnant mice. *J Exp Med* 214: 2303–2313
- Capoccia BJ, Jin RU, Kong YY, Peek Jr RM, Fassan M, Rugge M, Mills JC (2013) The ubiquitin ligase Mindbomb 1 coordinates gastrointestinal secretory cell maturation. *J Clin Invest* 123: 1475–1491
- Carrar A, Trefely S, Zhao S, Campbell SL, Norgard RJ, Schultz KC, Sidoli S, Parris JLD, Affronti HC, Sivanand S et al (2019) Acetyl-CoA metabolism supports multistep pancreatic tumorigenesis. *Cancer Discov* 9: 416–435
- Chen T, Oh S, Gregory S, Shen X, Diehl AM (2020) Single-cell omics analysis reveals functional diversification of hepatocytes during liver regeneration. *JCI Insight* 5: e141024
- Cheung EC, DeNicola GM, Nixon C, Blyth K, Labuschagne CF, Tuveson DA, Vousden KH (2020) Dynamic ROS Control by TIGAR Regulates the Initiation and Progression of Pancreatic Cancer. *Cancer Cell* 37: 168–182
- Choi E, Means AL, Coffey RJ, Goldenring JR (2019) Active Kras expression in gastric isthmal progenitor cells induces foveolar hyperplasia but not metaplasia. *Cell Mol Gastroenterol Hepatol* 7: 251–253
- Dekaney CM, King S, Sheahan B, Cortes JE (2019) Mist1 expression is required for paneth cell maturation. *Cell Mol Gastroenterol Hepatol* 8: 549–560
- Engevik AC, Feng R, Choi E, White S, Bertaux-Skeirik N, Li J, Mahe MM, Aihara E, Yang Li, DiPasquale B et al (2016) The development of spasmolytic polypeptide/TFE2-expressing metaplasia (SPEM) during gastric repair is absent in the aged stomach. *Cell Mol Gastroenterol Hepatol* 2: 605–624
- Fahling M, Mathia S, Paliege A, Koesters R, Mrowka R, Peters H, Persson PB, Neumayer HH, Bachmann S, Rosenberger C (2013) Tubular von Hippel-Lindau knockout protects against rhabdomyolysis-induced AKI. *J Am Soc Nephrol* 24: 1806–1819
- Fahling M, Mathia S, Paliege A, Koesters R, Mrowka R, Peters H, Persson PB, Neumayer HH, Bachmann S, Rosenberger C (2013) Gene Expression

- Omnibus GSE44925 (<https://www.ncbi.nlm.nih.gov/geo/query/acc.cgi?acc=GSE44925>). [DATASET]
- Faust F, Gomez-Lazaro M, Borta H, Agricola B, Schrader M (2008) Rab8 is involved in zymogen granule formation in pancreatic acinar AR42J cells. *Traffic* 9: 964–979
- Fazio EN, Young CC, Toma J, Levy M, Berger KR, Johnson CL, Mehmood R, Swan P, Chu A, Cregan SP et al (2017) Activating transcription factor 3 promotes loss of the acinar cell phenotype in response to cerulein-induced pancreatitis in mice. *Mol Biol Cell* 28: 2347–2359
- Fazio EN, Young CC, Toma J, Levy M, Berger KR, Johnson CL, Mehmood R, Swan P, Chu A, Cregan SP et al (2017). Gene Expression Omnibus GSE60250 (<https://www.ncbi.nlm.nih.gov/geo/query/acc.cgi?acc=GSE60250>) [DATASET]
- Fukuda M (2008) Regulation of secretory vesicle traffic by Rab small GTPases. *Cell Mol Life Sci* 65: 2801–2813
- Gerber T, Murawala P, Knapp D, Masselink W, Schuez M, Hermann S, Gac-Santel M, Nowoshilow S, Kageyama J, Khattak S et al (2018) Single-cell analysis uncovers convergence of cell identities during axolotl limb regeneration. *Science* 362: eaa0681
- Gerber T, Murawala P, Knapp D, Masselink W, Schuez M, Hermann S, Gac-Santel M, Nowoshilow S, Kageyama J, Khattak S et al (2018). Gene Expression Omnibus GSE106269 (<https://www.ncbi.nlm.nih.gov/geo/query/acc.cgi?acc=GSE106269>). [DATASET]
- Gey M, Wanner R, Schilling C, Pedro MT, Sinske D, Knoll B (2016) Atf3 mutant mice show reduced axon regeneration and impaired regeneration-associated gene induction after peripheral nerve injury. *Open Biol* 6: 160091
- Giroux V, Rustgi AK (2017) Metaplasia: tissue injury adaptation and a precursor to the dysplasia-cancer sequence. *Nat Rev Cancer* 17: 594–604
- Goldenring JR (2018) Pyloric metaplasia, pseudopyloric metaplasia, ulcer-associated cell lineage and spasmolytic polypeptide-expressing metaplasia: reparative lineages in the gastrointestinal mucosa. *J Pathol* 245: 132–137
- Grant CE, Bailey TL, Noble WS (2011) FIMO: scanning for occurrences of a given motif. *Bioinformatics* 27: 1017–1018
- Guerra F, Bucci C (2016) Multiple roles of the small GTPase Rab7. *Cells* 5: 34
- Hai T, Wolfgang CD, Marsee DK, Allen AE, Sivaprasad U (1999) ATF3 and stress responses. *Gene Expr* 7: 321–335
- Hartman MG, Lu D, Kim ML, Kociba GJ, Shukri T, Buteau J, Wang X, Frankel WL, Guttridge D, Prentki M et al (2004) Role for activating transcription factor 3 in stress-induced beta-cell apoptosis. *Mol Cell Biol* 24: 5721–5732
- Hess DA, Humphrey SE, Ishibashi J, Damsz B, Lee AH, Glimcher LH, Konieczny SF (2011) Extensive pancreas regeneration following acinar-specific disruption of Xbp1 in mice. *Gastroenterology* 141: 1463–1472
- Hong KU, Reynolds SD, Giangreco A, Hurley CM, Stripp BR (2001) Clara cell secretory protein-expressing cells of the airway neuroepithelial body microenvironment include a label-retaining subset and are critical for epithelial renewal after progenitor cell depletion. *Am J Respir Cell Mol Biol* 24: 671–681
- Hou Y, Ernst SA, Stuenkel EL, Lentz SI, Williams JA (2015) Rab27A is present in mouse pancreatic acinar cells and is required for digestive enzyme secretion. *PLoS One* 10: e0125596
- Huh WJ, Esen E, Geahlen JH, Bredemeyer AJ, Lee AH, Shi G, Konieczny SF, Glimcher LH, Mills JC (2010) XBP1 controls maturation of gastric zymogenic cells by induction of MIST1 and expansion of the rough endoplasmic reticulum. *Gastroenterology* 139: 2038–2049
- Huh WJ, Khurana SS, Geahlen JH, Kohli K, Waller RA, Mills JC (2012) Tamoxifen induces rapid, reversible atrophy, and metaplasia in mouse stomach. *Gastroenterology* 142: 21–24
- Hunt D, Raivich G, Anderson PN (2012) Activating transcription factor 3 and the nervous system. *Front Mol Neurosci* 5: 7
- Inoue K, Zama T, Kamimoto T, Aoki R, Ikeda Y, Kimura H, Hagiwara M (2004) TNF α -induced ATF3 expression is bidirectionally regulated by the JNK and ERK pathways in vascular endothelial cells. *Genes Cells* 9: 59–70
- Itoh T, Satoh M, Kanno E, Fukuda M (2006) Screening for target Rabs of TBC (Tre-2/Bub2/Cdc16) domain-containing proteins based on their Rab-binding activity. *Genes Cells* 11: 1023–1037
- Jin RU, Mills JC (2014) RAB26 coordinates lysosome traffic and mitochondrial localization. *J Cell Sci* 127: 1018–1032
- Jin RU, Mills JC (2019) The cyclical hit model: how paligenesis might establish the mutational landscape in Barrett's esophagus and esophageal adenocarcinoma. *Curr Opin Gastroenterol* 35: 363–370
- Johnson CL, Kowalik AS, Rajakumar N, Pin CL (2004) Mist1 is necessary for the establishment of granule organization in serous exocrine cells of the gastrointestinal tract. *Mech Dev* 121: 261–272
- Jones JC, Brindley CD, Elder NH, Myers Jr MG, Rajala MW, Dekaney CM, McNamee EN, Frey MR, Shroyer NF, Dempsey PJ (2019) Cellular plasticity of Defa4(Cre)-expressing paneth cells in response to notch activation and intestinal injury. *Cell Mol Gastroenterol Hepatol* 7: 533–554
- Karki A, Humphrey SE, Steele RE, Hess DA, Taparowsky EJ, Konieczny SF (2015) Silencing Mist1 gene expression is essential for recovery from acute pancreatitis. *PLoS One* 10: e0145724
- Keeley TM, Horita N, Samuelson LC (2019) Tamoxifen-induced gastric injury: effects of dose and method of administration. *Cell Mol Gastroenterol Hepatol* 8: 365–367
- Khurana SS, Riehl TE, Moore BD, Fassin M, Ruggie M, Romero-Gallo J, Noto J, Peek Jr RM, Stenson WF, Mills JC (2013) The hyaluronic acid receptor CD44 coordinates normal and metaplastic gastric epithelial progenitor cell proliferation. *J Biol Chem* 288: 16085–16097
- Kjos I, Borg Distefano M, Saetre F, Repnik U, Holland P, Jones AT, Engedal N, Simonsen A, Bakke O, Progidia C (2017) Rab7b modulates autophagic flux by interacting with Atg4B. *EMBO Rep* 18: 1727–1739
- Kowalik AS, Johnson CL, Chadi SA, Weston JY, Fazio EN, Pin CL (2007) Mice lacking the transcription factor Mist1 exhibit an altered stress response and increased sensitivity to caerulein-induced pancreatitis. *Am J Physiol Gastrointest Liver Physiol* 292: G1123–G1132
- Kowalik AS, Johnson CL, Chadi SA, Weston JY, Fazio EN, Pin CL (2007) Gene Expression Omnibus GSE3644 (<https://www.ncbi.nlm.nih.gov/geo/query/acc.cgi?acc=GSE3644>) [DATASET]
- Kreft L, Soete A, Hulpiau P, Botzki A, Saeyns Y, De Bleser P (2017) ConTra v3: a tool to identify transcription factor binding sites across species, update 2017. *Nucleic Acids Res* 45: W490–W494
- Kusaba T, Lalli M, Kramann R, Kobayashi A, Humphreys BD (2014) Differentiated kidney epithelial cells repair injured proximal tubule. *Proc Natl Acad Sci USA* 111: 1527–1532
- Langemeyer L, Frohlich F, Ungermann C (2018) Rab GTPase function in endosome and lysosome biogenesis. *Trends Cell Biol* 28: 957–970
- Lennerz JKM, Kim S-H, Oates EL, Huh WJ, Doherty JM, Tian X, Bredemeyer AJ, Goldenring JR, Lauwers GY, Shin Y-K et al (2010) The transcription factor MIST1 is a novel human gastric chief cell marker whose expression is lost in metaplasia, dysplasia, and carcinoma. *Am J Pathol* 177: 1514–1533
- Leushacke M, Tan SH, Wong A, Swathi Y, Hajamohideen A, Tan LT, Goh J, Wong E, Denil SLIJ, Murakami K et al (2017) Lgr5-expressing chief cells drive epithelial regeneration and cancer in the oxyntic stomach. *Nat Cell Biol* 19: 774–786

- Li HF, Cheng CF, Liao WJ, Lin H, Yang RB (2010) ATF3-mediated epigenetic regulation protects against acute kidney injury. *J Am Soc Nephrol* 21: 1003–1013
- Li X, Wu J, Sun X, Wu Q, Li Y, Li K, Zhang Q, Li Y, Abel ED, Chen H (2020) Autophagy reprograms alveolar progenitor cell metabolism in response to lung injury. *Stem Cell Reports* 14: 420–432
- Lin H, Li HF, Chen HH, Lai PF, Juan SH, Chen JJ, Cheng CF (2014) Activating transcription factor 3 protects against pressure-overload heart failure via the autophagy molecule Beclin-1 pathway. *Mol Pharmacol* 85: 682–691
- Liou GY, Doppler H, DelGiorno KE, Zhang L, Leitges M, Crawford HC, Murphy MP, Storz P (2016) Mutant KRas-induced mitochondrial oxidative stress in acinar cells upregulates EGFR signaling to drive formation of pancreatic precancerous lesions. *Cell Rep* 14: 2325–2336
- Lizundia R, Chaussepied M, Naissant B, Masse GX, Quevillon E, Michel F, Monier S, Weitzman JB, Langsley G (2007) The JNK/AP-1 pathway upregulates expression of the recycling endosome rab11a gene in B cells transformed by Theileria. *Cell Microbiol* 9: 1936–1945
- Lo H-Y, Jin RU, Sibbel G, Liu D, Karki A, Joens MS, Madison BB, Zhang Bo, Blanc V, Fitzpatrick JAJ et al (2017) A single transcription factor is sufficient to induce and maintain secretory cell architecture. *Genes Dev* 31: 154–171
- Mackiewicz P, Wyroba E (2009) Phylogeny and evolution of Rab7 and Rab9 proteins. *BMC Evol Biol* 9: 101
- Mareninova OA, Vegh ET, Shalbuva N, Wightman CJ, Dillon DL, Malla S, Xie Y, Takahashi T, Rakonczay Z, French SW et al (2021) Dysregulation of mannose-6-phosphate dependent cholesterol homeostasis in acinar cells mediates pancreatitis. *J Clin Invest* <https://doi.org/10.1172/JCI146870>
- Marubashi S, Fukuda M (2020) Rab7B/42 is functionally involved in protein degradation on melanosomes in keratinocytes. *Cell Struct Funct* 45: 45–55
- Meyer AR, Engevik AC, Willet SG, Williams JA, Zou Y, Massion PP, Mills JC, Choi E, Goldenring JR (2019) Cystine/Glutamate antiporter (xCT) is required for chief cell plasticity after gastric injury. *Cell Mol Gastroenterol Hepatol* 8: 379–405
- Meyer AR, Goldenring JR (2018) Injury, repair, inflammation and metaplasia in the stomach. *J Physiol* 596: 3861–3867
- Miao ZF, Adkins-Threats M, Burclaff JR, Osaki LH, Sun JX, Kefalov Y, He Z, Wang ZN, Mills JC (2020a) A metformin-responsive metabolic pathway controls distinct steps in gastric progenitor fate decisions and maturation. *Cell Stem Cell* 26: 910–925
- Miao Z-F, Lewis MA, Cho CJ, Adkins-Threats M, Park D, Brown JW, Sun J-X, Burclaff JR, Kennedy S, Lu J et al (2020b) A dedicated evolutionarily conserved molecular network licenses differentiated cells to return to the cell cycle. *Dev Cell* 55: 178–194
- Miao ZF, Sun JX, Adkins-Threats M, Pang MJ, Zhao JH, Wang X, Tang KW, Wang ZN, Mills JC (2021) DDIT4 licenses only healthy cells to proliferate during injury-induced metaplasia. *Gastroenterology* 160: 260–271
- Mills JC, Sansom OJ (2015) Reserve stem cells: Differentiated cells reprogram to fuel repair, metaplasia, and neoplasia in the adult gastrointestinal tract. *Sci Signal* 8: re8
- Mills JC, Taghert PH (2012) Scaling factors: transcription factors regulating subcellular domains. *BioEssays* 34: 10–16
- Moore BD, Jin RU, Osaki L, Romero-Gallo J, Noto J, Peek RK, Mills JC (2015) Gene Expression Omnibus GSE71580 (<https://www.ncbi.nlm.nih.gov/geo/query/acc.cgi?acc=GSE71580>). [DATASET]
- Moore BD, Jin RU, Osaki L, Romero-Gallo J, Noto J, Peek RK, Mills JC (2015) Identification of alanyl aminopeptidase (CD13) as a surface marker for isolation of mature gastric zymogenic chief cells. *Am J Physiol Gastrointest Liver Physiol* 309: G955–G964
- Nam KT, Lee H, Sousa JF, Weis VG, O'Neal RL, Finke PE, Romero-Gallo J, Shi G, Mills JC, Peek RM et al (2010) Mature chief cells are cryptic progenitors for metaplasia in the stomach. *Gastroenterology* 139: 2028–2037
- Niederer C, Ferrell LD, Grendell JH (1985) Caerulein-induced acute necrotizing pancreatitis in mice: protective effects of proglumide, benzotript, and secretin. *Gastroenterology* 88: 1192–1204
- Nozaki K, Ogawa M, Williams JA, Lafleur BJ, Ng V, Drapkin RI, Mills JC, Konieczny SF, Nomura S, Goldenring JR (2008) A molecular signature of gastric metaplasia arising in response to acute parietal cell loss. *Gastroenterology* 134: 511–522
- Ohnishi H, Ernst SA, Wys N, McNiven M, Williams JA (1996) Rab3D localizes to zymogen granules in rat pancreatic acini and other exocrine glands. *Am J Physiol* 271: G531–G538
- Otu HH, Naxerova K, Ho K, Can H, Nesbitt N, Libermann TA, Karp SJ (2007) Gene Expression Omnibus GSE6998 (<https://www.ncbi.nlm.nih.gov/geo/query/acc.cgi?acc=GSE6998>). [DATASET]
- Otu HH, Naxerova K, Ho K, Can H, Nesbitt N, Libermann TA, Karp SJ (2007) Restoration of liver mass after injury requires proliferative and not embryonic transcriptional patterns. *J Biol Chem* 282: 11197–11204
- Pereira-Leal JB, Seabra MC (2000) The mammalian Rab family of small GTPases: definition of family and subfamily sequence motifs suggests a mechanism for functional specificity in the Ras superfamily. *J Mol Biol* 301: 1077–1087
- Petersen CP, Mills JC, Goldenring JR (2017) Murine models of gastric corpus preneoplasia. *Cell Mol Gastroenterol Hepatol* 3: 11–26
- Pin CL, Rukstalis JM, Johnson C, Konieczny SF (2001) The bHLH transcription factor Mist1 is required to maintain exocrine pancreas cell organization and acinar cell identity. *J Cell Biol* 155: 519–530
- Progida C, Cogli L, Piro F, De Luca A, Bakke O, Bucci C (2010) Rab7b controls trafficking from endosomes to the TGN. *J Cell Sci* 123: 1480–1491
- Radyk MD, Burclaff J, Willet SG, Mills JC (2018) Metaplastic cells in the stomach arise, independently of stem cells, via dedifferentiation or transdifferentiation of chief cells. *Gastroenterology* 154: 839–843
- Ramsey VG, Doherty JM, Chen CC, Stappenbeck TS, Konieczny SF, Mills JC (2007) The maturation of mucus-secreting gastric epithelial progenitors into digestive-enzyme secreting zymogenic cells requires Mist1. *Development* 134: 211–222
- Raven A, Lu W-Y, Man TY, Ferreira-Gonzalez S, O'Duibhir E, Dwyer BJ, Thomson JP, Meehan RR, Bogorad R, Koteliensky V et al (2017) Cholangiocytes act as facultative liver stem cells during impaired hepatocyte regeneration. *Nature* 547: 350–354
- Römermann D, Ansari N, Schultz-Moreira AR, Michael A, Marhenke S, Hardtke-Wolenski M, Longerich T, Manns MP, Wedemeyer H, Vogel A et al (2020) Absence of Atg7 in the liver disturbed hepatic regeneration after liver injury. *Liver Int* 40: 1225–1238
- Rosenfeldt MT, O'Prey J, Morton JP, Nixon C, MacKay G, Mrowinska A, Au A, Rai TS, Zheng L, Ridgway R et al (2013) p53 status determines the role of autophagy in pancreatic tumour development. *Nature* 504: 296–300
- Saenz JB, Burclaff J, Mills JC (2016) Modeling murine gastric metaplasia through tamoxifen-induced acute parietal cell loss. *Methods Mol Biol* 1422: 329–339
- Saenz JB, Mills JC (2018) Acid and the basis for cellular plasticity and reprogramming in gastric repair and cancer. *Nat Rev Gastroenterol Hepatol* 15: 257–273
- Saenz JB, Vargas N, Mills JC (2018) Tropism for spasmolytic polypeptide-expressing metaplasia allows helicobacter pylori to expand its intragastric niche. *Gastroenterology* 156: 160–174

- Saera-Vila A, Kish PE, Louie KW, Grzegorski SJ, Klionsky DJ, Kahana A (2016) Autophagy regulates cytoplasmic remodeling during cell reprogramming in a zebrafish model of muscle regeneration. *Autophagy* 12: 1864–1875
- Saluja A, Saito I, Saluja M, Houlihan MJ, Powers RE, Meldolesi J, Steer M (1985) In vivo rat pancreatic acinar cell function during supramaximal stimulation with caerulein. *Am J Physiol* 249: G702–G710
- Shimizu T, Sohn Y, Choi E, Petersen CP, Prasad N, Goldenring JR (2020) Decrease in MiR-148a expression during initiation of chief cell transdifferentiation. *Cell Mol Gastroenterol Hepatol* 9: 61–78
- Sood V, Sharma KB, Gupta V, Saha D, Dhapola P, Sharma M, Sen U, Kitajima S, Chowdhury S, Kalia M et al (2017) ATF3 negatively regulates cellular antiviral signaling and autophagy in the absence of type I interferons. *Sci Rep* 7: 8789
- Storz P (2017) Acinar cell plasticity and development of pancreatic ductal adenocarcinoma. *Nat Rev Gastroenterol Hepatol* 14: 296–304
- Stroupe C (2018) This is the end: regulation of Rab7 nucleotide binding in endolysosomal trafficking and autophagy. *Fron Cell Dev Biol* 6: 129.
- Takahashi K, Mashima H, Miura K, Maeda D, Goto A, Goto T, Sun-Wada GH, Wada Y, Ohnishi H (2017) Disruption of small GTPase Rab7 exacerbates the severity of acute pancreatitis in experimental mouse models. *Sci Rep* 7: 2817
- Tata PR, Mou H, Pardo-Saganta A, Zhao R, Prabhu M, Law BM, Vinarsky V, Cho JL, Breton S, Sahay A et al (2013) Dedifferentiation of committed epithelial cells into stem cells in vivo. *Nature* 503: 218–223
- Tian X, Jin RU, Bredemeyer AJ, Oates EJ, Blazewska KM, McKenna CE, Mills JC (2010) RAB26 and RAB3D are direct transcriptional targets of MIST1 that regulate exocrine granule maturation. *Mol Cell Biol* 30: 1269–1284
- Tsai WW, Matsumura S, Liu W, Phillips NG, Sonntag T, Hao E, Lee S, Hai T, Montminy M (2015) ATF3 mediates inhibitory effects of ethanol on hepatic gluconeogenesis. *Proc Natl Acad Sci USA* 112: 2699–2704
- van Es JH, Sato T, van de Wetering M, Lyubimova A, Yee Nee AN, Gregorieff A, Sasaki N, Zeinstra L, van den Born M, Korving J et al (2012) Dll1+ secretory progenitor cells revert to stem cells upon crypt damage. *Nat Cell Biol* 14: 1099–1104
- Wandering-Ness A, Zerial M (2014) Rab proteins and the compartmentalization of the endosomal system. *Cold Spring Harb Perspect Biol* 6: a022616
- Wang L, Deng S, Lu Y, Zhang Y, Yang L, Guan Y, Jiang H, Li H (2012) Increased inflammation and brain injury after transient focal cerebral ischemia in activating transcription factor 3 knockout mice. *Neuroscience* 220: 100–108
- Weis VG, Petersen CP, Weis JA, Meyer AR, Choi E, Mills JC, Goldenring JR (2017) Maturity and age influence chief cell ability to transdifferentiate into metaplasia. *Am J Physiol Gastrointest Liver Physiol* 312: G67–G76
- Willet SG, Lewis MA, Miao ZF, Liu D, Radyk MD, Cunningham RL, Burclaff J, Sibbel G, Lo HG, Blanc V et al (2018) Regenerative proliferation of differentiated cells by mTORC1-dependent paligenesis. *EMBO J* 37: e98311
- Wroblewski LE, Choi E, Petersen C, Delgado AG, Piazzuelo MB, Romero-Gallo J, Lantz TL, Zavros Y, Coffey RJ, Goldenring JR et al (2019) Targeted mobilization of Lrig1(+) gastric epithelial stem cell populations by a carcinogenic Helicobacter pylori type IV secretion system. *Proc Natl Acad Sci USA* 116: 19652–19658
- Yang M, Chen T, Han C, Li N, Wan T, Cao X (2004) Rab7b, a novel lysosome-associated small GTPase, is involved in monocytic differentiation of human acute promyelocytic leukemia cells. *Biochem Biophys Res Commun* 318: 792–799
- Yue L, Wan R, Luan S, Zeng W, Cheung TH (2020) Dek modulates global intron retention during muscle stem cells quiescence exit. *Dev Cell* 53: 661–676
- Yue L, Wan R, Luan S, Zeng W, Cheung TH (2020) Gene Expression Omnibus GSE113631 (<https://www.ncbi.nlm.nih.gov/geo/query/acc.cgi?acc=GSE113631>). [DATASET]
- Zhao Y, Wu X, Qian L, Guo L, Liao J, Wu X (2017) Activating transcription factor 3 protects mice against pseudomonas aeruginosa-induced acute lung injury by interacting with lipopolysaccharide binding protein. *Mol Immunol* 90: 27–32
- Zhou J, Edgar BA, Boutros M (2017) ATF3 acts as a rheostat to control JNK signalling during intestinal regeneration. *Nat Commun* 8: 14289
- Zhu Q, Wang H, Jiang B, Ni X, Jiang L, Li C, Wang X, Zhang F, Ke B, Lu L (2018) Loss of ATF3 exacerbates liver damage through the activation of mTOR/p70S6K/ HIF-1alpha signaling pathway in liver inflammatory injury. *Cell Death Dis* 9: 910

Annual Review of Physiology

Paligenosis: Cellular Remodeling During Tissue Repair

Jeffrey W. Brown,^{1,*} Charles J. Cho,^{1,2,*}
and Jason C. Mills^{1,2,3,4}

¹Division of Gastroenterology, Department of Medicine, Washington University School of Medicine in St. Louis, St. Louis, Missouri, USA

²Current affiliation: Section of Gastroenterology and Hepatology, Department of Medicine, Baylor College of Medicine, Houston, Texas, USA

³Departments of Pathology and Immunology and Developmental Biology, Washington University School of Medicine in St. Louis, St. Louis, Missouri, USA

⁴Current affiliation: Departments of Medicine, Pathology and Immunology, and Molecular and Cellular Biology, Baylor College of Medicine, Houston, Texas, USA; email: jason.mills@bcm.edu

Annu. Rev. Physiol. 2022. 84:461–83

First published as a Review in Advance on
October 27, 2021

The *Annual Review of Physiology* is online at
physiol.annualreviews.org

<https://doi.org/10.1146/annurev-physiol-061121-035954>

Copyright © 2022 by Annual Reviews.
All rights reserved

*These authors contributed equally to this article

Keywords

dedifferentiation, regeneration, injury, metaplasia

Abstract

Complex multicellular organisms have evolved specific mechanisms to replenish cells in homeostasis and during repair. Here, we discuss how emerging technologies (e.g., single-cell RNA sequencing) challenge the concept that tissue renewal is fueled by unidirectional differentiation from a resident stem cell. We now understand that cell plasticity, i.e., cells adaptively changing differentiation state or identity, is a central tissue renewal mechanism. For example, mature cells can access an evolutionarily conserved program (paligenosis) to reenter the cell cycle and regenerate damaged tissue. Most tissues lack dedicated stem cells and rely on plasticity to regenerate lost cells. Plasticity benefits multicellular organisms, yet it also carries risks. For one, when long-lived cells undergo paligenotic, cyclical proliferation and redifferentiation, they can accumulate and propagate acquired mutations that activate oncogenes and increase the potential for developing cancer. Lastly, we propose a new framework for classifying patterns of cell proliferation in homeostasis and regeneration, with stem cells representing just one of the diverse methods that adult tissues employ.

ANNUAL REVIEWS **CONNECT**

www.annualreviews.org

- Download figures
- Navigate cited references
- Keyword search
- Explore related articles
- Share via email or social media

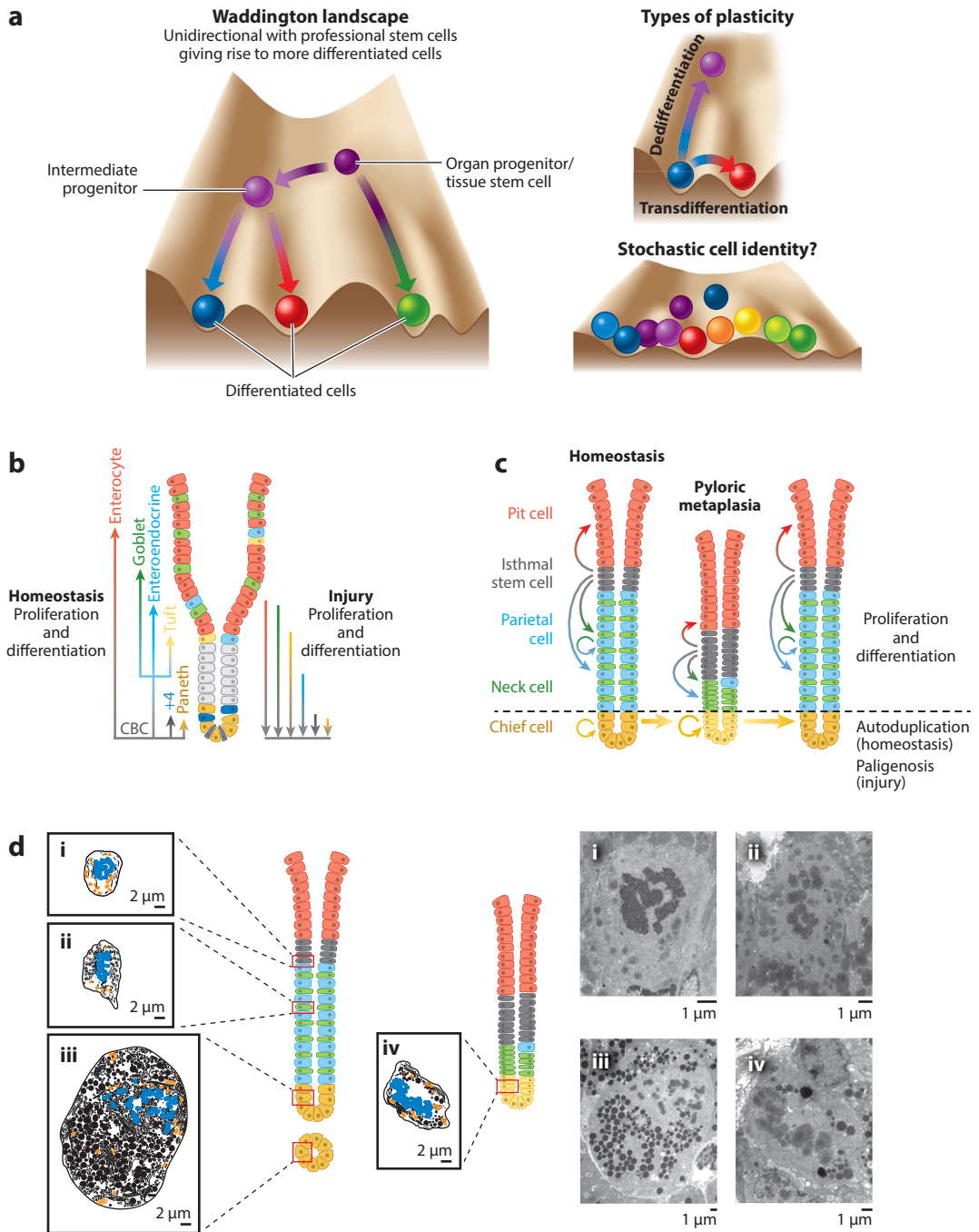
1. INTRODUCTION

For most of the last half of the twentieth and early part of the twenty-first centuries, the canonical model for proliferation in adult tissue was the epigenetic landscape proposed initially by the geneticist Conrad Waddington (1), which implied that a stem cell is constantly present in every tissue. The stem cell self-renews and, when necessary, spawns differentiated cells in a unidirectional flow (**Figure 1a**). Such a professional stem cell is by definition self-replicative as well as multipotent (i.e., it can give rise to multiple cell types) and thus relatively undifferentiated (i.e., it lacks both specific markers attributable to differentiated cell types as well as specific mature cell architectural features like secretory granules).

However, with tools like genetic and chemical lineage tracing and single-cell RNA sequencing (scRNA-seq), and with the advent of cellular reprogramming to generate induced pluripotent stem cells (2, 3), it has become clear that cell behavior in tissue can be far more complicated (see, e.g., 4, 5). For example, single-cell expression profiling shows that there might not even be clear grooves on the Waddington landscape, but instead, cell identity might be fluid, with the behavior and phenotype of a single differentiated cell being better modeled by a stochastic electron-cloud-like representation (**Figure 1a**). In other words, cell identity may be loosely constrained by a genetic/epigenetic envelope but perpetually restless in response to environmental, hormonal, and paracrine signals. We have likely missed such heterogeneity of adult cell identity because the techniques we traditionally employ to assess cell identity sample the cell at a single time point, using limited biomarkers. Moreover, in the setting of injury, the constraining envelope (i.e., Waddington groove) for a cell is perturbed, with mature cells able to access states not available during homeostasis. For example, they can undergo dedifferentiation to a stem cell–like state, or they can change phenotype to replace other adult cell lineages via transdifferentiation (6, 7) (**Figure 1a**).

An individual cell can be injured in numerous ways: chemical, thermal, inflammatory, hypoxic/ischemic, infectious, autoimmune, or physical or by starvation or being crushed. However, the fundamental response decision matrix is the same: (a) repair the damage (e.g., via induction and resolution of cell stress pathways like the unfolded protein response), (b) die (e.g., via apoptosis, pyroptosis, necroptosis, or anoikis, a noninjury-associated process), or (c) enter the cell cycle. Additionally, extracellular signals from immune cells and the mesenchyme can further modify cellular responses, such as coaxing cells to change identity (transdifferentiate) to replace other cell types lost by injury. Here, we focus not on extracellular signals but on the intrinsic aspects of a cell's response either to its own injury or to injury in neighboring cells. Cell repair is the optimal choice if the insults are minor. Cell death benefits the organism if the cell itself is irreparably damaged, has acquired mutations that would predispose toward oncogenesis, or is harboring a pathogen. Cell proliferation may be necessary to regenerate tissue if other cells are dead or injured beyond repair. For example, after liver cell loss (e.g., chemical or partial hepatectomy) the liver must maintain metabolic and synthetic functions while it increases cell mass (7).

Most tissues do not actually have professional stem cells, in which case homeostatic proliferation is via mature cells autoduplicating: cytokinesis without significant prior loss or the degradation of differentiated features. Indeed, many nonvertebrate organisms may lack adult professional stem cells entirely. Thus, in most cases where cell proliferation is needed to regenerate tissue after injury, mature cells that are performing a differentiated function must be recruited. It is likely, given the universality of this tissue need, that mature cells have evolved a conserved program (akin to mitosis or apoptosis) that interprets stress as a signal to retool their differentiated cell architecture and reenter the cell cycle. We have termed this program paligenosis from pali/n/m (meaning backward or recurrence) + genea (born of, producing) + osis (an action or process).



(Caption appears on following page)

Figure 1 (Figure appears on preceding page)

Schematic representation of homeostatic behavior and injury-induced cellular plasticity in the exocrine pancreas as well as epithelia of the gastric corpus and small intestine. (a) Illustration of cell fate decisions and plasticity within an adult tissue. (Left) Waddington landscape in which a stem cell at the top of the hill has the potential to roll down one of several grooves to a specific, differentiated state at the bottom of the landscape implying irreversible terminal differentiation. (Upper right) Examples of cell plasticity in adult tissue: Dedifferentiation (differentiated cells at the bottom to roll uphill) and transdifferentiation (differentiated cells located at a specific groove move to another one, overcoming the hurdle). (Lower right) Single-cell analyses such as RNA-seq suggest that cell state may be a fluid and not deterministic process as has been implied by traditional fixed tissues and histological approaches. (b) Homeostatic lineage differentiation from the professional stem cell (LGR5⁺ CBC) at homeostasis and injury-induced dedifferentiation. (c) Juxtaposition of the two proliferative zones within the gastric corpus at homeostasis and depiction of the divergent response to injury. (d) Scaled schematic representation demonstrating the dramatic differences in cellular differentiation between both different lineages and changes following injury. (Left panels) Schematic illustration of size-matched representative TEM images (right panels) of mitotic cells in the murine stomach corpus and pancreas at homeostasis and after injury: (i) isthmal stem cell (type I), (ii) mucous neck cell (type II), (iii) pancreas acinar cell (type III), and (iv) dedifferentiated gastric chief cell during paligenosis (type IV). Colchicine was used to halt progression through mitosis and increase the likelihood of catching rare, homeostatic autoduplication events in TEM. Condensed chromosome (blue) and mitochondria (orange) are colorized. Right panels are the original TEM images of cells depicted in the left panels. Abbreviations: CBC, crypt base columnar cell; RNA-seq, RNA sequencing; TEM, transmission electron microscopy.

Here, we discuss both homeostatic and postinjury reparative processes and primarily focus on paligenosis, contrasting paligenosis to other reparative processes and discussing how paligenosis might have evolved. We also discuss risks of endowing cells with the capacity to undergo paligenosis. Our focus centers on—but is not exclusive to—tissues of the gastrointestinal tract, where cross-tissue comparison of cellular behavior during homeostasis and following injury is relatively straightforward.

2. RECONSIDERING STEMNESS IN HOMEOSTASIS AND INJURY

The tissue that pioneered a Waddington, unidirectional hierarchy of adult stem cell behavior was arguably the hematopoietic system of vertebrates. At homeostasis, blood cells largely develop in the bone marrow from multipotent stem cells that spawn various lineages of differentiated cells via sequential fate choices, each of which restricts lineage options along Waddington differentiation grooves (8). There is also evidence in blood for another classical notion of professional stem cell behavior: that stem cells can remain undifferentiated but dormant for days, weeks, and months, activated only when needed (9–11). Such a notion that true, professional stem cells at the top of a multipotent hierarchy would be largely quiescent originated with early nucleotide analog tracing experiments (e.g., with ³H-thymidine) showing that some cells could take up label (i.e., proliferate, which, in the thinking of the era, meant they must be stem or progenitor cells) and then retain it for weeks or months after chase without label (12). Outside the hematopoietic system, the quiescent satellite cells in skeletal muscle (13), and potentially the occasionally proliferative +4 reserve stem cell in the small intestine (12), little evidence has emerged for such so-called label-retaining stem cells. Rather, professional stem cells largely devote their daily activity to stochastic decisions about whether to proliferate or differentiate and are not quiescent at all (14).

Although the long-held notion of slow-cycling stem cells may actually apply only to blood at homeostasis, other tissues with professional stem cells do seem to adhere more or less to the unidirectional stem cell differentiation behavior illustrated by the Waddington landscape (1, 15) (Figure 1a,b). However, even in such stem cell-maintaining adult tissues, injury seems to scramble this behavior, with genetic lineage tracing studies clearly demonstrating that injury can induce diverse examples of cell plasticity. Moreover, most tissues or tissue compartments (and many entire organisms) lack professional stem cells and regenerate damaged tissue entirely by recruitment of mature cells into the cell cycle. In this section, we examine examples of how tissues self-maintain in homeostasis and injury in agreement or in contrast to Waddington stem cell dynamic models.

2.1. Dynamics of Professional Stem Cell Behavior at Homeostasis

Outside the hematopoietic system (and possibly skin), the tissue that has arguably been best studied in terms of its classical, hierarchical stem cell differentiation behavior is the small intestine, wherein the professional stem cell, the crypt base columnar cell (CBC), sits at the base of the intestinal crypt nestled between Paneth cells (16–18). This cell is most commonly identified by the biomarker LGR5, a cell surface receptor for R-spondin that augments WNT signaling (19). The CBC maintains itself by a stochastic mix of self-replication and generation of progeny (14) that go on to differentiate into all the principal intestinal lineages (16) (**Figure 1b**). Stem cells of the skin, including those of the epidermis and hair follicle, also largely follow classical differentiation at homeostasis (20, 21).

In the body of the stomach, the multipotent cell sits at the isthmus between the deeper glandular cells and those cells that rise to the surface of the gastric lumen (i.e., foveolar, surface, or pit) cells (**Figure 1c**). The isthmal stem cell seems to follow classical stem cell hierarchical dynamics at homeostasis: giving rise to multiple cell lineages in the epithelium (22). However, the digestive enzyme–secreting chief cells at the base seem to largely maintain their own population at homeostasis (23, 24) (**Figure 1c**).

2.2. Cellular Plasticity in Tissues with a Professional Stem Cell Following Injury

Injury induces cell plasticity, even in tissues with professional stem cells. For example, in the small intestine, there is a so-called +4 reserve stem cell population whose activity is induced by injury. The +4 cell has always been largely functionally defined, as it was previously the site of maximal label-retaining activity (12). More recently, it has been defined by lineage tracing that contrasts +4 cell behavior with CBC behavior. LGR5-negative, non-CBC stem cell activity localizes approximately to the +4 position using lineage tracing studies with various promoters, e.g., *Bmi1* (25, 26), *Hopx* (27), *mTERT* (28), and *Lrig1* (29, 30). Although there might be some homeostatic stem-like behavior of such +4 cells, they are likely at least partially differentiated, with most studies suggesting they are physiologically secretory cells that serve as reserve stem cells following injury (16, 31). However, their ability to be recruited as stem cells is far from unique when radiation or chemical injury has compromised or overwhelmed the professional CBC stem cells. For example, Paneth cells (32, 33), enterocytes (34–38), enteroendocrine cells (39), and even tuft cell lineages demonstrate significant plasticity (40, 41). Any of these cells seem capable of ultimately replacing a lost CBC, meaning all intestinal lineages may have some capacity for complete dedifferentiation back to the multipotent state. In tissues with a professional stem cell, such cellular plasticity is necessary to restore the homeostatic cell hierarchy when the stem cells are lost. In the absence of such plasticity, ablation of the stem cell population would result in collapse and complete loss of these rapidly cycling tissues.

2.3. Cellular Plasticity in Tissues without Professional Stem Cell or with Mixed Stem Cell Activity at Homeostasis

The epithelium of the gastric body (corpus) has a mixed phenotype of stem cell activity (**Figure 1c,d**). The professional, isthmal stem cell can repopulate the pit (surface/foveolar), neck, and parietal cell lineages (23, 24). However, using elegant lineage tracing, Han et al. (23) have demonstrated that the chief cells are responsible for maintaining their own population at homeostasis. Our work using BrdU/EdU pulse-chase labeling both at homeostasis and during injury corroborates their study (24). Thus, at homeostasis, chief cell dynamics resemble those of acinar salivary gland cells (42), exocrine pancreatic acinar cells (43), and hepatocytes (44): cell populations

that maintain their own census at homeostasis through autoduplication. The self-duplicating quality of acinar cells has not been extensively studied, but it may be that only subpopulations of cells have proliferative potential with either mutational burden or local concentrations of growth factors likely playing a role in promoting this behavior (45). Unlike induced proliferation following injury that is discussed below, it seems that the homeostatic autoduplication that differentiated cells undergo occurs without large-scale cell architecture remodeling or dedifferentiation.

2.4. Tissues without Professional Stem Cells after Injury

The cells in the parenchyma of most organs at homeostasis seem to be devoted to carrying out their differentiated function and are mitotically quiescent (46), so when injury is severe enough to merit proliferation to replace lost cells, there have to be mechanisms to license mature, differentiated cells into the cell cycle that do not involve professional stem cells. For example, other than the rare autoduplicating cells, the exocrine pancreas is largely mitotically quiescent. However, following injury that causes cell loss, the remaining cells demonstrate remarkable plasticity. Injury either transiently with cerulein, a cholecystokinin analog, or permanently, via pancreatic duct ligation, causes acinar cells to revert to a more embryonic-like phenotype, with proliferating ductular morphology characterized by a relative depletion of zymogenic granules and a more cuboidal morphology resembling ductal precursors (recently reviewed in 47). Because of the duct-like morphology and because acinar cells activate the expression of genes characteristic of mature ducts (e.g., *CK19*, *SOX9*), the changes that occur are known as acinar-to-ductal metaplasia (ADM). As a metaplasia, ADM cells are morphologically distinct from acinar cells at homeostasis, yet they are not dysplastic. However, the term acinar-to-ductal metaplasia is misleading, because ADM cells do not become mature pancreatic duct-like cells (e.g., a transdifferentiation event), as they continue to express genes normally present only in the acinar cells (e.g., amylase) (31).

The importance of ADM is underscored by lineage tracing experiments demonstrating that this metaplasia can progress to pancreatic intraepithelial neoplasia (PanIN) (48–52). PanINs are precursor lesions to pancreatic ductal adenocarcinoma harboring mutations characteristic of invasive cancer (53–55).

The liver is similar to the pancreas in being largely mitotically quiescent at homeostasis, with hepatocytes performing their various roles in regulating metabolism and secreting bile and blood proteins. Hepatocytes, however, are exceedingly plastic with hepatocytes in all histoanatomical zones and of all functions able to enter the cell cycle after injury (56).

In the body of the stomach, the professional isthmal stem cell increases proliferation in response to injury; however, the chief cells in the base undergo a dramatic reprogramming akin to pancreatic ADM (57) (**Figure 1c**). Injury induces chief cells to express markers traditionally restricted to mucous neck cells or embryonic glandular cells [e.g., the epitope for the *Griffonia simplicifolia* lectin II (GSII), trefoil factor family 2 (TFF2), and mucin 6 (MUC6)] (58). This metaplastic response is referred to as SPEM (spasmolytic polypeptide-expressing metaplasia) because TFF2 was originally called spasmolytic polypeptide (59). But like the pancreatic acinar cells, these metaplastic zymogenic cells retain markers restricted to zymogenic cells [e.g., gastric intrinsic factor (GIF) and pepsinogen C (PGC)].

The innate similarity of SPEM and ADM (large, mitotically quiescent cells reprogramming to express embryonic and wound-healing-associated genes) (153) leads to an obvious hypothesis that the cellular reprogramming program may be conserved across diverse organs. Indeed, the SPEM of chief cells always seems to occur in a broader gastric response that includes loss of acid-secreting parietal cells and increased proliferation of isthmal cells (mentioned above) and often hyperplasia of pit cells (foveolar hyperplasia). This overall pattern has been termed pyloric

(or pseudopyloric) metaplasia and is so named because the gastric units with pyloric metaplasia resemble normal units of the gastric pylorus or antrum (57) (**Figure 1c**). It has been proposed that SPEM and ADM as well as gastric metaplasia in inflammatory bowel disease, autoimmune gastritis, and portions of the metaplasia in the esophagus known as Barrett's esophagus are all manifestations of a common wound-induced pyloric metaplasia pattern that increases wound-healing factors such as trefoil factors and mucins and increases embryonic gene expression patterns that provide the right context for cells to enter the cell cycle and serve as progenitors to regenerate lost tissue (57–62).

3. PALIGENOSIS: A CONSERVED CELLULAR-MOLECULAR PROGRAM MATURE CELLS USE TO REENTER THE CELL CYCLE

We hypothesized that ADM and SPEM within pyloric metaplasia may be instances of an even broader cellular-molecular program that evolution has bestowed upon mature, differentiated cells of a tissue. As mentioned above, such a program, paligenosis, affords mature cells that need to regenerate lost tissue a route to reenter the cell cycle (**Figure 2a**). However, allowing mature cells to cycle between proliferative and long-lived quiescent, functional states has the downside that it increases the chance for accumulation, storage, and unmasking of oncogenic mutations (60, 63) (see below for more discussion).

3.1. Stages of Paligenosis

The pathologist George Adami described over a century ago what a mature cell would need to become proliferative again: It would need to switch energy use from fueling functional activity (e.g., secreting digestive enzymes) to fueling proliferation (64). We now know that paligenosis is just such a switch revolving around the cellular energy hub mTOR, mechanistic target of rapamycin complex 1 (mTORC1) (65), with mTORC1 elevated in homeostatic, differentiated cells to fuel protein production for secretion, mTORC1 switched off as the cell activates autophagy and lysosomes to downscale the large cellular architecture of a differentiated cell, and then mTORC1 switched back on to fuel cell cycle reentry (65) (**Figure 2a**).

It is not yet clear how the mixture of cell-intrinsic and -extrinsic signals dictates whether a cell will successfully undergo paligenosis. Expression of ATF3 is one of the earliest events in paligenosis, which transcriptionally regulates autophagy via induction of RAB7B (66). We and others have found that reactive oxygen species (ROS) are clearly an upstream event, as ROS-handling programs are induced and critical for normal paligenosis progression (67). Management of ROS depends on the xCT cysteine/glutamate transporter, which ensures progression through paligenosis, at least in gastric chief cells (67). Despite these cell-intrinsic phenomena, it has also been shown that macrophages (68), group 2 lymphoid cells (69), and a variety of cytokines are involved in orchestrating paligenotic metaplasia (70–72). Clearly, much future work is needed to understand how all of these aforementioned and other signals are assimilated by the cell to drive the reciprocal mTORC1/autophagy cycle characteristic of paligenosis. Here, we review our current understanding of the orderly series of cellular-molecular events in paligenosis by which a mature, differentiated cell undergoes paligenosis to become a primitive proliferative cell.

Paligenosis begins when a differentiated cell tunes down mTORC1 activity and upregulates autophagy in order to downscale the mature cellular machinery (Stage 1). This results in a less differentiated, more plastic cell that later begins to express metaplastic genes (e.g., *SOX9*) coincident with tuning mTORC1 activity (Stage 2) back up to enter the cell cycle (Stage 3) (65).

If lysosomal function is compromised as in the *Gnptab*^{-/-} mouse (65), which lacks the ability to transport lysosomal hydrolases, or by treatment with hydroxychloroquine (66), the cell's

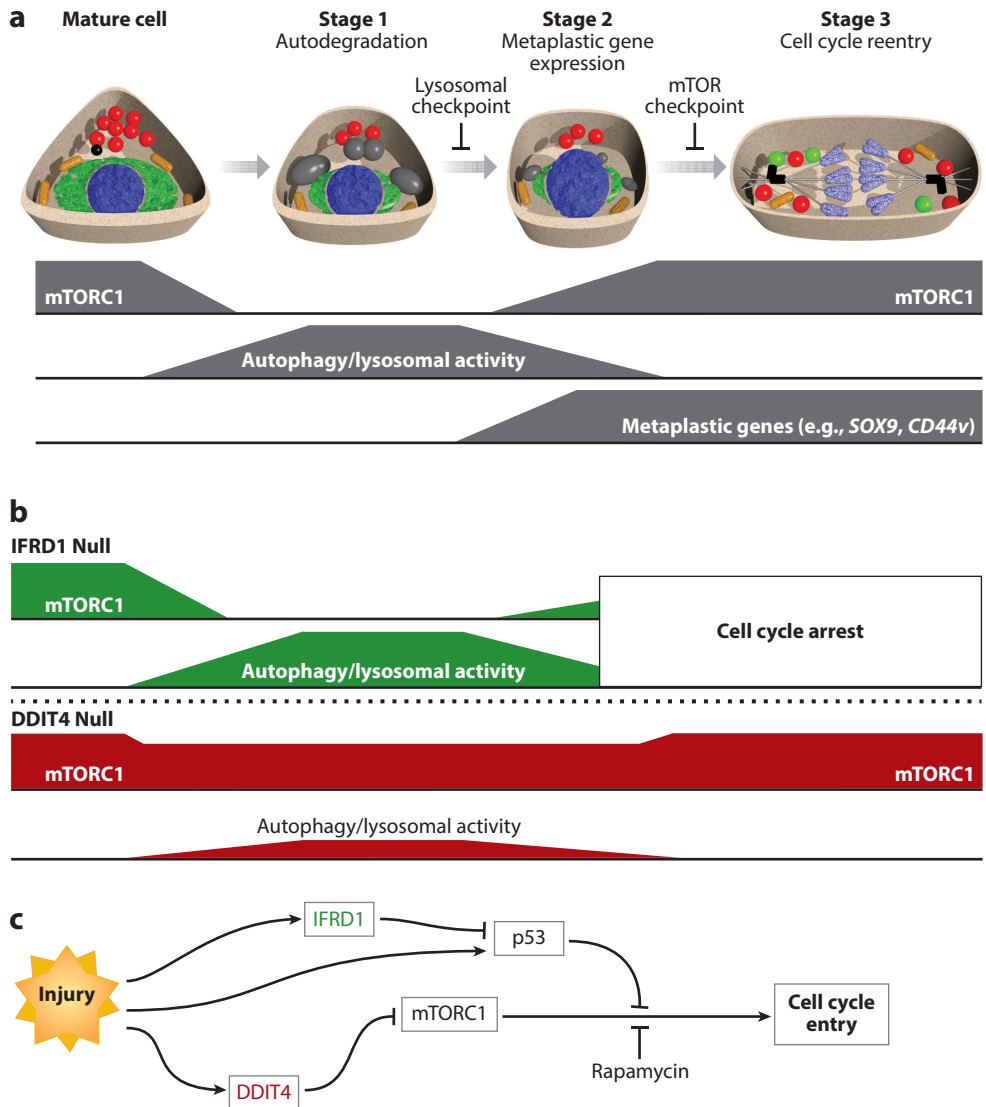


Figure 2

Schematic representation of the dynamic modulation of mTOR and autophagy involved in paligenesis. (a) Temporal model of cellular architectural changes through the three stages of paligenesis overlain on the modulation of mTOR and autophagic activity as well as the expression of metaplastic genes. (b) The molecular and cytologic consequences of IFRD1 and DDIT4 knockout on mTOR and autophagy in paligenesis. (c) Molecular schema of how IFRD1, DDIT4, and p53 orchestrate paligenesis. Abbreviations: DDIT4, DNA damage-inducible transcript 4; mTORC1, mechanistic target of rapamycin complex 1.

ability to undergo even the initial stages of paligenesis is compromised. Without functional lysosomes, most paligenotic cells do not scale down differentiated cell architecture, fail to express metaplasia-associated genes, and reenter the cell cycle. In addition, failure at this stage (which also occurs when cells lack ATF3 to induce lysosomes) causes increased cell death (66, 73). If we inhibit mTORC1 function with rapamycin, cells downscale and express metaplastic genes

but do not proliferate. Thus, we conclude that there are at least three stages of paligenosis: Stage 1 with autophagy/lysosomal degradation of architecture, Stage 2 with induced expression of embryonic/wound-healing/metaplastic genes (e.g., *CD44v*, *SOX9*, nuclear *YAP1*, and others mentioned above), and Stage 3 with cell cycle reentry (**Figure 2a**).

In accordance with the concept of paligenosis, various forms of autophagy have been implicated as important in zebrafish muscle reprogramming (74), pancreatic duct cell transdifferentiation into endocrine cells (4), beige-to-white fat conversion (75–77), hepatocyte proliferation posthepatectomy (78), and skin repair (79). mTORC1 has also been shown to be a key driver of emergence from quiescence (reviewed in 80, 81), as muscle satellite cells reenter the cell cycle during regeneration (82), as so-called +4 intestinal cells are recruited following crypt injury (83), and in reprogramming of differentiated cells into induced pluripotent stem cells (84).

3.2. Genes Essential to Paligenosis

We hypothesized that there would be a core set of conserved, shared genes/proteins responsible for the precise orchestration of paligenosis the way caspases and BCL family members are critical for apoptosis. These genes would be dispensable at homeostasis and thus there would be no overt phenotype in knockout mice. Further, they would be upregulated following a diverse range of injury models, species and tissues. Accordingly, we screened genes upregulated during injury and known to modulate mTORC signaling. In a recent in silico screen, only two genes fulfilled these criteria: *IFRD1* and *DDIT4* [DNA damage-inducible transcript 4 (85)].

3.3. *IFRD1*, a Paligenosis Gene

IFRD1 [interferon-related developmental regulator, also known as PC4 (86) and Tis7 (87)] is a stress-induced protein conserved even in *Schizosaccharomyces pombe* (85). There is no apparent ortholog in budding yeast. The importance of this protein in regeneration and disease has been demonstrated by its activity as a disease modifier in models of short bowel syndrome (88) and cystic fibrosis (89). *IFRD1* has also been demonstrated to alter bone repair and axonal regrowth (85) in addition to the injury models discussed here. A puzzlingly diverse array of cellular functions have been ascribed to *IFRD1*, including modulating histone deacetylase activity (89, 90), inhibiting NF- κ B/RelA acetylation (90), repressing PGC-1 α expression (91), and negatively regulating BMP-2 signaling (92).

Following injury, *IFRD1* mRNA levels increase within hours and, unlike most other mRNAs whose translation is suppressed, translation of *IFRD1* mRNA is increased due to phosphorylation of eIF2-mediated leaky scanning of upstream ORF and reinitiation at the major AUG codon (93, 94). Despite mRNA and protein levels of *IFRD1* increasing early, loss of *IFRD1* manifests later in paligenosis. In *Ifrd1*^{-/-} mice following injury we observed that paligenotic cells had the expected initial decrease in mTORC1 activity and increase in autophagy as well as the induction of metaplastic genes. However, paligenotic cells lacking *IFRD1* do not efficiently reactivate mTORC1 and favor cell death over proliferation (85) (**Figure 2b**). This effect is at least partially due to stabilization of p53, as the phenotype of *Ifrd1* null mice was ameliorated in the double knockout [*Ifrd1*^{-/-}, *Trp53*^{-/-} (85)] (**Figure 2c**). However, other mechanisms are likely involved given the multiple pathways *IFRD1* affects (89–92). p53 itself seems to have a critical role in paligenosis, as it suppresses mTORC1 until DNA damage is cleared, thereby performing a key role in preventing mature cells (that may have accrued mutations in previous rounds of paligenosis or via recent ROS) from entering the cell cycle until their genome is intact, an aspect of paligenosis we detail below.

3.4. *DDIT4*, Another Paligenosis Gene

DDIT4, also known as *REDD1* (regulated in development and DNA damage 1), was identified in our screen for paligenosis-related genes. *DDIT4* appears to have evolved after *IFRD1* because there is no orthologous protein identified in yeast. *DDIT4* is best known to suppress mTORC1 indirectly via the TSC2 protein (95, 96), which is believed to occur via *DDIT4* releasing TSC2 from associating with its inhibitory 14-3-3 protein (97–100). Although it was originally proposed that *DDIT4* directly binds 14-3-3, structural evidence for this interaction is lacking (101). With 14-3-3 inhibition, TSC2 is released, facilitating the hydrolytic activity of RHEB (102), which is required for mTORC1 activity (103–108).

Like others, we found that suppression of mTORC depends on *DDIT4*, as *Ddit4*^{-/-} mice fail to tune down mTORC activity following injury (85). Accordingly, the autophagic response in the presence of persistent mTORC1 is not as robust, and consequently paligenotic cells proceed earlier to mitosis, often prior to fully scaling down cell architecture (85) (**Figure 2b,c**). The phenotype was similar to that observed in the *Trp53* null mice following injury (85).

3.5. Paligenosis-Like Processes

Paligenosis has been defined as a cellular process whereby a differentiated cell modulates mTORC1 and autophagy to augment plasticity and access a proliferative embryonic-like cell state (**Figure 2a**). We hypothesize that similar, but perhaps not identical, reactions to injury likely occur elsewhere and potentially in tissues that do not have the ability to proliferate. Moreover, it is clear that the decision to proliferate after injury can be separated from the downscaling and gene expression changes. For example, as discussed above, rapamycin-mediated inhibition of mTORC1 can block cells in a downscaled state expressing metaplastic genes yet not proliferating. In human tissue and in other, more chronic SPEM-inducing situations in mice, cells can reprogram into the SPEM phenotype without proliferating (109–111). Indeed, most SPEM in humans and in chronic mouse models (e.g., in mice infected with *Helicobacter* spp.) is actually not proliferative, so it is possible the first two stages of paligenosis may happen frequently while entry into the third stage is differentially regulated. Alternatively, we speculate that after a brief period of proliferation, redifferentiation may be required prior to another proliferative burst, and this may be an infrequent event (e.g., there is an additional unrecognized checkpoint that prevents dedifferentiated, metaplastic cells from continuously proliferating).

Another example of a paligenosis-like process is the regeneration after axotomy of neurons. It had been previously established that induction of autophagy promotes axonal regeneration (112) and similarly demonstrated that high mTORC1 activity is required for the process to occur (113, 114). Accordingly, we have observed that *IFRD1* was also necessary (85), and others have shown that ATF3 is critical for axon regeneration (115). Thus, even in cell types without the ability to proliferate, conserved molecular networks control reaction to injury. We look forward to having a much more extensive understanding of the conserved interaction of mTORC1, p53, *DDIT4*, *IFRD1*, and ATF3 across tissues and species.

4. PALIGENOSIS IS ADAPTIVE FOR MULTICELLULARITY BUT CARRIES RISKS FOR TUMORIGENESIS

Summarizing what we have discussed so far, we can say that the patterns of cell self-renewal and regeneration of tissues at homeostasis and after injury are diverse, and the Waddington, unidirectional model with a professional stem cell in a strict hierarchy is the exception, not the rule. In this

section, we examine multicellularity and paligenosis in an evolutionary context, beginning with how paligenosis might have evolved from stress responses in unicellular eukaryotes.

4.1. The Foundation of Paligenosis May Date Back to Yeast

The foundation of paligenosis, a process whereby differentiated cells in a multicellular organism change their differentiation state and are licensed to proliferate, may have originated in unicellular organisms. For example, following injury, *S. pombe* change from division via fission/mitosis to a meiotic state, which involves changes in differentiation including the generation of a shmoo. Mating via meiosis increases genetic diversity and provides the species a greater likelihood of surviving death or injury. To proceed to the meiotic phenotype following stress, *S. pombe* must downregulate mTOR (116–120) and induce autophagy (121, 122), completely analogous to Stages 1 and 2 of paligenosis. Interestingly, mutant screens in *S. pombe* implicate its IFRD1 ortholog in stress-induced meiosis and shmoo formation.

It is puzzling in some ways that the Waddington, professional stem cell theory of proliferation regulation grew to such hegemony given that the single-celled common ancestors of metazoans were able to (or had to) balance maintaining all their key organelles and special architecture while also being able to divide. In other words, being able to maintain cells with limited specialized subcellular architecture, whose only function is to divide and fuel other cells, is a special luxury of multicellular organisms. Studies of choanoflagellates, the closest known relative to animals, have been particularly helpful in understanding how multicellularity (and stem cells and paligenosis) might have evolved (123–125). These protists are generally unicellular organisms, but some species (e.g., *Salpingoeca rosetta*) also show facultative multicellularity, thereby modeling the transition from unicellularity to multicellularity (126, 127). Choanoflagellates are equipped with not only a nucleus/nucleolus and cell membrane, but also mitochondria, endoplasmic reticulum, a Golgi apparatus and associated vesicles, food vacuoles, and flagellum. Thus, a single cell is capable of accomplishing multiple functions that, by division of labor, would be shared by multiple specialized cell types in multicellular organisms (125, 128, 129). In terms of overall organismal complexity, such redundancy is inherently inefficient.

In another protist, the facultatively multicellular *Dictyostelium discoideum*, some additional division of cell labor has evolved with these organisms undergoing aggregative multicellularity versus the clonal multicellularity of choanoflagellates (125, 130). In *Dictyostelium*, mTOR plays a central role in cell dedifferentiation (80, 131), suggesting that paligenosis may be a universal feature of cell reprogramming.

Teleologically, multicellular organisms evolved in part because having a large number of cells allows division of labor, with cells differentiating to each be uniquely suited for a specific function. In the process of differentiation, cells scale up some subcellular features at the expense of others (132). However, when a multicellular organism relies on division of labor among multiple different cell types executing a different function, survival requires the ability to regulate cell numbers and health at homeostasis and replace damaged and lost cell populations following injury. In more complex multicellular organisms, cellular differentiation occurs within specialized organs comprising long-lived differentiated cells, with specific and diverse mechanisms required for cell renewal in homeostasis and after injury (133). Paligenosis likely evolved as one way for organisms to harmonize maximal, differentiated division of labor while retaining a contingency plan for regeneration after large-scale tissue damage.

Specialization also permits diverse organismal behavior, protecting the organism from predators and permitting adaptation into new environmental niches. Only in the context of a complex, organ-containing organism does a professional stem cell make adaptive sense. Even in this

context, the specialized professional stem cell, whose sole function is to proliferate, would be useful only to replace specific tissue compartments that are continuously lost. Accordingly, the somatic tissues in vertebrates with such professional stem cells are largely those subject to environmental insult: the skin, the lumen of the gastrointestinal tract, portions of the genitourinary tract, and the hematopoietic lineages. Tissues that interact daily with the external environment have a programmed loss of cell mass via shedding (i.e., anoikis) that creates a need for continuous renewal. Blood cells similarly undergo programmed loss via death/pruning (e.g., erythrocytes in the spleen or the kamikaze nature of neutrophils). In the vast majority of organ systems, the parenchyma comprises long-lived specialized cells that only rarely undergo programmed death. In such organs, existence of a cell maintained in a constantly less-specialized (undifferentiated) state, whose sole function is to divide and differentiate, would be as superfluous as it is in less complex organisms lacking dedicated organs.

Although large-scale regeneration of the type seen in more primitive metazoans or in plants (e.g., of limbs, heads, or branches) does not occur in many higher metazoans (134, 135), paligenosis may be a unique vestige of these ancestral injury-induced regenerative pathways. There is limited information on whether paligenosis functions in more primitive multicellular organisms, but that is potentially only because this question has not yet been asked.

4.2. Paligenosis Is a Double-Edged Sword: Critical for Repair but Risky for Cancer

In some ways, cancer is a unique phenomenon of complex multicellular organisms. The invasion, metastases, and death caused by cancer are possible only if there is a complex multicellular organism able to provide support and a niche for the high metabolic demands of these invasive rogue cells. Interestingly, in addition to the infrastructure provided by complex multicellular organisms, it appears that the genetic regulatory pathways that allow cancer to occur are also unique to complex multicellular organisms (136, 137). Trigou et al. (136) have suggested that cancer represents a breakdown of the molecular pathways evolved in higher organisms to restrain unicellular proliferative pathways. Accordingly, when TP53 is exogenously expressed in unicellular organisms (*S. pombe*) that lack an ortholog, it restrains proliferation (138), corroborating the hypothesis that TP53 suppresses ancestral proliferative pathways.

DDIT4 exemplifies the risks inherent to paligenosis. As discussed above, its best-described role is suppressing mTOR in the setting of DNA damage. Loss of *Ddit4* in mice causes cell cycle reentry in paligenosis despite DNA damage, which eventually, through cycles of paligenosis, increases tumorigenesis (139). The checkpoint that halts cells with DNA damage depends on TP53 suppressing the mTORC1 reactivation required for cell cycle reentry (**Figure 2**). Thus, it appears that the modulation of mTOR and autophagy are used by higher organisms as a pause/checkpoint to assess the state of the cell, allowing only healthy cells to proliferate. Another group has described a similar p53/*Ddit4*/mTOR checkpoint in tumor suppression (140). Thus, although cell plasticity may be essential to maintain cell populations that lack a stem cell after injury, it must be tightly regulated because the breakdown of licensing checkpoints can be fatal for the organism.

Another aspect of paligenosis with respect to tumorigenesis and multicellularity is that differentiated, functional cells in a complex organism are often long-lived. It is energetically wasteful to elaborate all the complex architecture to make such cells perform their function efficiently and then have those cells constantly turn over. However, paligenosis affords such long-lived cells a route to reenter the cell cycle and then redifferentiate over multiple cycles. Thus, such cells can accumulate mutations over time, each of which may be relatively innocuous, but eventually, an oncogenic mutation may arise, and certain combinations of mutations can lead to cancer. Such

a phenomenon has been illustrated in pancreatic acinar cells. Induction of constitutively active Kras^{G12D} GTPase promotes tumors; however, activated Kras is not sufficient to drive dedifferentiation in the absence of injury or inflammation (53, 141–143). Rather, mutant Kras^{G12D} must be expressed in cells that have undergone ADM for it to cause uncontrolled growth. Thus, mature differentiated cells can store an oncogenic mutation that becomes unmasked during paligenosis.

We have called this potentially dangerous, mutation-accumulating and -unmasking aspect of paligenosis the cyclical hit model (31, 60, 139). Given that professional stem cells have evolved to constantly generate cells that are quickly shed, we have argued that differentiated, paligenotic cells are much more likely the cells in which the multiple hits of mutations that cause tumors occur (31). Overall, although it is necessary for maintenance of many tissues that lack a professional stem cell, it would seem that licensing differentiated cells to proliferate is inherently dangerous. Moreover, because injury and/or inflammation induce paligenosis, it is possible that the long-understood correlation between inflammation and the development of adult cancer stems in part from this relationship.

5. A PROPOSED CLASSIFICATION OF TYPES OF CELLULAR PROLIFERATION IN ADULT TISSUES

As in most nascent fields, terminology and nomenclature are inconsistent, and this can lead to inappropriate interpretation of data (144). The take-home message from our review of the extant literature is that cell plasticity terminology is still a moving target and may need to be adjusted as future data and technologies become available.

Here, we propose a classification of different types of proliferative, regenerative cell behavior that occur in homeostasis and during injury. We do this in part to underscore that a unidirectional hierarchy model based on a multipotent professional stem cell is only one aspect of the complex patterns of proliferative cell behavior in multicellular organisms. Currently, we believe there is evidence for five different cell types (**Table 1**; see also **Figure 1d**). Type I is the professional stem cell. As discussed, many tissues and tissue compartments do not have such a cell and rely

Table 1 Proposed cell type classification based on basal and injury-induced plasticity

Type	Nomenclature	Proliferation time	Description	Examples
I	Constitutively dividing professional stem cell	Homeostasis, postinjury	Constantly dividing Undifferentiated	Intestine: LGR5 ⁺ CBC Stomach: isthmal stem cell Skin: basal epithelial cell Bone marrow: stem cell
II	Inducible progenitor	Homeostasis, postinjury	Mildly proliferative Some differentiated features	Skeletal muscle: satellite cell Intestine: +4 cell
III	Autoduplication	Homeostasis, paligenosis	Infrequent division Differentiated	Pancreas: acinar cell Stomach: chief cell Liver: hepatocyte
IV	Differentiated	Postinjury	No basal proliferation Differentiated	Intestine: Paneth cell Intestine: enterocyte Intestine: enteroendocrine cell
V	Terminally differentiated	Not applicable	No proliferation Differentiated	Heart: cardiomyocyte Nervous system: neuron

Abbreviation: CBC, crypt base columnar cell.

on the parenchyma for maintenance of cell population. This cell is constitutively proliferative and lacks differentiated cell features (note the small, granule-free isthmal gastric epithelial stem cell in **Figure 1d, subpanel i**). It is capable of self-replication and is multipotent, meaning it is able to generate multiple other distinct cell types in the tissue compartment. A subset of type I cells are highly proliferative progenitors that are more differentiated than the multipotent stem cells in a tissue and even more proliferative; this subset would include transit-amplifying cells in the small intestine and the various hematopoietic intermediate progenitor cell types like myeloid or lymphoid progenitors. Type II cells are less proliferative than the constitutively active stem cells but can be proliferative when activated. Like professional stem cells type II cells have some subcellular specialization. Intestinal stem cells exemplify this behavior. The behavior of mucous neck cells in the gastric epithelium has been less well described owing to the lack of good lineage tracing promoters, but they may also eventually be classified as type II (note that in **Figure 1d, subpanel ii**, the homeostatic, dividing neck cell is small but does have characteristic mucous granules). Type III cells are highly differentiated cells that maintain their own population at homeostasis via autoduplication (see, e.g., **Figure 1d, subpanel iii**). They are typically (if not always) in tissue compartments without professional stem cells. At times of need (e.g., after injury) they can be recruited as more proliferative, progenitor-like cells via paligenosis. This process involves downscaling of elaborate mature cell architecture and change in gene expression (metaplasia) that allows for more rapid regeneration of cells than can occur via single autoduplication events. Compare the large, autoduplicating pancreatic acinar cell in **Figure 1d, subpanel iii** (with all of its elaborate secretory function-associated machinery like abundant rough endoplasmic reticulum and secretory granules) with the much smaller paligenotic cell (**Figure 1d, subpanel iv**), which maintains only scattered granules (consistent with its origin as a digestive enzyme-secreting cell) and trace rough endoplasmic reticulum after massive downscaling for proliferation. Type IV cells have largely been defined in the intestine, where there has been abundant lineage tracing to determine relatively subtle differences in cell behavior. They are differentiated cells, known to be mostly maintained in homeostasis by a professional stem cell (type I). Genetic lineage tracing has demonstrated that injury-induced ablation of the stem cell causes these cells to revert to the stem cell lineage that originally spawned them. The cellular-molecular mechanisms that govern this reversion have not been described: they could potentially be similar to paligenosis in modulating mTOR and autophagy; however, this has not been specifically studied. Finally, type V cells are terminally differentiated and unable to reenter the cell cycle after embryonic development.

6. PALIGENOSIS OUTSIDE NORMAL TISSUE: IN VITRO MODELS AND CANCER CELLS

As described in the previous section, the behavior of cells in tissue is complex within each cell, even in how they execute mitosis, displaying considerable variation. One reason why paligenosis has taken so long to manifest itself as an innate cell program (versus mitosis, which was discovered centuries ago and apoptosis a half century ago) may be because it is a program of differentiated cells in tissue. Tissue culture is designed to make cells undergo mitosis, and cellular pathways governing mitosis involve numerous checkpoints that lead to apoptosis if cells cannot divide. Both processes are thus easy to model in vitro. However, paligenosis occurs in cells that do not grow—cells that remain quiescent mitotically but are highly active when metabolically performing their functions. The whole purpose of tissue culture, even of normal cells (as opposed to transformed cell lines), has largely been to coax cells to grow, which, by definition, means cultured cells are not maintained in a long-lived quiescent, functionally active state.

As previously discussed, paligenosis is likely critical for inducing a regenerative program that is precancerous (i.e., is metaplastic). But what about tumors themselves? If tumor cells originate from metaplasias that emerged via paligenosis, do tumors undergo some sort of paligenosis? The questions about tumor paligenosis and tissue culture paligenosis are linked because most in vitro models involve cultures of cells derived originally from tumors, with genes required for normal error checking in paligenosis (e.g., *TP53*) frequently mutated in cancer cell lines.

Evidence for paligenosis in tumors stems from studies like those of Rehman et al. (145), who recently demonstrated that following chemotherapy, colorectal cancer decreased mTOR activity and increased autophagy to enter a dedifferentiated state that they likened to embryonic diapause. In this state (akin to the end of paligenosis Stage 1), they found the cells able to resist chemotherapy, slowly cycling, and able to emerge from relative quiescence after injury. They also found that autophagy was required to maintain viability as energy was shifted from anabolic to catabolic. All of these features are consistent with the molecular features of paligenosis that give differentiated cells the ability to become proliferative. Because cancer generally maintains some differentiated features from its parent tissue (e.g., pathologists grade them histologically as poorly, moderately, or highly differentiated), perhaps tumor cells have a low threshold for paligenosis that allows them to cycle between the mitotically quiescent (i.e., a quasi-differentiated state) and proliferative states. Clearly, much remains to be investigated along these lines.

Organoids may offer a unique opportunity to study paligenosis in normal or cancerous tissues in vitro. Organoids can be derived from biopsied or resected adult tissue as well as differentiated entirely in vitro from embryonic or induced pluripotent stem cells. In both cases, normal organoids would be presumably free of the types of mutations that permit the cancer cell lines to grow indefinitely in an unrestrained fashion. Unlike most cancer cell lines, organoids can be coaxed from a proliferative state that increases cell mass to differentiate by either reducing the concentration of specific media components or growing the organoids on a substrate, allowing media on one side and open atmospheric air on the other (the air-liquid interface) (146–149). Some investigators have referred to organoids that grow without substantial differentiation as stem cell organoids (150, 151), but such continuously proliferating organoids also exemplify a type of perpetual tissue plasticity because organoids have to continuously react to the stress of passaging, a sort of tissue injury. It will be interesting to see the behavior of epithelial cells in organoids as organoid culture becomes more sophisticated: adding mesenchyme and other cells that might mimic the cellular niche as opposed to growing organoids in a generic complex of extracellular proteins and with a cocktail of growth factors. Establishing such conditions that recapitulate the tonic stimulation present in vivo could continuously promote a differentiated state. Truly being able to switch organoids from an in vivo, quiescent, differentiating state to an injury-responsive state might help us study in vitro-specific mechanisms of paligenosis-like modulation of mTORC1 activity and autophagy along with specific paligenosis-related signaling cascades.

Clearly, much work needs to be done to better understand paligenosis in tumors and to develop in vitro models of paligenosis, but organoids appear to be a useful starting point.

7. CONCLUSIONS AND FUTURE DIRECTIONS

Considering how widespread tissue plasticity is following injury, in the formation of cancer, and potentially at homeostasis, the precise, conserved cellular-molecular events that govern switches in cellular identity should be a central focus of study. We have taken some forays into studying such mechanisms using rapid, drug-induced mouse injury models. However, there is huge potential for studying roles for autophagy and mTOR (and IFRD1 and DDIT4) in numerous systems where plasticity plays a critical role. For example, potential differences between our proposed

type III and type IV cell proliferation behavior might be elucidated by delving into the sequence of cellular-molecular events within each intestinal epithelial cell type sequentially over time after initial injury. There is some indication that the process involves modulation of mTOR (83, 152); however, earlier time points are necessary to determine whether there is biphasic modulation, as we have demonstrated in the stomach and pancreas (65, 85).

Numerous other fundamental questions abound. Do some differentiated cells maintain this ancestral, cell cycle reentry mechanism, whereas others lose it? In the stomach, acid-secreting parietal cells never seem to reenter the cell cycle; they either survive injury or undergo programmed cell death. So, are chief cells the only cell type in the stomach capable of paligenosis? As alluded to above, are any mature cells and/or their partially differentiated progenitor in the small intestine capable of paligenosis? Following injury, they are clearly capable of dedifferentiating into a professional stem cell.

Clearly, we are just at the beginning of what we can learn about how cell plasticity informs our understanding of evolution, regeneration, and cancer. Moreover, plasticity-specific pathways, in particular, those governing paligenosis, might be exploited for therapy to encourage regeneration and discourage cancer in novel ways that differ from our current therapeutic strategies that largely target apoptosis and mitosis. Paligenosis-modulating drugs may have advantages, given that, unlike apoptosis and mitosis, paligenosis is largely a feature restricted to the injury response and so, in an otherwise normal person, paligenotic pathways may be specific to regeneration and impose cell fidelity checkpoints that would discourage the formation of cancer.

DISCLOSURE STATEMENT

The authors are not aware of any affiliations, memberships, funding, or financial holdings that might be perceived as affecting the objectivity of this review.

ACKNOWLEDGMENTS

J.W.B. is supported by the US Department of Defense, through the PRCRP under award W81XWH-20-1-0630; US National Institutes of Health (NIH) grants T32 DK007130-42 and NIH R21 AI156236; the Digestive Disease Research Core Centers Pilot and Feasibility Grant as part of P30 DK052574; the Doris Duke Charitable Foundation Fund to Retain Clinical Scientists; and the American Gastroenterological Association grant AGA2021-5101. C.J.C. is supported by the NIH National Cancer Institute grant T32 CA009547. J.C.M. is supported by the NIH National Cancer Institute (R01CA239645, R01CA246208), National Institute of Diabetes and Digestive and Kidney Diseases (R21 DK111369, R01DK094989, R01DK105129, R01DK110406), and the BETRNet (U54 CA163060).

LITERATURE CITED

1. Waddington CH. 1940. *Organisers and Genes*. Cambridge, UK: Cambridge Univ. Press
2. Takahashi K, Yamanaka S. 2006. Induction of pluripotent stem cells from mouse embryonic and adult fibroblast cultures by defined factors. *Cell* 126:663-76
3. Takahashi K, Tanabe K, Ohnuki M, Narita M, Ichisaka T, et al. 2007. Induction of pluripotent stem cells from adult human fibroblasts by defined factors. *Cell* 131:861-72
4. Spatz LB, Jin RU, Mills JC. 2021. Cellular plasticity at the nexus of development and disease. *Development* 148:dev197392
5. Shivdasani RA, Clevers H, de Sauvage FJ. 2021. Tissue regeneration: Reserve or reverse? *Science* 371:784-86

6. Rajagopal J, Stanger BZ. 2016. Plasticity in the adult: How should the Waddington diagram be applied to regenerating tissues? *Dev. Cell* 36:133–37
7. Chen T, Oh S, Gregory S, Shen X, Diehl AM. 2020. Single-cell omics analysis reveals functional diversification of hepatocytes during liver regeneration. *JCI Insight* 5:e141024
8. Luyten A, Zang C, Liu XS, Shivdasani RA. 2014. Active enhancers are delineated de novo during hematopoiesis, with limited lineage fidelity among specified primary blood cells. *Genes Dev.* 28:1827–39
9. Fukushima T, Tanaka Y, Hamey FK, Chang CH, Oki T, et al. 2019. Discrimination of dormant and active hematopoietic stem cells by G0 marker reveals dormancy regulation by cytoplasmic calcium. *Cell Rep.* 29:4144–58.e7
10. Baldrige MT, King KY, Boles NC, Weksberg DC, Goodell MA. 2010. Quiescent haematopoietic stem cells are activated by IFN- γ in response to chronic infection. *Nature* 465:793–97
11. Haas S, Hansson J, Klimmeck D, Loeffler D, Velten L, et al. 2015. Inflammation-induced emergency megakaryopoiesis driven by hematopoietic stem cell-like megakaryocyte progenitors. *Cell Stem Cell* 17:422–34
12. Hume WJ, Potten CS. 1982. A long-lived thymidine pool in epithelial stem cells. *Cell Tissue Kinet.* 15:49–58
13. Fujita R, Jamet S, Lean G, Cheng HCM, Hebert S, et al. 2021. Satellite cell expansion is mediated by P-eIF2 α -dependent *Tacc3* translation. *Development* 148:dev194480
14. Snippert HJ, van der Flier LG, Sato T, van Es JH, van den Born M, et al. 2010. Intestinal crypt homeostasis results from neutral competition between symmetrically dividing Lgr5 stem cells. *Cell* 143:134–44
15. Waddington CH. 1957. *The Strategy of the Genes: A Discussion of Some Aspects of Theoretical Biology*. London: Allen & Unwin
16. Bankaitis ED, Ha A, Kuo CJ, Magness ST. 2018. Reserve stem cells in intestinal homeostasis and injury. *Gastroenterology* 155:1348–61
17. Barker N, van Es JH, Kuipers J, Kujala P, van den Born M, et al. 2007. Identification of stem cells in small intestine and colon by marker gene *Lgr5*. *Nature* 449:1003–7
18. Sato T, Vries RG, Snippert HJ, van de Wetering M, Barker N, et al. 2009. Single Lgr5 stem cells build crypt-villus structures *in vitro* without a mesenchymal niche. *Nature* 459:262–65
19. de Lau W, Barker N, Low TY, Koo BK, Li VS, et al. 2011. Lgr5 homologues associate with Wnt receptors and mediate R-spondin signalling. *Nature* 476:293–97
20. Burclaff J, Mills JC. 2018. Plasticity of differentiated cells in wound repair and tumorigenesis, part II: skin and intestine. *Dis. Model Mech.* 11:dmm035071
21. Li L, Clevers H. 2010. Coexistence of quiescent and active adult stem cells in mammals. *Science* 327:542–45
22. Willet SG, Mills JC. 2016. Stomach organ and cell lineage differentiation: from embryogenesis to adult homeostasis. *Cell. Mol. Gastroenterol. Hepatol.* 2:546–59
23. Han S, Fink J, Jorg DJ, Lee E, Yum MK, et al. 2019. Defining the identity and dynamics of adult gastric isthmus stem cells. *Cell Stem Cell* 25:342–56.e7
24. Burclaff J, Willet SG, Saenz JB, Mills JC. 2020. Proliferation and differentiation of gastric mucous neck and chief cells during homeostasis and injury-induced metaplasia. *Gastroenterology* 158:598–609.e5
25. Yan KS, Chia LA, Li X, Ootani A, Su J, et al. 2012. The intestinal stem cell markers Bmi1 and Lgr5 identify two functionally distinct populations. *PNAS* 109:466–71
26. Sangiorgi E, Capecchi MR. 2008. Bmi1 is expressed *in vivo* in intestinal stem cells. *Nat. Genet.* 40:915–20
27. Takeda N, Jain R, LeBoeuf MR, Wang Q, Lu MM, Epstein JA. 2011. Interconversion between intestinal stem cell populations in distinct niches. *Science* 334:1420–24
28. Montgomery RK, Carlone DL, Richmond CA, Farilla L, Kranendonk ME, et al. 2011. Mouse telomerase reverse transcriptase (mTert) expression marks slowly cycling intestinal stem cells. *PNAS* 108:179–84
29. Powell AE, Wang Y, Li Y, Poulin EJ, Means AL, et al. 2012. The pan-ErbB negative regulator Lrig1 is an intestinal stem cell marker that functions as a tumor suppressor. *Cell* 149:146–58
30. Wong VWY, Stange DE, Page ME, Buczaeki S, Wabik A, et al. 2012. Lrig1 controls intestinal stem-cell homeostasis by negative regulation of ErbB signalling. *Nat. Cell Biol.* 14:401–8
31. Mills JC, Sansom OJ. 2015. Reserve stem cells: differentiated cells reprogram to fuel repair, metaplasia, and neoplasia in the adult gastrointestinal tract. *Sci. Signal* 8:re8

32. Jones JC, Brindley CD, Elder NH, Myers MG Jr., Rajala MW, et al. 2019. Cellular plasticity of *Defa4^{Cre}*-expressing paneth cells in response to notch activation and intestinal injury. *Cell. Mol. Gastroenterol. Hepatol.* 7:533–54
33. Schmitt M, Schewe M, Sacchetti A, Feijtel D, van de Geer WS, et al. 2018. Paneth cells respond to inflammation and contribute to tissue regeneration by acquiring stem-like features through SCF/c-Kit signaling. *Cell Rep.* 24:2312–28.e7
34. Asfaha S, Hayakawa Y, Muley A, Stokes S, Graham TA, et al. 2015. *Krt19⁺/Lgr5⁻* cells are radioresistant cancer-initiating stem cells in the colon and intestine. *Cell Stem Cell* 16:627–38
35. Buczacki SJ, Zecchini HI, Nicholson AM, Russell R, Vermeulen L, et al. 2013. Intestinal label-retaining cells are secretory precursors expressing Lgr5. *Nature* 495:65–69
36. Ishibashi F, Shimizu H, Nakata T, Fujii S, Suzuki K, et al. 2018. Contribution of ATOH1⁺ cells to the homeostasis, repair, and tumorigenesis of the colonic epithelium. *Stem Cell Rep.* 10:27–42
37. Tetteh PW, Basak O, Farin HF, Wiebrands K, Kretzschmar K, et al. 2016. Replacement of lost Lgr5-positive stem cells through plasticity of their enterocyte-lineage daughters. *Cell Stem Cell* 18:203–13
38. Tian H, Biehs B, Warming S, Leong KG, Rangell L, et al. 2011. A reserve stem cell population in small intestine renders Lgr5-positive cells dispensable. *Nature* 478:255–59
39. Yan KS, Gevaert O, Zheng GXY, Anchang B, Probert CS, et al. 2017. Intestinal enteroendocrine lineage cells possess homeostatic and injury-inducible stem cell activity. *Cell Stem Cell* 21:78–90.e6
40. van Es JH, Wiebrands K, Lopez-Iglesias C, van de Wetering M, Zeinstra L, et al. 2019. Enteroendocrine and tuft cells support Lgr5 stem cells on Paneth cell depletion. *PNAS* 116:26599–605
41. Chandrakesan P, May R, Qu D, Weygant N, Taylor VE, et al. 2015. Dclk1⁺ small intestinal epithelial tuft cells display the hallmarks of quiescence and self-renewal. *Oncotarget* 6:30876–86
42. Weng PL, Aure MH, Maruyama T, Ovitt CE. 2018. Limited regeneration of adult salivary glands after severe injury involves cellular plasticity. *Cell Rep.* 24:1464–70.e3
43. Sangiorgi E, Capecchi MR. 2009. *Bmi1* lineage tracing identifies a self-renewing pancreatic acinar cell subpopulation capable of maintaining pancreatic organ homeostasis. *PNAS* 106:7101–6
44. Yanger K, Knigin D, Zong Y, Maggs L, Gu G, et al. 2014. Adult hepatocytes are generated by self-duplication rather than stem cell differentiation. *Cell Stem Cell* 15:340–49
45. Wollny D, Zhao S, Everlien I, Lun X, Brunken J, et al. 2016. Single-cell analysis uncovers clonal acinar cell heterogeneity in the adult pancreas. *Dev. Cell* 39:289–301
46. Marescal O, Cheeseman IM. 2020. Cellular mechanisms and regulation of quiescence. *Dev. Cell* 55:259–71
47. Grimont A, Leach SD, Chandwani R. 2021. Uncertain beginnings: acinar and ductal cell plasticity in the development of pancreatic cancer. *Cell. Mol. Gastroenterol. Hepatol.* In press. <https://doi.org/10.1016/j.jcmgh.2021.07.014>
48. Habbe N, Shi G, Meguid RA, Fendrich V, Esni F, et al. 2008. Spontaneous induction of murine pancreatic intraepithelial neoplasia (mPanIN) by acinar cell targeting of oncogenic Kras in adult mice. *PNAS* 105:18913–18
49. Shi G, Zhu L, Sun Y, Bettencourt R, Damsz B, et al. 2009. Loss of the acinar-restricted transcription factor Mist1 accelerates Kras-induced pancreatic intraepithelial neoplasia. *Gastroenterology* 136:1368–78
50. Baumgart M, Werther M, Bockholt A, Scheurer M, Ruschoff J, et al. 2010. Genomic instability at both the base pair level and the chromosomal level is detectable in earliest PanIN lesions in tissues of chronic pancreatitis. *Pancreas* 39:1093–103
51. Hill R, Calvopina JH, Kim C, Wang Y, Dawson DW, et al. 2010. PTEN loss accelerates *Kras^{G12D}*-induced pancreatic cancer development. *Cancer Res.* 70:7114–24
52. Bailey JM, Alsina J, Rasheed ZA, McAllister FM, Fu YY, et al. 2014. DCLK1 marks a morphologically distinct subpopulation of cells with stem cell properties in preinvasive pancreatic cancer. *Gastroenterology* 146:245–56
53. Guerra C, Schuhmacher AJ, Canamero M, Grippo PJ, Verdager L, et al. 2007. Chronic pancreatitis is essential for induction of pancreatic ductal adenocarcinoma by K-Ras oncogenes in adult mice. *Cancer Cell* 11:291–302

54. Hruban RH, Adsay NV, Albores-Saavedra J, Anver MR, Biankin AV, et al. 2006. Pathology of genetically engineered mouse models of pancreatic exocrine cancer: consensus report and recommendations. *Cancer Res.* 66:95–106
55. Tuveson DA, Hingorani SR. 2005. Ductal pancreatic cancer in humans and mice. *Cold Spring Harb. Symp. Quant. Biol.* 70:65–72
56. Chen F, Jimenez RJ, Sharma K, Luu HY, Hsu BY, et al. 2020. Broad distribution of hepatocyte proliferation in liver homeostasis and regeneration. *Cell Stem Cell* 26:27–33.e4
57. Goldenring JR. 2018. Pyloric metaplasia, pseudopyloric metaplasia, ulcer-associated cell lineage and spasmodic polypeptide-expressing metaplasia: reparative lineages in the gastrointestinal mucosa. *J. Pathol.* 245:132–37
58. Bockerstett KA, Lewis SA, Wolf KJ, Noto CN, Jackson NM, et al. 2020. Single-cell transcriptional analyses of spasmodic polypeptide-expressing metaplasia arising from acute drug injury and chronic inflammation in the stomach. *Gut* 69:1027–38
59. Schmidt PH, Lee JR, Joshi V, Playford RJ, Poulson R, et al. 1999. Identification of a metaplastic cell lineage associated with human gastric adenocarcinoma. *Lab. Investig.* 79:639–46
60. Jin RU, Mills JC. 2019. The cyclical hit model: how paligenosis might establish the mutational landscape in Barrett's esophagus and esophageal adenocarcinoma. *Curr. Opin. Gastroenterol.* 35:363–70
61. Halldorsdottir AM, Sigurdardottrir M, Jonasson JG, Oddsdottir M, Magnusson J, et al. 2003. Spasmodic polypeptide-expressing metaplasia (SPEM) associated with gastric cancer in Iceland. *Dig. Dis. Sci.* 48:431–41
62. Lennerz JK, Kim SH, Oates EL, Huh WJ, Doherty JM, et al. 2010. The transcription factor MIST1 is a novel human gastric chief cell marker whose expression is lost in metaplasia, dysplasia, and carcinoma. *Am. J. Pathol.* 177:1514–33
63. Saenz JB, Mills JC. 2018. Acid and the basis for cellular plasticity and reprogramming in gastric repair and cancer. *Nat. Rev. Gastroenterol. Hepatol.* 15:257–73
64. Adami JG. 1900. On growth and overgrowth and on the relationship between cell differentiation and proliferative capacity; its bearing upon the regeneration of tissues and the development of tumors. In *Festschrift in Honor of Abraham Jacobi, M.D., L.L.D.: To Commemorate the Seventieth Anniversary of his Birth, May Sixth, 1900*, pp. 422–32. New Rochelle, NY: Knickerbocker Press
65. Willet SG, Lewis MA, Miao ZF, Liu D, Radyk MD, et al. 2018. Regenerative proliferation of differentiated cells by mTORC1-dependent paligenosis. *EMBO J.* 37:e98311
66. Radyk MD, Spatz LB, Pena BL, Brown JW, Burclaff J, et al. 2021. ATF3 induces RAB7 to govern autodegradation in paligenosis, a conserved cell plasticity program. *EMBO Rep.* 22:e51806
67. Meyer AR, Engevik AC, Willet SG, Williams JA, Zou Y, et al. 2019. Cystine/glutamate antiporter (xCT) is required for chief cell plasticity after gastric injury. *Cell. Mol. Gastroenterol. Hepatol.* 8:379–405
68. Petersen CP, Weis VG, Nam KT, Sousa JF, Fingleton B, Goldenring JR. 2014. Macrophages promote progression of spasmodic polypeptide-expressing metaplasia after acute loss of parietal cells. *Gastroenterology* 146:1727–38.e8
69. Meyer AR, Engevik AC, Madorsky T, Belmont E, Stier MT, et al. 2020. Group 2 innate lymphoid cells coordinate damage response in the stomach. *Gastroenterology* 159:2077–91.e8
70. De Salvo C, Pastorelli L, Petersen CP, Butto LF, Buela KA, et al. 2021. Interleukin 33 triggers early eosinophil-dependent events leading to metaplasia in a chronic model of gastritis-prone mice. *Gastroenterology* 160:302–16.e7
71. Bockerstett KA, Petersen CP, Noto CN, Kuehm LM, Wong CF, et al. 2020. Interleukin 27 protects from gastric atrophy and metaplasia during chronic autoimmune gastritis. *Cell. Mol. Gastroenterol. Hepatol.* 10:561–79
72. Bockerstett KA, Osaki LH, Petersen CP, Cai CW, Wong CF, et al. 2018. Interleukin-17A promotes parietal cell atrophy by inducing apoptosis. *Cell. Mol. Gastroenterol. Hepatol.* 5:678–90.e1
73. Miao ZF, Lewis MA, Cho CJ, Adkins-Threats M, Park D, et al. 2020. A dedicated evolutionarily conserved molecular network licenses differentiated cells to return to the cell cycle. *Dev. Cell* 55:178–94.e7
74. Saera-Vila A, Kish PE, Louie KW, Grzegorski SJ, Klionsky DJ, Kahana A. 2016. Autophagy regulates cytoplasmic remodeling during cell reprogramming in a zebrafish model of muscle regeneration. *Autophagy* 12:1864–75

75. Sarraf SA, Youle RJ. 2018. Parkin mediates mitophagy during beige-to-white fat conversion. *Sci. Signal* 11:eaat1082
76. Lu X, Altshuler-Keylin S, Wang Q, Chen Y, Henrique Sponton C, et al. 2018. Mitophagy controls beige adipocyte maintenance through a Parkin-dependent and UCP1-independent mechanism. *Sci. Signal* 11:eaap8526
77. Altshuler-Keylin S, Shinoda K, Hasegawa Y, Ikeda K, Hong H, et al. 2016. Beige adipocyte maintenance is regulated by autophagy-induced mitochondrial clearance. *Cell Metab.* 24:402–19
78. Espeillac C, Mitchell C, Celton-Morizur S, Chauvin C, Koka V, et al. 2011. S6 kinase 1 is required for rapamycin-sensitive liver proliferation after mouse hepatectomy. *J. Clin. Investig.* 121:2821–32
79. Crane ED, Wong W, Zhang H, O'Neil G, Crane JD. 2021. AMPK inhibits mTOR-driven keratinocyte proliferation after skin damage and stress. *J. Investig. Dermatol.* 141:2170–77.e3
80. Brunkard JO. 2020. Exaptive evolution of target of rapamycin signaling in multicellular eukaryotes. *Dev. Cell* 54:142–55
81. Johnson NM, Lengner CJ. 2020. MTORC1 and the rebirth of stemness. *Dev. Cell* 55:113–15
82. Rodgers JT, King KY, Brett JO, Cromie MJ, Charville GW, et al. 2014. mTORC1 controls the adaptive transition of quiescent stem cells from G₀ to G_{Alert}. *Nature* 510:393–96
83. Bohin N, McGowan KP, Keeley TM, Carlson EA, Yan KS, Samuelson LC. 2020. Insulin-like growth factor-1 and mTORC1 signaling promote the intestinal regenerative response after irradiation injury. *Cell. Mol. Gastroenterol. Hepatol.* 10:797–810
84. Wang S, Xia P, Ye B, Huang G, Liu J, Fan Z. 2013. Transient activation of autophagy via Sox2-mediated suppression of mTOR is an important early step in reprogramming to pluripotency. *Cell Stem Cell* 13:617–25
85. Miao ZF, Lewis MA, Cho CJ, Adkins-Threats M, Park D, et al. 2020. A dedicated evolutionarily conserved molecular network licenses differentiated cells to return to the cell cycle. *Dev. Cell* 55:178–94.e7
86. Tirone F, Shooter EM. 1989. Early gene regulation by nerve growth factor in PC12 cells: induction of an interferon-related gene. *PNAS* 86:2088–92
87. Viator I, Huber LA. 2007. Role of TIS7 family of transcriptional regulators in differentiation and regeneration. *Differentiation* 75:891–97
88. Garcia AM, Wakeman D, Lu J, Rowley C, Geisman T, et al. 2014. *Tis7* deletion reduces survival and induces intestinal anastomotic inflammation and obstruction in high-fat diet-fed mice with short bowel syndrome. *Am. J. Physiol. Gastrointest. Liver Physiol.* 307:G642–54
89. Gu Y, Harley IT, Henderson LB, Aronow BJ, Viator I, et al. 2009. Identification of *IFRD1* as a modifier gene for cystic fibrosis lung disease. *Nature* 458:1039–42
90. Tummers B, Goedemans R, Pelascini LP, Jordanova ES, van Esch EM, et al. 2015. The interferon-related developmental regulator 1 is used by human papillomavirus to suppress NFκB activation. *Nat. Commun.* 6:6537
91. Park G, Horie T, Kanayama T, Fukasawa K, Iezaki T, et al. 2017. The transcriptional modulator *Ifrd1* controls PGC-1α expression under short-term adrenergic stimulation in brown adipocytes. *FEBS J.* 284:784–95
92. Onishi Y, Park G, Iezaki T, Horie T, Kanayama T, et al. 2017. The transcriptional modulator *Ifrd1* is a negative regulator of BMP-2-dependent osteoblastogenesis. *Biochem. Biophys. Res. Commun.* 482:329–34
93. Andreev DE, O'Connor PB, Fahey C, Kenny EM, Terenin IM, et al. 2015. Translation of 5' leaders is pervasive in genes resistant to eIF2 repression. *eLife* 4:e03971
94. Zhao C, Datta S, Mandal P, Xu S, Hamilton T. 2010. Stress-sensitive regulation of *IFRD1* mRNA decay is mediated by an upstream open reading frame. *J. Biol. Chem.* 285:8552–62
95. Reiling JH, Hafen E. 2004. The hypoxia-induced paralogs *Scylla* and *Charybdis* inhibit growth by down-regulating S6K activity upstream of TSC in *Drosophila*. *Genes Dev.* 18:2879–92
96. Corradetti MN, Inoki K, Guan KL. 2005. The stress-induced proteins RTP801 and RTP801L are negative regulators of the mammalian target of rapamycin pathway. *J. Biol. Chem.* 280:9769–72
97. DeYoung MP, Horak P, Sofer A, Sgroi D, Ellisen LW. 2008. Hypoxia regulates TSC1/2-mTOR signaling and tumor suppression through REDD1-mediated 14–3–3 shuttling. *Genes Dev.* 22:239–51
98. Hernandez G, Lal H, Fidalgo M, Guerrero A, Zalvide J, et al. 2011. A novel cardioprotective p38-MAPK/mTOR pathway. *Exp. Cell Res.* 317:2938–49

99. Pieri BL, Souza DR, Luciano TF, Marques SO, Pauli JR, et al. 2014. Effects of physical exercise on the P38MAPK/REDD1/14-3-3 pathways in the myocardium of diet-induced obesity rats. *Horm. Metab. Res.* 46:621–27
100. Favier FB, Costes F, Defour A, Bonnefoy R, Lefai E, et al. 2010. Downregulation of Akt/mammalian target of rapamycin pathway in skeletal muscle is associated with increased REDD1 expression in response to chronic hypoxia. *Am. J. Physiol. Regul. Integr. Comp. Physiol.* 298:R1659–66
101. Vega-Rubin-de-Celis S, Abdallah Z, Kinch L, Grishin NV, Brugarolas J, Zhang X. 2010. Structural analysis and functional implications of the negative mTORC1 regulator REDD1. *Biochemistry* 49:2491–501
102. Zhang Y, Gao X, Saucedo LJ, Ru B, Edgar BA, Pan D. 2003. Rheb is a direct target of the tuberous sclerosis tumour suppressor proteins. *Nat. Cell Biol.* 5:578–81
103. Stocker H, Radimerski T, Schindelholz B, Wittwer F, Belawat P, et al. 2003. Rheb is an essential regulator of S6K in controlling cell growth in *Drosophila*. *Nat. Cell Biol.* 5:559–65
104. Garami A, Zwartkruis FJ, Nobukuni T, Joaquin M, Rocco M, et al. 2003. Insulin activation of Rheb, a mediator of mTOR/S6K/4E-BP signaling, is inhibited by TSC1 and 2. *Mol. Cell* 11:1457–66
105. Castro AF, Rebhun JF, Clark GJ, Quilliam LA. 2003. Rheb binds tuberous sclerosis complex 2 (TSC2) and promotes S6 kinase activation in a rapamycin- and farnesylation-dependent manner. *J. Biol. Chem.* 278:32493–96
106. Tee AR, Manning BD, Roux PP, Cantley LC, Blenis J. 2003. Tuberous sclerosis complex gene products, Tuberin and Hamartin, control mTOR signaling by acting as a GTPase-activating protein complex toward Rheb. *Curr. Biol.* 13:1259–68
107. Inoki K, Li Y, Xu T, Guan KL. 2003. Rheb GTPase is a direct target of TSC2 GAP activity and regulates mTOR signaling. *Genes Dev.* 17:1829–34
108. Long X, Lin Y, Ortiz-Vega S, Yonezawa K, Avruch J. 2005. Rheb binds and regulates the mTOR kinase. *Curr. Biol.* 15:702–13
109. Radyk MD, Burclaff J, Willet SG, Mills JC. 2018. Metaplastic cells in the stomach arise, independently of stem cells, via dedifferentiation or transdifferentiation of chief cells. *Gastroenterology* 154:839–43.e2
110. Jeong S, Choi E, Petersen CP, Roland JT, Federico A, et al. 2017. Distinct metaplastic and inflammatory phenotypes in autoimmune and adenocarcinoma-associated chronic atrophic gastritis. *United Eur. Gastroenterol. J.* 5:37–44
111. Riera KM, Jang B, Min J, Roland JT, Yang Q, et al. 2020. Trop2 is upregulated in the transition to dysplasia in the metaplastic gastric mucosa. *J. Pathol.* 251:336–47
112. He M, Ding Y, Chu C, Tang J, Xiao Q, Luo ZG. 2016. Autophagy induction stabilizes microtubules and promotes axon regeneration after spinal cord injury. *PNAS* 113:11324–29
113. Abe N, Borson SH, Gambello MJ, Wang F, Cavalli V. 2010. Mammalian target of rapamycin (mTOR) activation increases axonal growth capacity of injured peripheral nerves. *J. Biol. Chem.* 285:28034–43
114. Carlin D, Halevi AE, Ewan EE, Moore AM, Cavalli V. 2019. Nociceptor deletion of Tsc2 enhances axon regeneration by inducing a conditioning injury response in dorsal root ganglia. *eNeuro* 6:ENEURO.0168-19.2019
115. Gey M, Wanner R, Schilling C, Pedro MT, Sinske D, Knoll B. 2016. *Atf3* mutant mice show reduced axon regeneration and impaired regeneration-associated gene induction after peripheral nerve injury. *Open Biol.* 6:160091
116. Otsubo Y, Yamashita A, Ohno H, Yamamoto M. 2014. *S. pombe* TORC1 activates the ubiquitin-proteasomal degradation of the meiotic regulator Mei2 in cooperation with Pat1 kinase. *J. Cell Sci.* 127:2639–46
117. Nakase Y, Fukuda K, Chikashige Y, Tsutsumi C, Morita D, et al. 2006. A defect in protein farnesylation suppresses a loss of *Schizosaccharomyces pombe tsc2⁺*, a homolog of the human gene predisposing to tuberous sclerosis complex. *Genetics* 173:569–78
118. Matsumoto S, Bandyopadhyay A, Kwiatkowski DJ, Maitra U, Matsumoto T. 2002. Role of the Tsc1-Tsc2 complex in signaling and transport across the cell membrane in the fission yeast *Schizosaccharomyces pombe*. *Genetics* 161:1053–63
119. Valbuena N, Moreno S. 2010. TOR and PKA pathways synergize at the level of the Ste11 transcription factor to prevent mating and meiosis in fission yeast. *PLOS ONE* 5:e11514

120. Alvarez B, Moreno S. 2006. Fission yeast Tor2 promotes cell growth and represses cell differentiation. *J. Cell Sci.* 119:4475–85
121. Matsuhara H, Yamamoto A. 2016. Autophagy is required for efficient meiosis progression and proper meiotic chromosome segregation in fission yeast. *Genes Cells* 21:65–87
122. Nakashima A, Hasegawa T, Mori S, Ueno M, Tanaka S, et al. 2006. A starvation-specific serine protease gene, *isp6⁺*, is involved in both autophagy and sexual development in *Schizosaccharomyces pombe*. *Curr. Genet.* 49:403–13
123. Carr M, Leadbeater BS, Hassan R, Nelson M, Baldauf SL. 2008. Molecular phylogeny of choanoflagellates, the sister group to Metazoa. *PNAS* 105:16641–46
124. Ruiz-Trillo I, Roger AJ, Burger G, Gray MW, Lang BF. 2008. A phylogenomic investigation into the origin of metazoa. *Mol. Biol. Evol.* 25:664–72
125. Brunet T, King N. 2017. The origin of animal multicellularity and cell differentiation. *Dev. Cell* 43:124–40
126. Levin TC, Greaney AJ, Wetzel L, King N. 2014. The *rosetteless* gene controls development in the choanoflagellate *S. rosetta*. *eLife* 3:e04070
127. Leadbeater BSC. 2015. *The Choanoflagellates: Evolution, Biology, and Ecology*. Cambridge, UK: Cambridge Univ. Press
128. Laundon D, Larson BT, McDonald K, King N, Burkhardt P. 2019. The architecture of cell differentiation in choanoflagellates and sponge choanocytes. *PLOS Biol.* 17:e3000226
129. Arendt D, Denes AS, Jekely G, Tessmar-Raible K. 2008. The evolution of nervous system centralization. *Philos. Trans. R. Soc. B* 363:1523–28
130. Strassmann JE, Zhu Y, Queller DC. 2000. Altruism and social cheating in the social amoeba *Dictyostelium discoideum*. *Nature* 408:965–67
131. Nichols JM, Antolovic V, Reich JD, Brameyer S, Paschke P, Chubb JR. 2020. Cell and molecular transitions during efficient dedifferentiation. *eLife* 9:e55435
132. Mills JC, Taghert PH. 2012. Scaling factors: transcription factors regulating subcellular domains. *Bioessays* 34:10–16
133. Michod RE. 2007. Evolution of individuality during the transition from unicellular to multicellular life. *PNAS* 104(Suppl. 1):8613–18
134. Slack JM. 2017. Animal regeneration: ancestral character or evolutionary novelty? *EMBO Rep.* 18:1497–508
135. Ikeuchi M, Ogawa Y, Iwase A, Sugimoto K. 2016. Plant regeneration: cellular origins and molecular mechanisms. *Development* 143:1442–51
136. Trigou AS, Pearson RB, Papenfuss AT, Goode DL. 2017. Altered interactions between unicellular and multicellular genes drive hallmarks of transformation in a diverse range of solid tumors. *PNAS* 114:6406–11
137. Bussey KJ, Cisneros LH, Lineweaver CH, Davies PCW. 2017. Ancestral gene regulatory networks drive cancer. *PNAS* 114:6160–62
138. Bischoff JR, Casso D, Beach D. 1992. Human p53 inhibits growth in *Schizosaccharomyces pombe*. *Mol. Cell. Biol.* 12:1405–11
139. Miao ZF, Cho CJ, Wang ZN, Mills JC. 2020. Autophagy repurposes cells during paligenesis. *Autophagy* 17:588–89
140. Kon N, Ou Y, Wang SJ, Li H, Rustgi AK, Gu W. 2021. mTOR inhibition acts as an unexpected checkpoint in p53-mediated tumor suppression. *Genes Dev.* 35:59–64
141. Carriere C, Young AL, Gunn JR, Longnecker DS, Korc M. 2009. Acute pancreatitis markedly accelerates pancreatic cancer progression in mice expressing oncogenic Kras. *Biochem. Biophys. Res. Commun.* 382:561–65
142. Huang H, Daniluk J, Liu Y, Chu J, Li Z, et al. 2014. Oncogenic K-Ras requires activation for enhanced activity. *Oncogene* 33:532–35
143. Collins MA, Bednar F, Zhang Y, Brisset JC, Galban S, et al. 2012. Oncogenic Kras is required for both the initiation and maintenance of pancreatic cancer in mice. *J. Clin. Investig.* 122:639–53
144. Mills JC, Stanger BZ, Sander M. 2019. Nomenclature for cellular plasticity: Are the terms as plastic as the cells themselves? *EMBO J.* 38:e103148

145. Rehman SK, Haynes J, Collignon E, Brown KR, Wang Y, et al. 2021. Colorectal cancer cells enter a diapause-like DTP state to survive chemotherapy. *Cell* 184:226–42.e21
146. Ootani A, Li X, Sangiorgi E, Ho QT, Ueno H, et al. 2009. Sustained in vitro intestinal epithelial culture within a Wnt-dependent stem cell niche. *Nat. Med.* 15:701–6
147. Giandomenico SL, Mierau SB, Gibbons GM, Wenger LMD, Masullo L, et al. 2019. Cerebral organoids at the air-liquid interface generate diverse nerve tracts with functional output. *Nat. Neurosci.* 22:669–79
148. Gindele JA, Kiechle T, Benediktus K, Birk G, Brendel M, et al. 2020. Intermittent exposure to whole cigarette smoke alters the differentiation of primary small airway epithelial cells in the air-liquid interface culture. *Sci. Rep.* 10:6257
149. VanDussen KL, Marinshaw JM, Shaikh N, Miyoshi H, Moon C, et al. 2015. Development of an enhanced human gastrointestinal epithelial culture system to facilitate patient-based assays. *Gut* 64:911–20
150. Alexander KL, Serrano CA, Chakraborty A, Nearing M, Council LN, et al. 2020. Modulation of glycosyltransferase ST6Gal-I in gastric cancer-derived organoids disrupts homeostatic epithelial cell turnover. *J. Biol. Chem.* 295:14153–63
151. Yin X, Mead BE, Safaee H, Langer R, Karp JM, Levy O. 2016. Engineering stem cell organoids. *Cell Stem Cell* 18:25–38
152. Chen M-S, Lo Y-H, Butkus J, Zou W, Tseng Y-J, et al. 2018. Gfi1-expressing Paneth cells revert to stem cells following intestinal injury. bioRxiv 364133. <https://doi.org/10.1101/364133>
153. Ma Z, Lytle NK, Chen B, Jyotsana N, Novak SW, et al. 2021. Single-cell transcriptomics reveals a conserved metaplasia program in pancreatic injury. *Gastroenterology*. In press. <https://www.doi.org/10.1053/j.gastro.2021.10.027>

Gut check: can other microbes or communities phenocopy *H. pylori*'s early gastric pathology?

Jeffrey W Brown 

The gastric mucosa is exposed to billions of diverse microorganisms every day. To stymie gastric colonisation as well as to limit passage of potential pathogens to more distal segments of the GI tract, the stomach has several broadly active defence mechanisms: acidity, mucus and proteolytic enzymes. Other extragastric mechanisms may contribute: for example, glycosylation epitopes like 3'-Sulfo-Lewis A on salivary mucins cotransit with swallowed bacteria and associate with them when the pH drops in the stomach,¹ presumably preventing the bacteria from binding the mucosa.

Despite these defenses, at least one bacterial species, *Helicobacter pylori* is able to colonise the human stomach. This pathogen initially invades the gastric antrum, but it can also spread to the gastric body by inducing a metaplastic glandular response,² characterised by loss of acid-secreting parietal cells (oxyntic atrophy) and metaplastic glandular changes (ie, Spasmolytic Expressing Polypeptide Metaplasia or SPEM). In a small proportion of individuals, metaplasia can progress to dysplasia and gastric adenocarcinoma. Thus, identifying the early histological changes associated with *H. pylori* infection becomes clinically important.³

The decrease in or absence of acidity associated with oxyntic atrophy creates an environment permissive for colonisation by opportunistic microbes. Although the presence of these ectopic microbial communities correlates with oxyntic atrophy,⁴ previously there has been no clear demonstration that bacteria other than *H. pylori* were able to induce metaplastic changes (recently reviewed by Engstrand and Graham⁵). However, in *Gut* by Kwon *et al*, show that microbial communities lacking *H. pylori* may give rise to oxyntic atrophy and metaplasia with subsequent

progression even to dysplastic-like lesions in the murine stomach.⁶

Due to the inability of human strains of *H. pylori* to efficiently colonise the murine stomach, Kwon *et al* were able to study the effects of non-*H. pylori* microbes on the mouse gastric epithelium.⁶ They compared gnotobiotic mice inoculated with either morcellated biopsies or gastric aspirates from humans with superficial gastritis, intestinal metaplasia or gastric cancer. As expected, they found that *H. pylori* did not grow out from the inoculated murine stomach, but interestingly numerous other microbes were able to implant and persist for at least a year. Microscopic examination of inoculated murine stomachs demonstrated histological features that phenocopy those observed in chronic *H. pylori*-infected human stomachs, including oxyntic atrophy and SPEM. Intriguingly, a year after inoculation, patchy regions of dysplastic appearing glands were observed in the gastric corpus of some mice.

Two important caveats arise when trying to extend these findings to humans: (1) microbes do not act in an identical fashion in humans as they do in mice, and (2) these experiments were carried out in germ-free animals. Limitations aside, their results question whether *H. pylori* is unique in its ability to initiate metaplastic changes in the presence of other bacterial species or whether communities lacking *H. pylori* are capable of acting similarly. Along similar lines, since the abundance of *H. pylori* decreases in advanced stages of metaplasia and dysplasia, the authors' data suggest that other microbes could be partially responsible for perpetuating the inflammatory environment invariably associated with oncogenic transformation even if they are unable to initiate such changes in humans.

This line of reasoning may call into question the current end points for antibiotic treatment of *H. pylori* gastritis. Following a course of antibiotics and acid suppression, treatment 'success' is determined by negative tests assaying for unique characteristics of *H. pylori* (ELISAs against

H. pylori epitopes) or urease activity (campylobacter-like organism (CLO) or breath tests). However, if bacteria other than *H. pylori* (with different antibiotic sensitivities) can maintain an inflammatory metaplastic epithelium that correlates with risk of gastric cancer,³ strategies that target restoration of the homeostatic gastric epithelium may be better endpoints for antibiotic treatment. To this end, the most logical test would be restoration of parietal cell number on histology or parietal cell function (ie, gastric pH). Although, ablation of parietal cells does not cause metaplasia in murine models⁷ and conditions like autoimmune gastritis that also decrease parietal cell numbers are not associated with an increased risk for developing gastric adenocarcinoma, the parietal cell census (drastically reducing in response to any type of gastric inflammation) can be used to assess restoration of the homeostatic gastric epithelium after antibiotic treatment.

An interplay between the host genetic susceptibility and *H. pylori* strain explains at least a portion if not the majority of the divergent geographic or cultural risk of developing gastric adenocarcinoma.⁸ Dietary factors may also be relevant by modulating *H. pylori* gene expression.⁸ If, in fact, microbial communities lacking *H. pylori* can elicit or maintain the inflammatory metaplastic glandular response in humans, similar questions may be asked of these potential pathogens.⁹

Although not controlled for inoculum of viable bacteria, the authors show increased macrophage infiltration in mice inoculated with microbial communities from individuals with gastric cancer or intestinal metaplasia relative to sham or individuals with superficial gastritis; a mechanism which has previously been shown to be important in the pathogenesis of SPEM.¹⁰ It remains to be determined whether the entire immunologic profile of the metaplastic stomach is similar to that precipitated by chronic infection with murine-adapted strains of *H. pylori*.

Although the authors observed focal dysplastic-like histology in ~50% of germ-free mice inoculated with microbes from individuals with either intestinal metaplasia or gastric cancer, it should be noted that a large fraction, if not most dysplastic murine histology, is reversible on removal of the offending stimuli. Thus, it will be important to ascertain whether these microbial communities can truly lead to invasive cancers in humans like chronic *H. pylori* infection. If these microbial communities do not

Department of Medicine, Washington University in St Louis School of Medicine, St Louis, MO 63110-1010, USA

Correspondence to Dr Jeffrey W Brown, Department of Medicine, Division of Gastroenterology, Washington University in St Louis School of Medicine, St Louis, MO 63110-1010, USA; brownjw@wustl.edu

predispose toward true oncogenic transformation, then these focal dysplastic-appearing lesions are of unclear clinical significance.

Overall, the data presented by Kwon *et al*, in no way downplay the importance of *H. pylori* as a human pathogen and carcinogen; however, they do help open the door for considering key roles for other bacteria as well.

Twitter Jeffrey W Brown @JeffreyWadeBro1

Contributors I conceived of and wrote the manuscript.

Funding JWB is supported by the Department of Defence, through the PRCRP programme under Award No. W81XWH-20-1-0630, P30 DK052574, the American Gastroenterological Association AGA2021-5101, R21 AI156236, and the Doris Duke Fund to Retain Clinical Scientists.

Competing interests None declared.

Patient and public involvement Patients and/or the public were not involved in the design, or conduct, or reporting or dissemination plans of this research.

Patient consent for publication Not applicable.

Provenance and peer review Commissioned; internally peer reviewed.

© Author(s) (or their employer(s)) 2022. No commercial re-use. See rights and permissions. Published by BMJ.



To cite Brown JW. *Gut* 2022;**71**:1241–1242.

Received 7 September 2021

Accepted 19 September 2021

Published Online First 23 September 2021



► <http://dx.doi.org/10.1136/gutjnl-2021-324489>

Gut 2022;**71**:1241–1242.

doi:10.1136/gutjnl-2021-325749

ORCID iD

Jeffrey W Brown <http://orcid.org/0000-0002-3992-9613>

REFERENCES

- 1 Veerman EC, Bank CM, Namavar F, *et al*. Sulfated glycans on oral mucin as receptors for *Helicobacter pylori*. *Glycobiology* 1997;**7**:737–43.
- 2 Sáenz JB, Mills JC. Acid and the basis for cellular plasticity and reprogramming in gastric repair and cancer. *Nat Rev Gastroenterol Hepatol* 2018;**15**:257–73.
- 3 Lee JWJ, Zhu F, Srivastava S, *et al*. Severity of gastric intestinal metaplasia predicts the risk of gastric cancer: a prospective multicentre cohort study (GCEP). *Gut* 2022;**71**:854–63.
- 4 Sheh A, Fox JG. The role of the gastrointestinal microbiome in *Helicobacter pylori* pathogenesis. *Gut Microbes* 2013;**4**:505–31.
- 5 Engstrand L, Graham DY. Microbiome and gastric cancer. *Dig Dis Sci* 2020;**65**:865–73.
- 6 Kwon S-K, Park JC, Kim KH, *et al*. Human gastric microbiota transplantation recapitulates premalignant lesions in germ-free mice. *Gut* 2022;**71**:1267–77.
- 7 Burclaff J, Osaki LH, Liu D, *et al*. Targeted apoptosis of parietal cells is insufficient to induce metaplasia in stomach. *Gastroenterology* 2017;**152**:762–6.
- 8 Amieva M, Peek RM. Pathobiology of *Helicobacter pylori*-induced gastric cancer. *Gastroenterology* 2016;**150**:64–78.
- 9 Abreu MT, Peek RM. Gastrointestinal malignancy and the microbiome. *Gastroenterology* 2014;**146**:1534–46. e3.
- 10 Petersen CP, Weis VG, Nam KT, *et al*. Macrophages promote progression of spasmodic polypeptide-expressing metaplasia after acute loss of parietal cells. *Gastroenterology* 2014;**146**:1727–38.